Archives of Computational Methods in Engineering (2022) 29:5663–5721
https://doi.org/10.1007/s11831-022-09786-9

REVIEW ARTICLE

State-of-the-Art Review of Machine Learning Applications in Additive Manufacturing; from Design to Manufacturing and Property Control

Garshasp Keyvan Sarkon[1] · Babak Safaei[1,2] · Mohammad Saleh Kenevisi[3] · Samaneh Arman[4] · Qasim Zeeshan[1]

Received: 21 April 2022 / Accepted: 26 June 2022 / Published online: 22 July 2022

Abstract
In this review, some of the latest applicable methods of machine learning (ML) in additive manufacturing (AM) have been presented and the classification of the most common ML techniques and designs for AM have been evaluated. Generally, AM methods are capable of creating complex designs and have shown great efficiency in the customization of intricate products. AM is also a multi-physical process and many parameters affect the quality in the development. As a result, ML has been considered as a competent modeling tool for further understanding and predicting the process of AM. In this work, most commonly implemented AM methods and practices that have been paired with ML methods along with their specific algorithms for optimization are considered. First, an overview of AM and ML techniques is provided. Then, the main steps in AM processes and commonly applied ML methods, as well as their applications, are discussed in further detail, and an outlook of the future of AM in the fourth industrial revolution is given. Ultimately, it was inferred from the previous papers that the most widely applied AM techniques are powder bed fusion, direct energy deposition, and fused deposition modeling. Also, there are other AM methods which are mentioned. The application of ML in each of the renowned techniques are reviewed more explicitly. It was found that, the lack of training data due to the novelty of AM, limitations of available materials to be applied in AM methods, non-standardization in AM data and process, and computational capability were some of the constraints of the application of ML in AM methods.

1 Introduction

1.1 Additive Manufacturing

The practice of manufacturing has been one of the key components of human development and progress through the ages. Some of the most significant methods include metal forming, machining, joining, casting, powder metallurgy, and three-dimensional printing or additive manufacturing (AM) [1]. AM is already in high demand in many industries such as aerospace and medical engineering [2, 3]. Moreover, considered to be an integral aspect leading to industry 4.0 [4]. In medical applications, AM has become the most commonly applied manufacturing method in hearing aid gadgets, dental implants and prosthetic bones and cartilages [5]. With the availability and commercialization of this technology, even novice, non-technical household applications have been reported to be functional and practical for either maintenance or self-customization [6]. The methods used in AM can create objects with sophisticated geometries layer after layer [7–17]. Although there are distinct methods under the class of AM, generally the process steps of each method follow the same stages and each step of different methods of AM fall under the same process step as depicted below (Fig. 1) [18].

The most applied AM methods are powder bed fusion (PBF), direct energy deposition (DED), and binder jetting (BJ) [19]. A classification of AM processes is presented below (Fig. 2) [20]. Each technique is different in terms of used material, layer formation and printed product. For each material and manufacturing method, different measures and considerations need to be taken to finish the product and to

✉ Babak Safaei
babak.safaei@emu.edu.tr

[1] Department of Mechanical Engineering, Eastern Mediterranean University, Famagusta, North Cyprus Via Mersin 10, Turkey

[2] Department of Mechanical Engineering Science, University of Johannesburg, Gauteng 2006, South Africa

[3] Department of Mechanical Engineering, Tsinghua University, Beijing 100084, China

[4] School of Science and Technology, The University of Georgia, Tbilisi 0171, Georgia

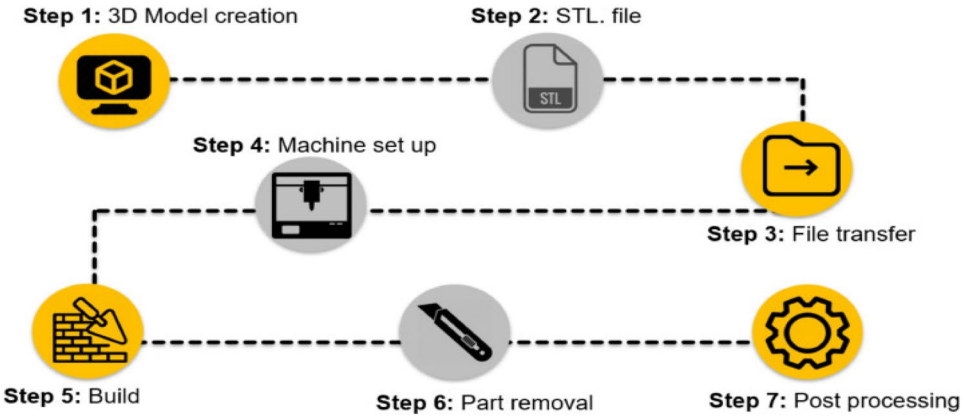

Fig. 1 The process steps in AM [18]

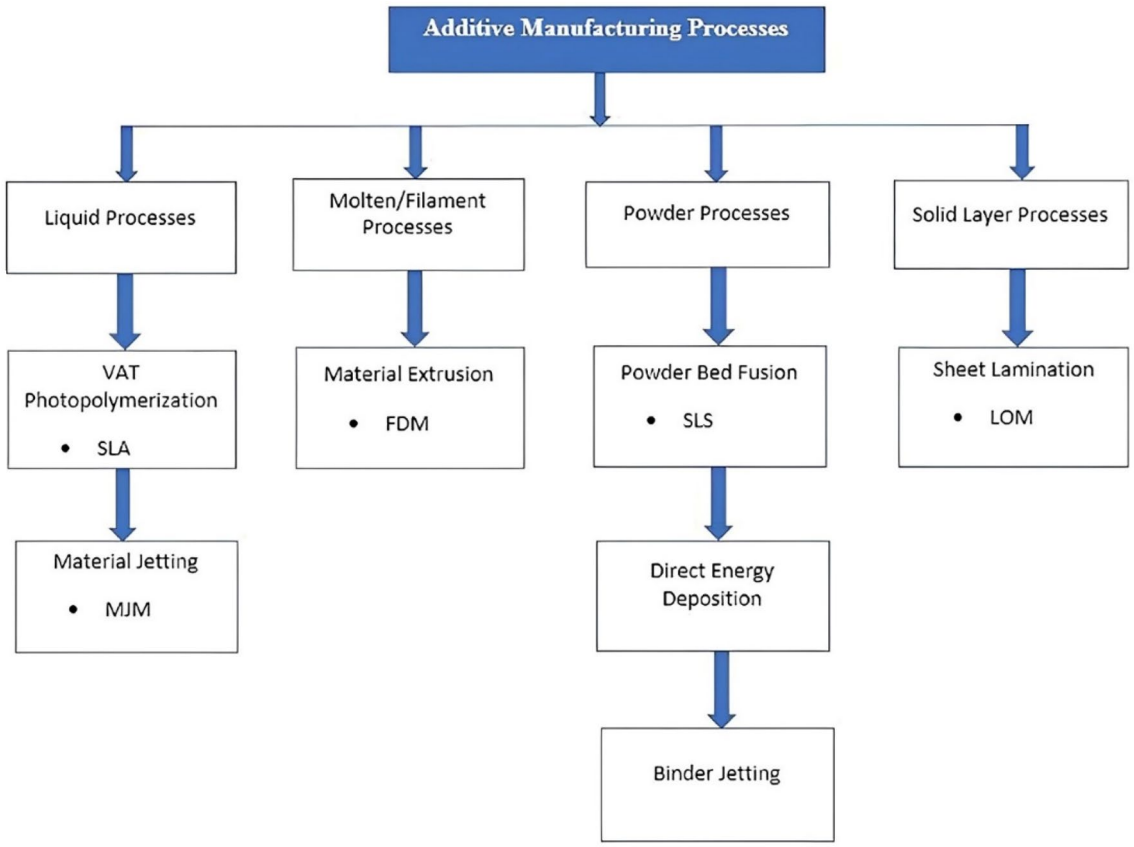

Fig. 2 Classification of notable methods of AM [20]

achieve the highest quality. The considerations and steps required to establish a solid database are distinctive based on their difference in printing. Therefore, sampling, testing and material analysis in 3D printing methods are explained. Since each printing method is chosen based on the properties and applications of printed parts, properties differ in terms of surface smoothness, strength, durability, dimension preciseness and geometrical complexity [21].

Overall, AM has lots of distinct advantages over traditional manufacturing methods. However, the preliminary parameters are quite hard to tune since they may significantly affect the microstructure of parts being printed and the overall quality of printed objects. Understanding process structure property performance (PSPP) relationship for 3D printing by using novel numerical and analytical modeling is a hurdle on its own, and nowadays, artificial intelligence (AI), particularly machine learning (ML) and neural networks (NN), are capable of performing advanced regression analyses and complex pattern recognition without the need to create analytical and physical models [22]. In this review,

the aim is to identify and discuss the applications of ML in some commonly used AM processes. The general process is depicted in Fig. 3 and gives an intuition of how these two methods could work together along with their functionalities and considerations[23]. The application of ML techniques, identification of challenges and advantages, and possibility of improvement in future works as well as the integration of these two concepts (ML and AM) are of utmost importance for a thorough understanding. Also, different provisions need to be considered for the maintenance of the aforementioned AM installments due to rapid growth of AM. Therefore, to tackle this shortcoming, a practice known as prognostics and health management (PHM) which is a combined practice of state monitoring for refining the accessibility and competence of high-value industrial apparatus and plummeting the maintenance expenses [24].As it happens, a method known as quantum ML technique is very helpful for health monitoring purposes of the installments and other approaches which will be discussed in the AM outlook section of the paper. Conventional ML methods are shown to be not competent when it comes to handling large amounts of data in real-time [25].

In the following, AM methods are evaluated as a preliminary introduction for painting a general picture regarding the capabilities of different AM methods.

1.1.1 Powder Bed Fusion

PBF is a state-of-the-art AM method that has progressed through many research works and advancements in industry [26]. PBF is subdivided into laser beam melting (LBM) or laser powder bed fusion (LPBF), electron beam melting (EBM) and selective laser sintering (SLS). Generally, in PBF, energy source directly melts and sinters the materials which are typically in powdered form [27]. Both metal and polymer-based procedures can be implemented for end-use manufactured parts and typically, this method is very demanding in terms of energy consumption [28]. Figure 4 [29] shows the aforementioned process. LPBF is particularly

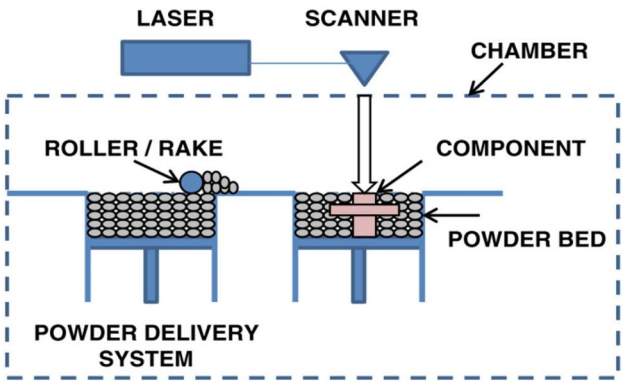

Fig. 4 Laser powder bed fusion device setting [29]

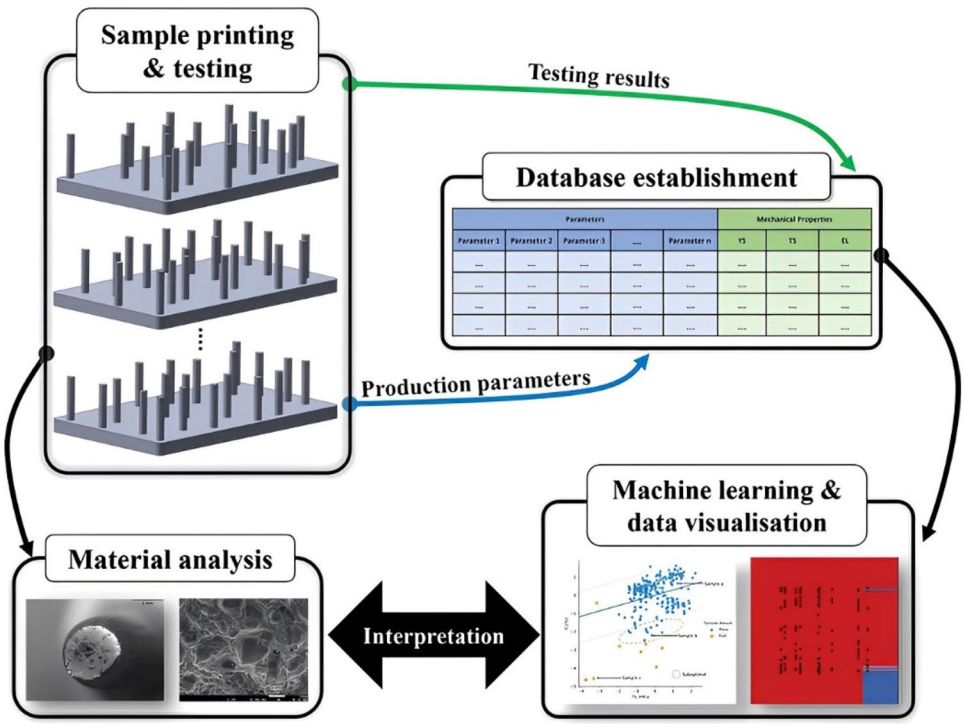

Fig. 3 Graphical representation of the steps taken in the application of ML in AM [23]

one of the well-established methods which has made notable progress to become fully commercialized [30–32].

1.1.2 Directed Energy Deposition

DED technique allows manufacturing objects by liquidizing materials while being deposited. This method is mostly used for metallic powders. DED can be easily paired with conventional subtractive methods for machining. Furthermore, DED is very applicable in maintenance and repairing since it has high deposition rate that could be used in repairing large components [33, 34]. This process generates three-dimensional parts by melting materials as it is placed by means of intense thermal energy such as electron beam, laser, or plasma arc. A scaffold system or robotic arm operates both energy source and material nozzle. A portable compartment is fixed along with a laser emitting source. Metal powder is concurrently directed into the nozzle to the required area; laser melts the powder which is then solidified to form a layer. Portable compartments are not fixed at specific axes and have the freedom to move along different orientations. Some of the notable hindrances are low building resolution of manufactured parts, high cost of manufacturing, and supportless structures [35]. Figure 5 shows a DED laser process [36].

1.1.3 Material Extrusion/Fused Deposition Modeling

FDM, sometimes referred to as fused filament fabrication (FFF), (Fig. 6) method is extensively used for manufacturing geometrically complex objects in a noticeably short time span to suit customer needs [37]. With control and command over processing parameters due to the enhanced capability of operating machines, customized biomedical parts are becoming easier to produce [38]. In FDM, an uninterrupted

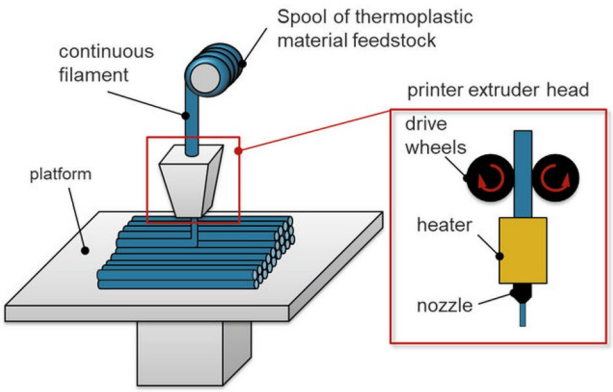

Fig. 6 Fused deposition modelling process of polymer material [42]

strand of a thermoplastic polymer is used to 3D print layers of materials. The process of FDM is generally described as the extrusion of heated feedstock plastic filaments via a nozzle tip to deposit multiple layers onto a platform to build up the structure layer after layer from a digital CAD model of the part [19, 39]. However, FDM full-scale use is compromised by limited materials available in the market. As a result, it is important to fix process parameters in the stage of fabrication [40, 41].

1.1.4 Vat-photopolymerization

Vat-photopolymerization (VATP) methods are considered as one of the low-cost AM processes in terms of required energy input [43, 44]**.** Moreover, this method has been very effective because of its high resolution and printing speed, especially in drug delivery and bespoke medical devices [45]. The very essence of material formation is based on a chemical process known as photopolymerization, which

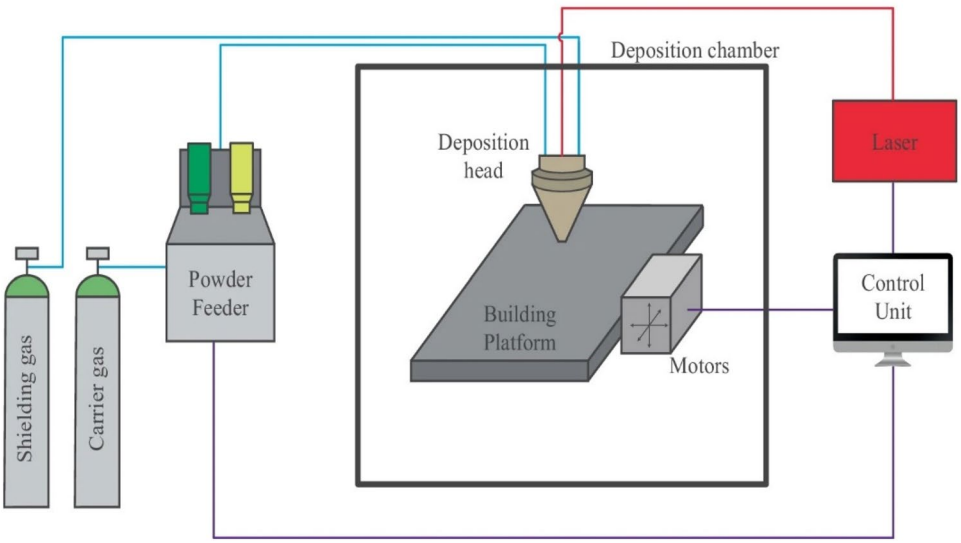

Fig. 5 Laser DED installment [36]

occurs under light exposure in photocurable polymers resulting in cross-linking of the material to a 3D form. Some different approaches include mask-image-projection-based stereolithography, laser writing stereolithography, and continuous light interface process (CLIP) [46–50]. In this section, we put CLIP approach under scope due to its potential for continuous AM and discrete layer segmentation. In CLIP approach, the most important parameter to monitor is continuous elevation speed which is shown by letter V in Fig. 7. Non-accurate speed elevation results in poor bonding of solidified materials if CLIP is too fast and adhesion to oxygen preamble window occurs if CLIP is too slow. The knowledge behind the proper elevation speed is mostly derived from experimental data and because printing geometry differs for each design purpose. The data from the empirical trial and error methods could not always be helpful, thus propelling researchers to consider data-driven and ML approaches to set the right parameters for each design [51].

1.1.5 Jetting Based AM Processes

Several distinct jetting processes based on the classification made by ASTM [53] are binder jetting and material jetting. In general, droplets of build material are jetted to a build platform similar to two dimensional inkjet printing, either jetted countinusly or with drop on demand method. Material, and for binder jetting, liquid bonding agent, is jetted to bind powder materials. While both material jetting and binder jetting share some similar traits, they have their own applications, advantages and strategies. Material jetting is very accurate with a minimum amount of waste and a variation of material parts and hues of color could be printed under one process, but there are only waxes and some polymers that could be used as print material whereas in binder jetting, a plethora of materials with much better and reliable mechanical properties such as metals, ceramics and polymers are used. Furthermore, in binder jetting method, there are many possibilities in the creation of parts with different mechanical properties while material jetting method does not have this important advantage [54].

i. Binder Jetting

BJ printing is a process where a binder material and a base material which are typically powder, are treated. Liquid binders are extended through a jetting nozzle which is referred to as inkjet printer. Inkjet printers spread powders and powdered materials are selectively combined into a solidified layer; needless to say the bound layer is only two dimensional [55].

ii. Material Jetting

Material jetting (MJ), was first established by Objet Geometries Ltd. in 2000 and was later adopted by the company Stratasys in 2012 [56]. In accordance with the standards set by ISO/ASTM52900, the printing method is explained as droplets selectively deposited from the feedstock. There are variances between the steps printing devices operate based on, but the general process remains the same. This method has other variations such as Electrohydrodynamic jet printing, where instead of heat, pneumatic or piezo electric force is used. The electrical field exerts the liquid out of the nozzle, which helps immensely in printing electronic apparatuses [57]. In order to store the photopolymer materials, an air-excluding tanker is implemented to exert deposits of aforementioned materials from the tank to the nozzle to form a very thin layer on the construction platform. Afterward, ultra violet (UV) light with wavelengths of 190 and 400 nm is used as post-processing for curing [58, 59]. When curing is done, the construction platform is lowered until a certain layer thickness is achieved and then, the process gets repeated until the desired part is constructed. Furthermore, the support materials for overhung parts are a sort of gel-like material that can be removed by sonication in a vat of sodium hydroxide, heating, or waterjet [60, 61]. Figure 8 shows how MJ operation takes place [62].

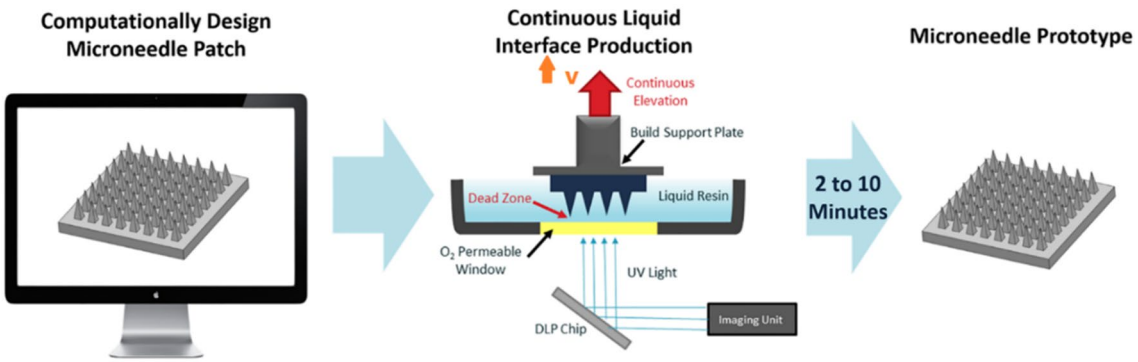

Fig. 7 A CLIP process for prototyping microneedle species. The orientation of the most important parameter 'V' is shown in orange [52]

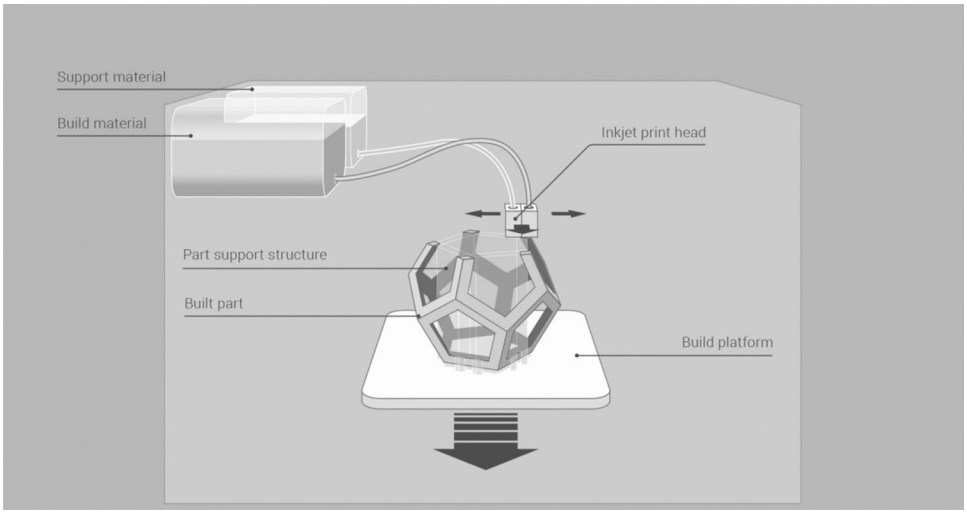

Fig. 8 A general depection of a material jetting process [62]

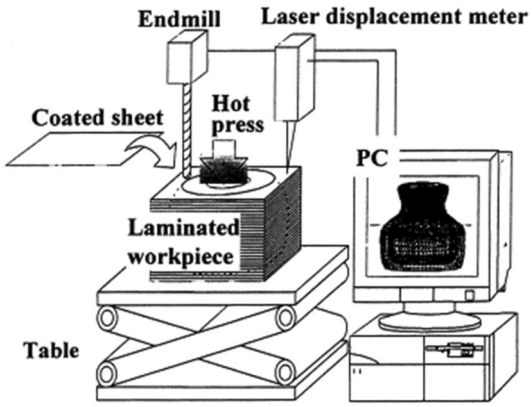

Fig. 9 A sheet lamination installment [64]

1.1.6 Sheet Lamination

Sheet lamination (SL) is a sub-branch of AM which was coined by Helisys of Torrance, in 1991. SL is sometimes also referred to as selective deposition lamination. However, the most prominent mode of SL is ultrasonic AM, which could have steps of other manufacturing techniques such as CNC milling, ultrasonic welding, and laminated object manufacturing. Generally, in SL methods, to make partitions, cuts are made via laser and contrariwise, In order to make bonds between sheets, typically ultrasound waves are implemended [63]. Figure 9 depicts how the process is undertaken [64].

This method mostly consists of a mechanism in which sheets are directed above the build platform. A roller which acts as a heater applies the necessary pressure to attach the sheet above to the one below. After performing laser cut to the layer, build platform is lowered to the thickness of the pre-existing sheet, which is mostly between 0.002 and 0.020 inches. Thus, one iteration is completed and another sheet advances on the top. The former sheet is deposited, while the platform rises again and the roller heating source enforces pressure to make another bond. As mentioned, this method has a number of names used by academia and industry. To the best of the authors knowledge, there is no explicit research done relating to the optimization of SL by ML and data-driven approaches. In general, it is shown that SL has high fabrication speed and there is no need for support structures. It also has low warping and internal stress. Moreover, multi-material and multi-color modes can be used. However, the shortcomings of this approach which require further study and improvement, are high amount of waste creation and issues with removing support entrapped in internal cavities. Moreover, thermal cutting produces harmful gasses and the lamination is likely to happen due to the heat of laser [63].

1.2 Machine Learning

ML techniques function as a medium for understanding complex patterns. Visual words and histogram of oriented gradients (HOG) are some of the features that are used in ML for image analysis [65]. These features mostly fall in the unsupervised category, hindering the proper consistency of the outcome of recognition task. In this approach, ML applies NN and convolutional deep neural network (CDNN) methods with the aid of supervised learning. This method picks up underlying patterns that could not be identified easily by automatic image processing. This method, which is exclusively inspired by the visual cortex of brain, has proven to be effective in inspection, motion detection, etc. [66–68]. While implementing ML, some assumptions are considered initially. The underlying premises and assumptions applied to develop an ML model need to be thoroughly understood to avoid any misconception. Figure 10 shows a classification

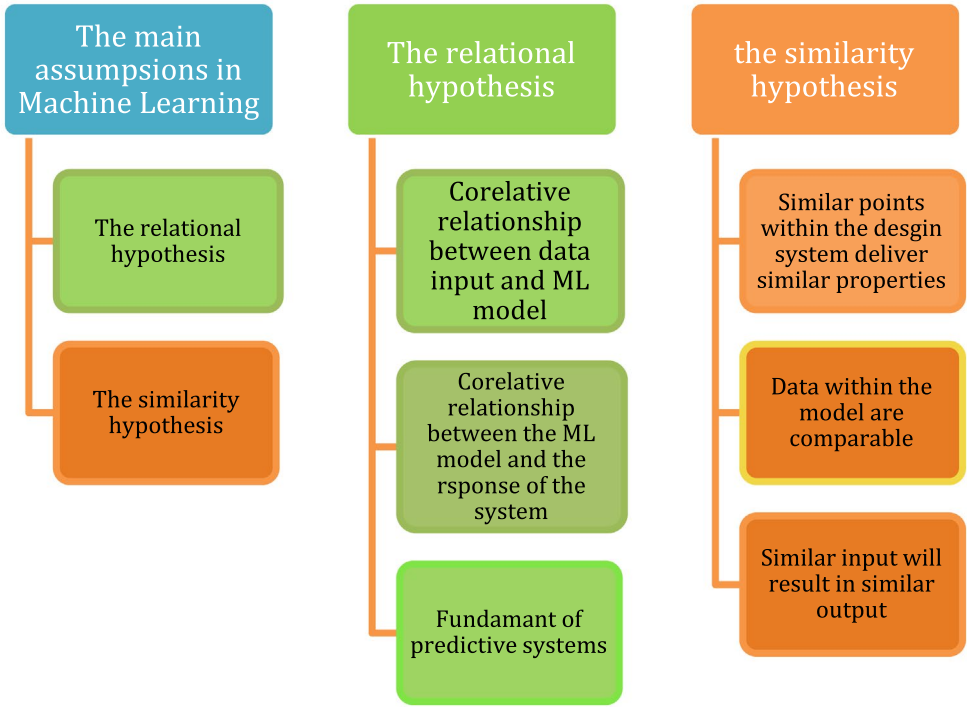

Fig. 10 Types of assumptions in ML

of some of the most important assumptions in this type of modeling.

ML models should be applied according to the assumptions considered in the model. Thus, resulting in a thorough assessment of the development of the model [69]. It is often believed that when a machine changes its configurations over time in a way that it performs better and more optimally, it has articulated learning behavior. Changes could vary between enhancement of an already applicable system or developing a totally new system. What a machine considers to change based on its experience could be a set of data or a structure of a program relating to the feedback it receives from its interaction with external information. ML is a branch of AI relating to changes that perform objectives in a more efficient way and it is associated with the AI. These tasks could be prediction, forecasting, diagnoses, robot control or planning Based on most classifications, ML could be classified into three paradigms (Fig. 11) [70].

1.2.1 Supervised ML

Supervised learning is the most commonly implemented ML method. In this method, ML models need to learn functions in a way that inputs fit the outputs. Then, the function reveals information from categorized training data and each input is related to its assigned value. The algorithm embedded in a ML model is capable of making novel observations never made before or uncovering patterns in a training data set [71]. Some considerations need to be made and some initial steps are required in order to perform this task [72–74].

- Acquiring a dataset and data processing
- Feature selection (target variable)
- Splitting the dataset (training, cross-validation, testing)
- Hyperparameter tuning and prediction

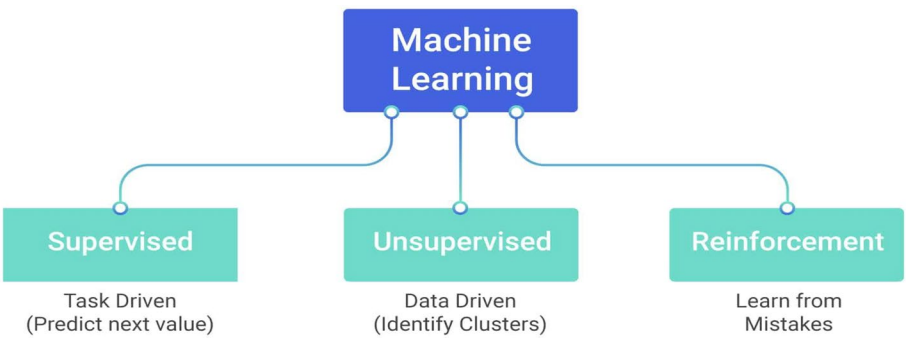

Fig. 11 Main paradigms of ML [70]

Figure 12 shows the structure of a supervised ML model [72]. One of the most approached predictive statistical analysis in supervised method is linear regression [75]. Each analysis is carried out by a specific algorithm which should be chosen with prior knowledge based on linearity or non-linearity of the problem. However, by comparing error metrics of each regression, best algorithm could be identified [76].

In the following, the aforementioned steps are discussed in more detail.

i. Dataset acquisition and processing

Data acquisition can be regarded as a concept where physical events that happened in real world gets transformed into electrical signals, converted, and scaled in digital format for further analysis, processing, and storage within the computer memory storage. In general data acquisition systems are not only for gathering data but also for operating on the data [77]. Having complete data is very important for ML models to perform better and get a robust analysis [78]. Nowadays, DL models can even operate as good as real ophthalmologists in detecting diabetic eye issues from an image, all owning to the computational power of models and large amount of data to train the models [79]. With modernization and new fields of science used in the industry, lack of prior data is a problem that should be dealt with, particularly with deep learning models that require even more data than traditional ML. Initially, data acquisition approaches are used to harvest, augment, or generate of novel data sets. Afterwards, data labeling should be done and then, training the already achieved or improve the labeling and accuracy of the gathered dataset. In this aspect, ML engineers and data scientists and data managers should work together. In the following, a diagram of steps in data collection, acquisition and processing is presented (Fig. 13) [80].

ii. Target variable selection

As the name indicates, the target variable is the feature that we aim to get or achieve in the ML task. Whether classification or regression, the features should be clear, such as the target variable. Target variables in the form of labeled targets are the pivotal point where supervised ML algorithms use historical data to pick apart patterns and discover relations amongst the other unknown features of the dataset and the set target variable. Without properly labeled data, supervised ML tasks would not be able to plot data to outcomes [81].

iii. Splitting the dataset

Based on most references and as a convention, it is understood that it is best to split the dataset to prevent overestimation and overfitting. In the following, we discuss the most noticeable sets of grouping: training set, cross-validation set, and testing test. The training test is mostly the largest set. The model trains based on the insight that it gains from the data that is fed from the training set. The training set is basically the subset of the whole data set available. In this phase, we can forecast the weights, the bias of the model if it's a NN. Therefore, we can optimize the hyperparameters, which are the parameters that control the initial setting of the system. They are immensely important because after setting them, they cannot be changed like the weights or biases or the parameters of the system. In the cross-validation phase,

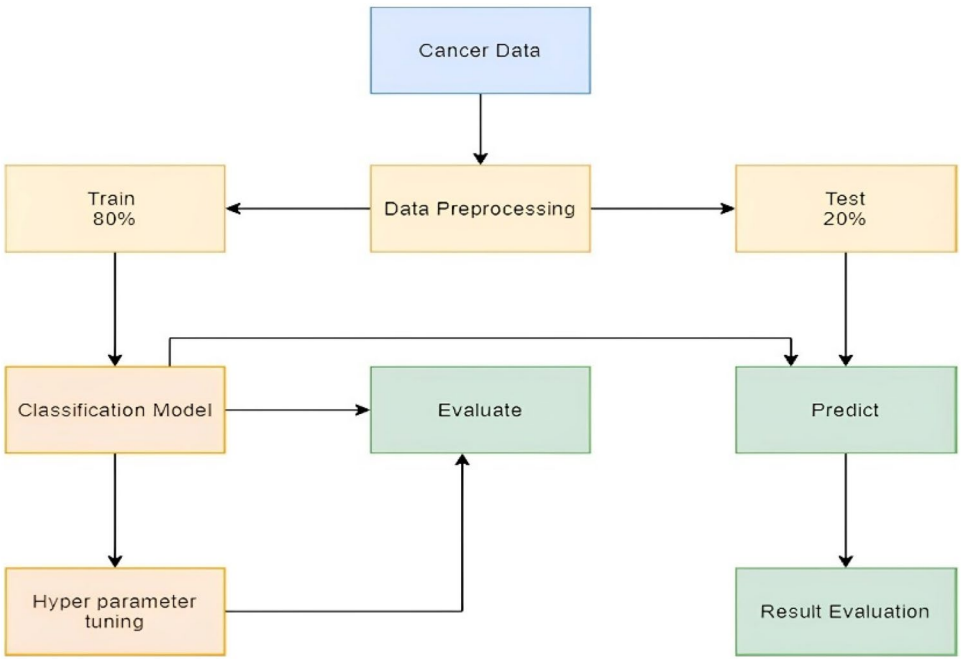

Fig. 12 General schematic diagram of a supervised ML model processing data related to cancer [72]

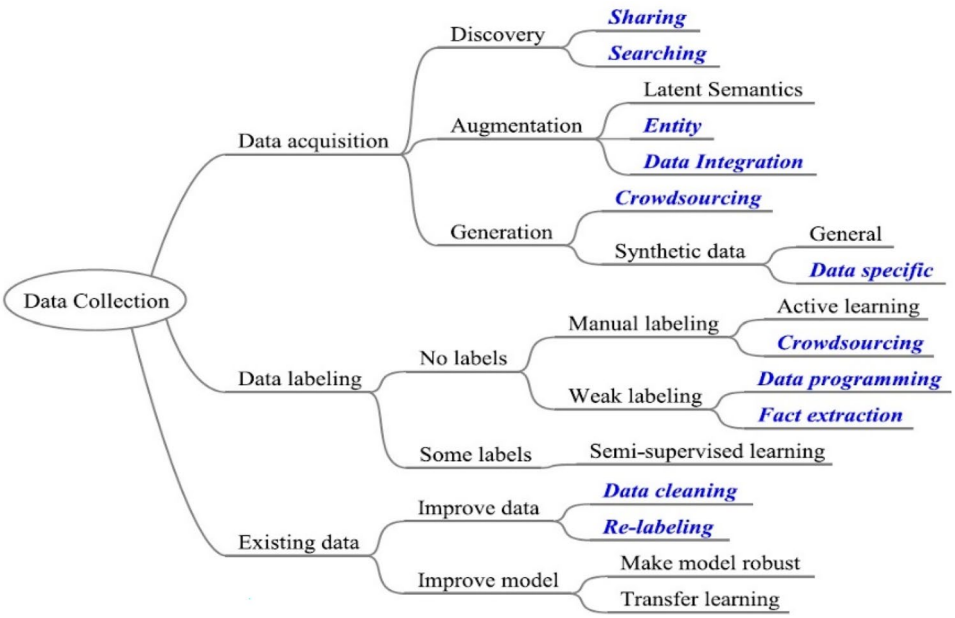

Fig. 13 Study landscape of data collection for ML [80]

we estimated the loss function or error of the system, and therefore minimizing it to get the best prediction. And then finally, we use the testing set, which is the smallest of the aforementioned sets and results in a non-bias result because the testing data are new to the model. This stage acts as a close simulation to a real life occurrence and demonstrates how the model would operate in a real situation [82].

iv. Hyperparameter tuning and prediction

Hyperparameters are very important due to the fact that they should be set before each iteration, and they define the very fundamentals of an ML model, unlike process parameters that can be manipulated while data learning process is in process. In the case of a DNN, a part of it is determining the number of hidden layers, nods, neurons, step size, and batch size. One needs to differentiate between the hyperparameters that are related to the algorithm, such as the aforementioned step size, batch size, and the ones that are related to the structure of the model, such as the number of hidden layers, method of nods connecting to each other and the number of nods. As is maintained, hyperparameters are constant while in operation, but process parameters can change. The progression to tuning or optimization of hyperparameters could be achieved when enough number of tests runs and trials are undertaken. The pace of training of a DL model is determined by the rate of convergence. There are methods known as super convergence methods where the crucial foundations of super-convergence Are training with a singular learning rate cycle and a hefty maximum learning rate [83, 84]. By comparison of the results of the test runs and making vigilant comparisons to real values of each data iteration, the accuracy of the model can be evaluated, and thereafter, we gain insight as to find the best values for the system to make a better combination of hyperparameters and more accurate predictions. A hyperparameter metric is a personal specification of a single target variable that is specified by choice of a human operator. The model accuracy is defined by a metric value and, therefore, can be determined if it is maximization or minimization that is the desired goal for our specified metric to fulfill [85].

1.2.2 Unsupervised ML

Methods classified as unsupervised ML are capable tools for the detection of similarities, thus drawing conclusions out of unclassified data by clustering them based on their similarities. When high dimensional problems are needed to be dealt with, these methods act fantastically in terms of finding correlations and patterns in such unclustered and vast environments and their visualization of many clusters that they classified. Furthermore, telling irrelevant inputs in models apart and eventually finding ways to produce materials under the same conditions and with the same quality are some features of unsupervised ML [86].

In industrial applications, a specific type of unsupervised ML, known as unsupervised transfer learning (UTL), has been found to be effective such that it could be considered as a robust anomaly detector that could be updated based on changing operating conditions. Needless to say, these models need comprehensive datasets [87]. Also, unsupervised learning could be used in cases where cyber-physical attack uncovering in AM is required [88].

1.2.3 Reinforced ML

ML approaches are very effective in dealing with repetitive tasks. Reinforced learning (RL) is very capable in the environments that machines are gathering field knowledge. There is no specific need for direct programming, and no human intervention is involved. The way this process undergoes is by defining objectives for the machine as rewards in the case of positive progress and punishments should the machine regresses away from the set objective. Figure 14 is a general workflow of a RL agent [89].

As the illustration above shows, there is an iteration shown as the observation phase O_t, in this iteration, everything that needs to be observed and acknowledged by the agent will be monitored and unveiled and the consensus is that there will be no information which will be concealed in this iteration. The embedded policy within the learning process signifies the agent's decisions and reaction to the observation that it conveyed. There are typically two form of policies, deterministic and stochastic. A deterministic policy is a precise action over a current state of observation $a = \pi(.|Ot)$. Contrariwise, a stochastic policy is a distribution of actions over a current state of observation $a = \mu(Ot)$. Moreover, a reward signal is the objective of the RL problem and it's directly influenced by the ongoing observation state and the actions taken in $r = R(Ot, a)$. The ultimate aspiration of the system is to maximize the reward it accumulates and maximization of the return rate Gt with discount rate $\gamma \in [0\ 1]$.

$$Gt = Rt + 1 + \gamma Rt + 2 + \gamma 2Rt + 3 + \ldots \quad (1)$$

Modelling of the environment allows for a deeper understanding and accurate postulation as to how the environment would behave. The dynamics of the environment could be mnemonically expressed as P, that could be either deterministic ($Ot = p(Ot, a)$) or stochastic $Ot = p(Ot, a)$ [90].

There are many possible applications of this ML approach, for instance if we consider an engineering design process, each decision taken in the process of design could have either positive or negative impact depending on the design objective**.** Numerous actions and approaches will be taken until the satisfactionary results will be achieved and each one of them has their rewards or punishments in the development of the process. There have been numerous reports of novel applications of RL method. In robotics, RL is a promising prospect for optimization and further enhancing robotic manipulations [90]. RL models are still somewhat considered as black box models. However, with methods to elucidate the intricate decision making of RL models and agent's behavior, RL models could help in acquiring scientific insight on the complex approaches it takes [91]. In a study in order to make Corrections in the framework for process control of robotic wire arc AM (WAAM) RL was used and the results signified that by using RL, learning architecture can be used in conjunction with real parts printing giving better chance of in-situ study, therefore minimizing the obligatory training time and material depletion. The

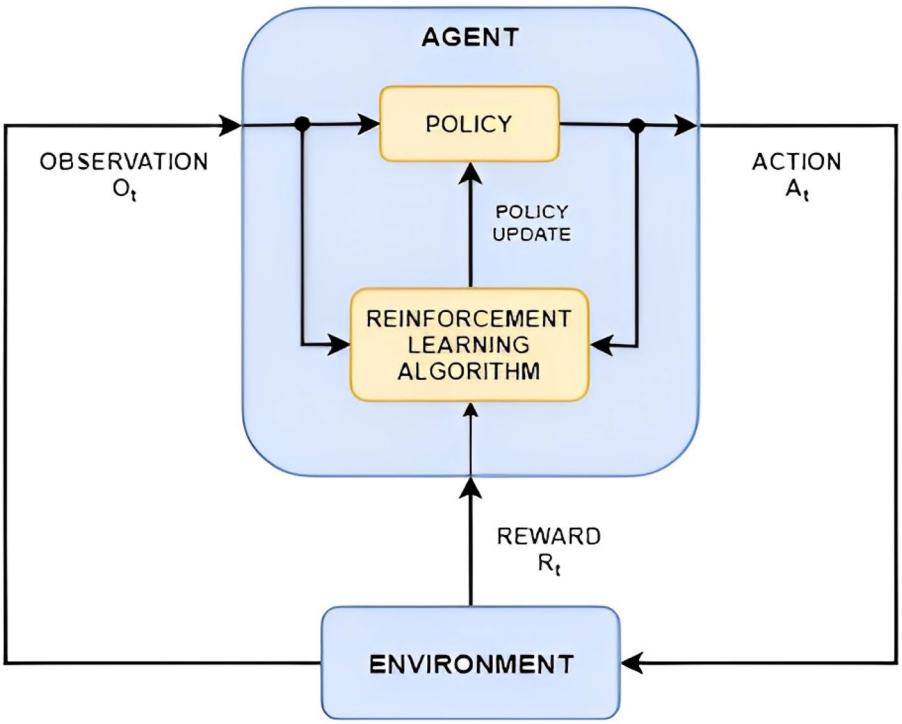

Fig. 14 Generic depiction of process steps of a reinforced ML model [89]

proposed learning framework is applied on an actual robotic WAAM system and empirically assessed [92].

1.2.4 Evaluation of ML Model Performance

In ML model performance, availability of data is an important factor. Tasks regarding voice recognition, natural language processing or image recognition have vast data availability, and in contrast, in a field like bio-informatics where data acquisition tasks are very hard to come by and are generated at quite a high price. In ML, there are three particular options to tackle the model evaluation (predictor). Independent dataset test, cross-validation test, and re-substituting. In the independent dataset approach for model evaluation, all the data sets are divided in a random fashion between two uneven parts, meaning that one part is deliberately smaller and the other larger, reason being that the larger part is designated as the training data and the smaller part for the final testing of the model. This approach is sometimes referred to as sub-sampling as well. The method however, operates on a small testing pool of datasets, which would result in volatile results on each testing evaluation. In simple terms, in each test, the results could be different from one another, which will result in inconsistency in results between real life results and test results, often higher or lower. In the resubstituting test, there is no difference between the testing pool and the training pool of data, and that becomes problematic as the model evaluation results are often far too optimistic and not very accurate. For example, a 99% accuracy could mean that the model is overestimated and rendered inoperable in real applications. The next type of model evaluation is known as cross-validation. Even though all the data available are used for testing, the way they are used are far more different compared to the resubstituting test, such that the whole data set is haphazardly divided in an arbitrary segmentation, denoted as 'n' part of equal magnitude. Furthermore, the testing and training operation will be carried out for 'n' times and in an arbitrary number of times where the objective is reached, denoted as 'kth' time, the 'kth' part will be used as the testing set while the remaining n-1 parts are still in training, and finally, after n rounds, every set of samples are used for testing phase for just once and by averaging the whole forecasting results over all the dataset, a better result for evaluation would be achieved (Fig. 15) [93].

Some other important measures of accuracy and precision of an ML model are described by confusion matrix and it could be expressed in four statements, as false negative (FN), false positive (FP), true negatives (TN), true positives (TP). Accuracy is therefore defined by how truthful the prediction of a model is. And it can be calculated as,

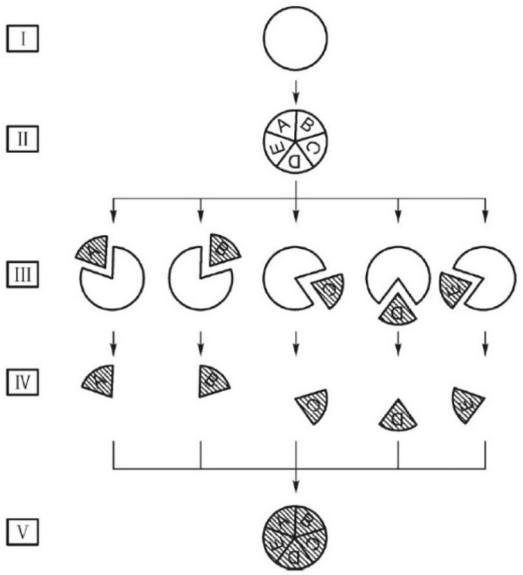

Fig. 15 A depiction of n-fold cross-validation [93]

$$\text{Accuracy (Acc)} = (\text{True Positives} + \text{True Negatives}) / \text{Total Samples count} \quad (2)$$

$$\text{Total Samples count(N)} = \text{TP} + \text{TN} + \text{FP} + \text{FN} \quad (3)$$

Precision is the amount of correct/ true positive cases divided by the number of real (true positive + false positive) examples forecasted by the classifier. The recall is the number of true positive instances divided by the number of predicted (true positive + false negative) instances by the classifier [94].

1.2.5 Deep Learning and Neural Networks Approach

In the past 40 years, ML and deep learning (DL) approaches to ML have proven to be very efficient and have made a huge impact in multiple industries [95]. Overall, both ML and DL belong to the much broader science of AI. The reason deep learning is addressed by this name is merely because of the multiple numbers of layers incorporated between the input layer, which is the first layer, and the last layer, which is the output layer [96]. Conventional NN models or multi-layer perceptrons have a singular nature that makes them well suited for binary problems via feeding them given inputs, which is inspired by the human's brain learning and perception pattern. Dong

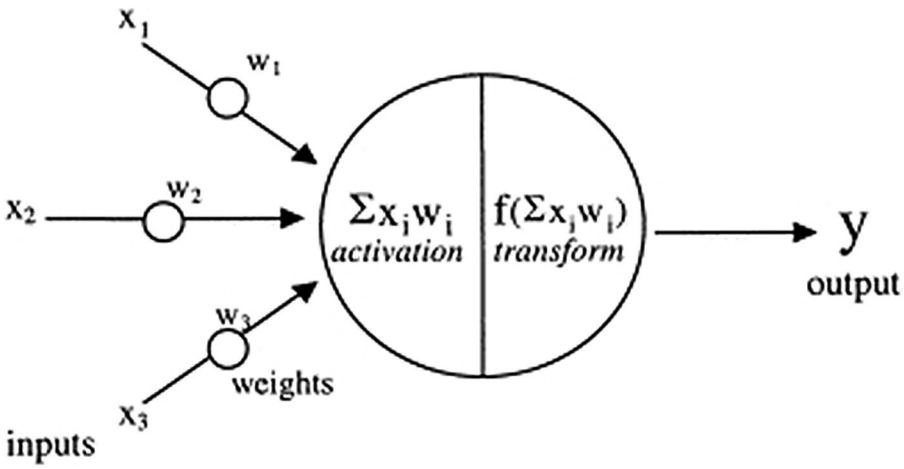

Fig. 16 A single artificial neuron [106]

et al. [97] generally break DL models down as 'merely a great many classifiers working organized, which are grounded on linear regression followed by some activation functions. A variation of DL, known as convolutional neural networks (CNN), is proven to be very suitable for image recognition tasks. Image recognition data are multi-layered data and are well designed for such tasks [98]. This DL method has been applied in many different fields [99–102]. For the case of 3D topology optimization [103], a CNN method known as one-shot has been successfully used [104] . Furthermore, because of the broad usage and variety of applications of DL models, the following will be dedicated to the breakdown of different DL models. Additionally, Recurrent neural networks (RNN) are very complicated and intricated due to the fact that aside from the inputs that they are fed with, an internal addition task is also carried out, which is nothing but some older internal tasks which are recognized as a part of the output for the system [105].

i. Classical neural networks (multi-layer perceptrons)

Conventional NN models or multi-layer perceptrons have a singular nature that makes them well suited for binary problems via feeding them given inputs, which is inspired by the human's brain learning and perception pattern. Figure 16 [106] depicts genesis of the aforementioned models. This method was initially developed by an American psychology practitioner by the name of Frank Rosenblatt in 1958. Typically, a NN model with two sets of inner layers is a classical NN.

This method is best used for its adaptability and flexibility to different types of data, regression or classification task, under the condition when a real set of values are fed to it as inputs and are also very well implemented for datasets that are in the form of vectors or matrices [107, 108].

ii. Convolutional neural networks

CNN can be considered as a more complicated and advanced form of classic NN. Capable of more complex preprocessing and data computation, these models have been used for image processing and handwritten digits (Fig. 17) [109] for the most part. However, it can also reach satisfactory results with non-image data as well. How this model makes its calculations is that the initial layers will pick apart traits like curves, edges, and lines of an image, the layers in between will group and assemble them and the final layers will recreate the image from the scratch all over. Moreover, there are some aspects where we can differentiate the CNN from its classic counterpart. Namely, the CNN models do not have to be directly connected to all out puts from the previous layers; or in other words, they have local connections. Second, the overlapping of input fields, within each layer. the neurons have the same weight in the whole layer and instead of the sigmoid function, it uses a non-linear function known as rectified linear function (RLF). Pooling layers will be combined with convolutional layers and the nominalization layers will be existent to keep the received signals in each level at the desired level. Overall, backpropagation will be used for training [110, 111].

iii. Recurrent neural network

Recurrent neural networks (RNN) are very complicated and intricated due to the fact that aside from the inputs that they are fed with, an internal addition task is also carried out, which is nothing but some older internal tasks which are recognized as a part of the output for the system (Fig. 18) [105]. Therefore, the RNN treats a part of its output as input for the next reoccurring step, and we could postulate that this is where the origin of the name Recurrent came from. The embedded algorithm selects the part of the output that is going to be used as an input. This internal state is also referred to as memory. This extra step as memory has proven

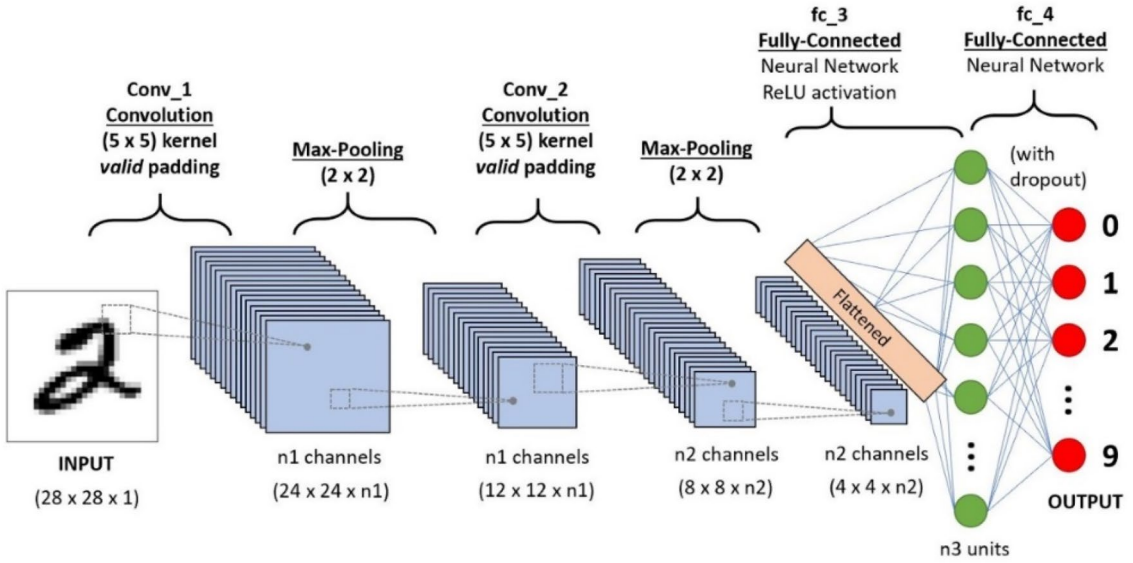

Fig. 17 A CNN sequence to classify handwritten digits [109]

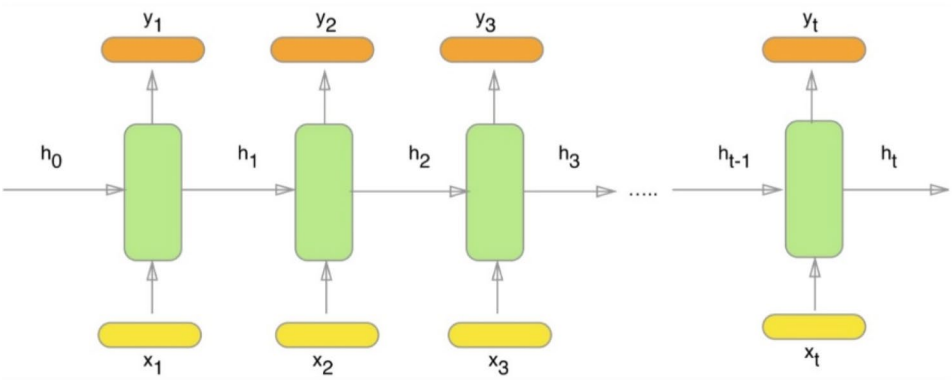

Fig. 18 A RNN, where x represent the input words from the text, y represent the predicted next words and h hold the info for the former input words [105]

to be very effective in chronological data, such as audio, text, time series, and allows to handle data and inputs of different sequence span. The long-short term memory (LSTM) and the gated recurrent unit (GRU) are some the famous algorithm applied and for accounting in for the inference on an output, only the network's output after the last phase of step is applied. Time series forecast has many applications in astro-and geophysics where many stimulating systems have unseen conditions that cannot be determined due to their novelty and need past observations to be determined [112].

1.2.6 Common Loss Functions in Machine Learning

During the recent decades, ML methods have achieved great feats and one of the most influential aspects of this achievement is the performance of their corresponding algorithms. As a result, one of the functions that keeps the algorithms in check is known as the loss function. In this section, we discuss some of the most pragmatic and known loss functions in ML. Basically, ML algorithms could be grouped in two sets, supervised and unsupervised. Within the supervised learning set, the most important tasks to be carried out are regression and classification tasks. In regression, a continuous value is under scope, but a discrete target value in classification tasks. In simple terms, the common objective of regression tasks is to learn about an arbitrary function f(x) that derives the minimum loss value related to all training data. Table 1 compares mathematical statement for regression and binary classification tasks [113].

Furthermore, it is noteworthy to bear in mind that each loss function results demand a different ML approach. For example, the famous support vector machine (SVM) algorithm[114] needs the hinge loss to operate, exponential loss [115] leads to the classic boosting method, and logistic loss function lead to logistic loss function. The logistic

Table 1 Regression task compared with classification in mathematical terms [113]

ML task	Regression task	Classification task
Mathematical expression	$min_{f(x)} \sum_{i=1}^{n} l\left(f(x_i) - y(i)\right) + R_\lambda(f)$	$min_{f(x)} \sum_{i=1}^{n} l\left(y_i f\left(x_i\right)\right) + R_\lambda(f)$
Components	f(x_i)-$y(_i)$ represent deviation of target value from the resultant value l represents the loss function R_λ, is a regularization term to hinder overfitting	$y_i f\left(x_i\right)$ represents devieation between the hyperplane and $f\left(x_i\right)$ l represents the loss function R_λ, is a regularization term to hinder overfitting y_i is the label of x_i

loss function is a classification-oriented loss function that is very prominent in ML problems and the mathematical expression for logistic regression goes as follows:

$$Log\ Loss = \sum_{(x,y)\in D} -ylog\left(y^{/}\right) - (1-y)\log\left(1-y^{/}\right) \quad (4)$$

where $(x, y) \in D$ is a set of data containing a great number of arbitrary labels, y is a label assigned to an example, and owning to the fact that logistic regression is a classification task, then y should be 1 or 0, and $y^{/}$ is the estimated value which could be any value between 0 and 1 [116]. Also, another important loss function that is very useful and worth mentioning is the cross-entropy loss function. This particular type of loss function is very useful for probability estimating of rare instances and stochastic environments and networks [117]. This powerful method has been nominated for applications such as importance sampling and optimal control [118] and probability density estimation [119].

2 Application of ML in AM

So far, the most commonly used ML method is supervised learning. This is due to its convenience in application and the fact that AM processes encompass several variables and complexities, which is a hurdle in exploiting full potential and advantages of ML. However, other ML methods are tested and implemented as well. For example, reports of using RL for toolpath optimization [120], unsupervised learning for anomaly detection [121], as well as finding trends in high dimensional data sets, constructing an analytical map of features detected in a manufacturing process, out of the inputs to the output responses for different problems, and finding patterns in dimensionally vast environments, are available [122]. ML models are classified as surrogate models and they are capable tools for studying non-linearities and could deliver good results with both simulated or experimental datasets [123]. Generally, ML modeling is often considered as surrogation modeling that could significantly speed up numerical simulation development [50]. Nonetheless, numerical methods such as finite element methods are quite common for the modeling of parameters such as heat source, feedstock, and melt pool dynamics [124–126]. Finite volume methods could also be implemented [127]. However, there are records of modifications on finite element analysis to best suit 3D printing process, such as quit/inactive method and other variations [128–130]. The most important aspect of ML is that it can be tuned by training data. In the case of AM, since it is a complex multi-physics process and a complex progression, there are many variables and parameters at play and therefore, considerable investments have been authorized to develop databases enriched with data informatics applicable within ML framework combined with legacy physics-based and Integrated Computational Materials Engineering (ICME). this combination had resulted in the development of tools to make predictive analysis regarding crack propagation due to fatigue and the nucleation, one example is known as DigitalClone® for AM which in a broader sense, is merely an ICME tool [131]. Consequently, this results in models with better process-structure property. Accurate grouping of each iteration of designed experiments improves and optimizes materials and designs [132]. ML models could only be efficient if it is fed with proper training data. Generally, the steps needed to be taken in an AM process could be divided into four major steps (Table 2) [133] and each step requires different considerations along its distinct ML method and algorithms. Considering the classifications presented in Fig. 19 [134], related common ML methods to the main process steps of AM are further described in Table 2.

2.1 AM Design

Typically, design for AM is a topic that could be divided into two segments; object design and the optimization of AM design. Also, owing to the novelty of the AM design, different materials and geometries need to be studied. Overall, matters related to topology optimization, design feature recommendation, shape deviations, material analysis for AM, and cost estimation fall within the scope of AM design. Therefore, studies regarding the aforementioned topics will

Table 2 Classification of main steps in an AM process with related ML method and application in process steps of AM [133]

Specified AM step	Common applied ML methods	AM applications in the related process
AM design	Hierarchical clustering, support vector machine, neural networks, lasso regression, elastic net regression, genetic algorithm, Feed-forward NN with backpropagation, Bayesian inference, random forest network	Design feature recommendation, part mass, support material and build-time prediction, cost estimation, topology, geometry compensation to counter thermal shrinkage and deformation, shape deviation
AM process and performance optimization	Back propagation (BP) NN, LS-SVM, genetic algorithm, self-organizing maps, Gaussian process regression BPNN, kriging, polynomial regression, genetic programming	Build precision perdition, melt pool depth and height, powder spreading prediction, melt pool width prediction, material toughness optimization, porosity prediction, wear strength prediction, part density prediction
In situ process control and monitoring	Bayesian–Dirichlet process, evidence theory, NN, Naïve Bayes clustering, SVM, quadratic discriminant analysis, support vector data description, probabilistic graph-based deep belief networks, spectral CNN, k-nearest neighbors (k-NN), feed forward NN, Bag-of-key points (words), Kmeans unsupervised clustering	Porosity detection, quality of fusion and defect detection, anomaly detection and classification, melt pool features and spatter detection, defect detection and classification with acoustic emissions, fault detection from multi-sensor data, quality monitoring using heterogeneous sensors in FDM, defect detection for laser powder bed fusion (LPBF) using in-situ images coupled with ex-situ CT scans
Testing and validation	Sparse representation, KNN, NN, naïve Bayes SVM, decision tree, augmented layer-wise spatial log Gaussian cox process	Classification of dimensional variation from laser scanned 3D point cloud data, defect detection (porosity)

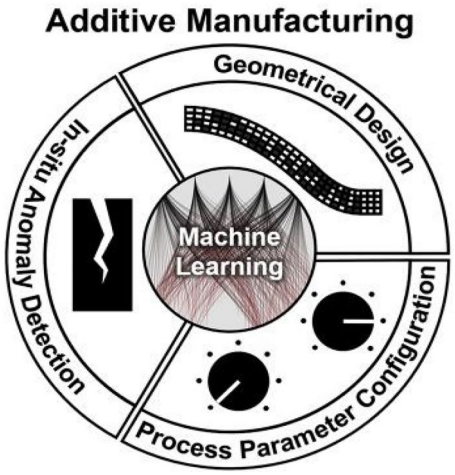

Fig. 19 Main process steps in AM [134]

be discussed in this section. The shape and dimensions of any desired part are among the initial phases that must be measured and considered. How efficiently and optimally the geometry of a shape is designed could go a long way and has major influences on price and even environmental pollution. An example of the importance of an optimal shape design is predominant in aeronautics, where reducing the volume of the material while still maintaining the quality and reliability can result in less fuel consumption. This can result in cheaper flights, less pollution, and lighter overall aeronautics [135]. One of the capabilities of AM methods is creating complex geometries and designs with intricate lattice structures. Also, the mass distribution of material [136, 137] in a part is well controlled and engineered in an AM design process. This new frontier of design poses its own challenges, including overhung structures [138, 139].

2.1.1 Topology Optimization

Topology optimization (TO) has started to gain attraction starting from the late 20'th century [140]. It became more popular as a reliable computational method for designing with less weight of parts being made in many fields including automotive and aerospace industries [135]. The main purpose of this step is to improve geometry to maximize load-bearing capacity while keeping stiffness and longevity at desired standard using as few materials as possible. TO methods also consider the optimization of natural frequency maximization and constraints and the minimization of constrictions. TO methods are applicable and have proven to be effective (Fig. 20) [141].

Nevertheless, TO faces many hurdles when paired with 3D printing. One of the main reasons stems from complex part shapes with overhung extensions, unique potential

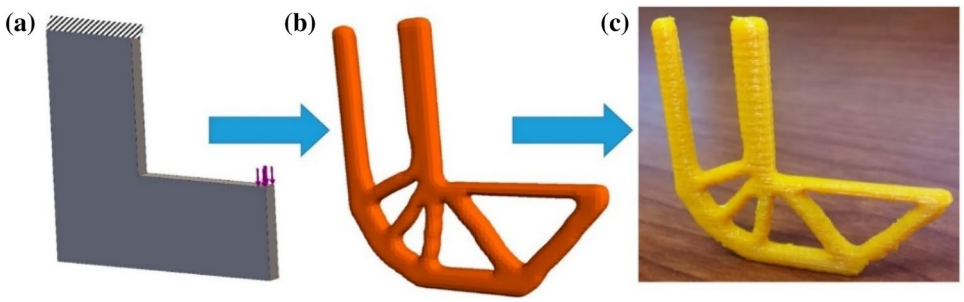

Fig. 20 **a** Basic structural forms of problem, **b** TO executed on the part, **c** 3D printed object [141]

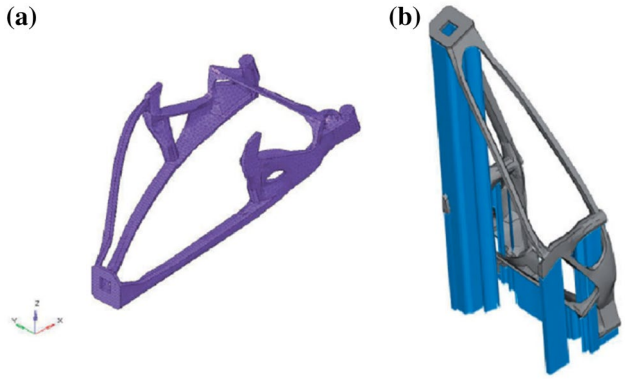

Fig. 21 **a** An additively manufactured part, **b** The support structure holding the shape upright, shown in blue [142]. (Color figure online)

sections of each product with different geometries and cross-section areas and angles exceeding their threshold vertical to printing bed. Depending on the type of material considered to be applied in printing process and the geometrical shape of part as well as its actual functionality, support structures are selected and used (Fig. 21) [142].

However, the removal of support structure is an extra effort; that is why although AM and TO are theoretically compatible, most TO considerations end up slightly challenging when a part is 3D printed [143, 144]. Thus, designing the shape to eliminate the need for support structure will result in a non-optimal shape. Therefore, a balance between the application of support structure while decreasing its significance in designing is a favorable tactic. Figure 22 [145] is an attempt to achieve such a goal by conducting analysis on the assemblage and the prediction made by ML on strength and toughness. Overall, the premise is to introduce the angles that are overhung, regarded as a penalty term, which could be considered as constraints in the design space. Also, linear regression can be applied to all voids in solid interfaces to detect the areas which need support structure. It needs to be mentioned that self-supporting designs mostly hinder the design from being practical. One commonly used approach to tackle this issue is assigning a soft penalty label to the amount of effort required to remove support structure to the design objective of choice with small controllable coefficients. The proposed method is to start solving in an unconstrained design space followed by further reorganization of the solution iteratively to minimize the so-called soft penalties with respect to design objective [134].

One of the capabilities of TO in AM designs is the ability to optimize heat and fluid transfer via TO methods. Optimizations could also be implemented to generate more enhanced heat sink designs [147]. AM has improved the

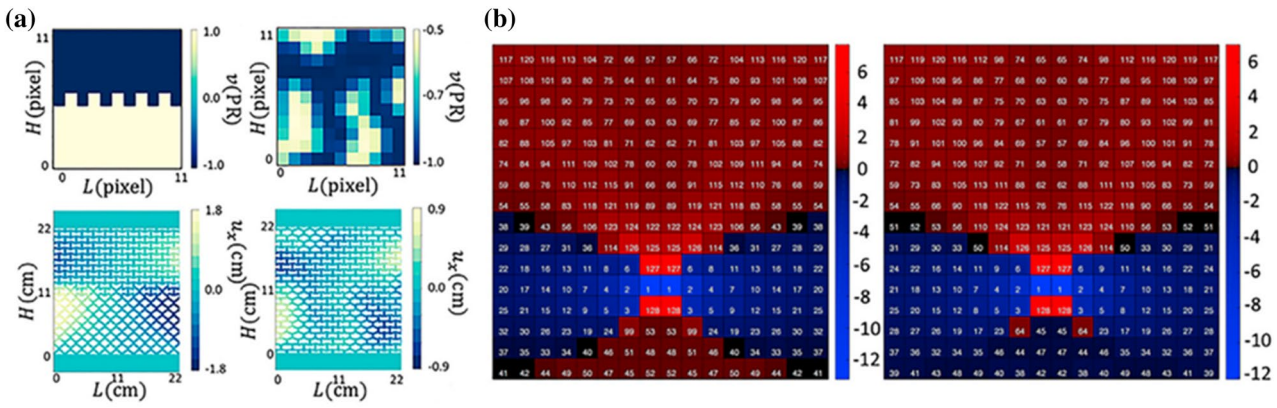

Fig. 22 **A** A sample DM and voxels representing varied domain assemblages [146], **B** Design manufacturing sensitivity analysis accomplished by linearly built models forecasting strength (right) and toughness (left) [145]

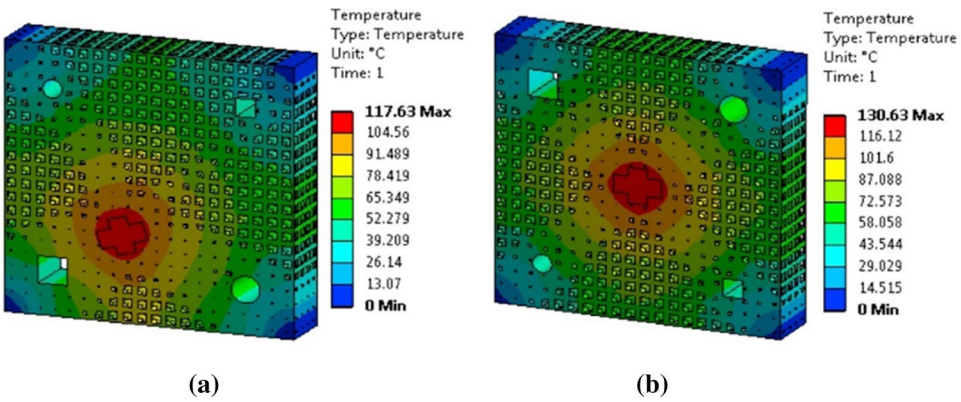

Fig. 23 Complete scale recreation for the design made by **a** simulated design and **b** fixed design [148]

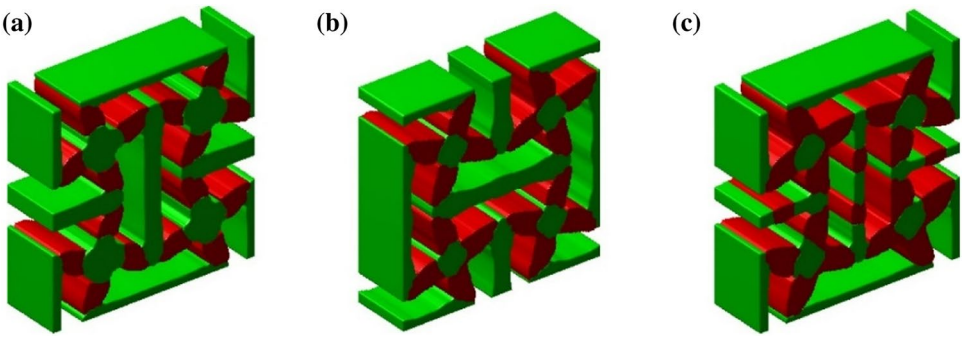

Fig. 24 Negative Poisson's ratio metamaterial designs with different volumetric ratios: **a** 20% for soft material and 40% for hard materials, green parts indicate hard materials and red parts present soft materials; **b** 35% green material and 25% red material; **c** 30% both hard and soft materials [149]

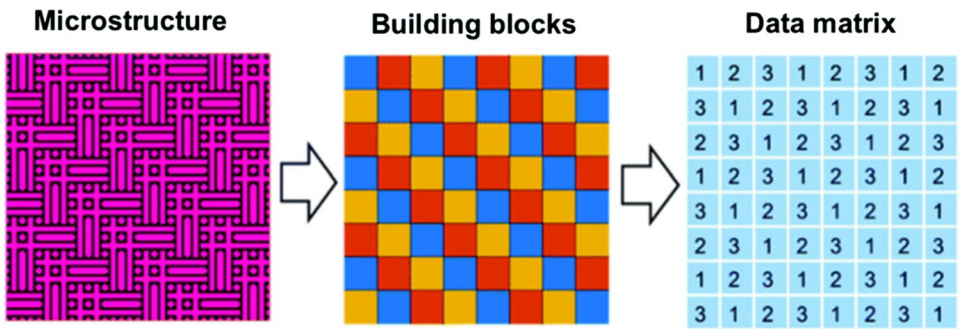

Fig. 25 Design of an AM product processed and fed to a ML model, each colored unit cell indicates complex assemblages of microstructures, giving each cell a number for the identification of each cell [155]

distribution of diverse lattice assemblies in designs (Fig. 23) [148]. Also, because of design freedom, the ability to include multiple materials in a part is practical and practiced today (Fig. 24) [149].

Shape and size optimization should also considered in TO [150–154]. Design and shape specifications related to each cell or voxel in each design could often be trained via ML methods by programming different material voxels as different features related to their assigned numbers (Fig. 25) [155].

In a case when buckling due to enforcing maximum load to a desired area is likely to happen, a particle swarm optimization (PSO) method was used in order to ensure shape optimization. The process could be stated in the following general form:

$$\text{Minimization of (X)} = \text{F(X)} = \frac{1}{Buckling} = \frac{Applied\ load}{Buckling}$$
$$\text{Subjected to } a_j \le X_j \le b_j \ \text{j} = 1, 2, \ \text{n} \tag{5}$$

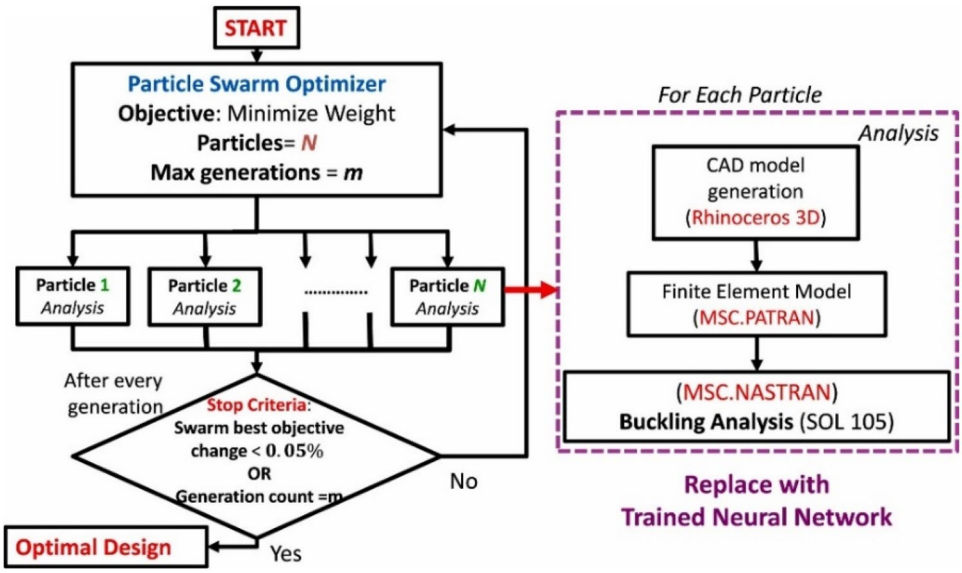

Fig. 26 Shape optimization via swarm particle optimization coupled with a trained DL model [156]

where function F(X) is the objective to be minimized, and by optimization of variable X and the lower and upper bounds enforced to the variable are set as a_j and b_j In general, PSO is regarded as a gradient-free optimization technique. A definite number of randomly chosen particles, also stated as designs, are introduced over a specified design domain so that each and every particle or design are processed based on the initial objective function. Upgrading is perceptible in the form of their social and individual variances, meaning alterations they receive as a particle or in a batch compared to pre-upgrading state. Depending on the best global value of each particle in the swarm and individual initial optimal value of interest. In this instance of the application of this optimization (Fig. 26) [156], shape X and shape design variables were successfully optimized via PSO [156]. Further details were also provided in a study by Singh et al. [157]. The right side of Fig. 15 illustrates a feature knows as Rhino. Python was used to assess the buckling load applied to the stiffened panel-shaped part under load for each particle of the optimized method. Furthermore, this feature could be used for the creation of panel geometry. When geometry is generated with a different set of parameters optimized by PSO, in order to automate the generation of geometry while PSO is being operated. Then, the prepared geometry is transferred to be processed in MSC Nastran software environment for buckling analysis [156, 158].

In other attempts to optimize TO, Sosnovik et al. [159] tried using CNN which resulted in significant positive results and overall acceleration in the process. The overall achievements were as following,

- After just a few numbers of iterations done by the algorithm known as penalization of solid isotropic materials (SIMP), the proper input volume was delivered.
- The SIMP algorithm delivered the output volume only after 100 iterations.

In the accounts of application of SIMP algorithm shown by Sosnovik et al. [159]. it was revealed that the computational effort was significantly reduced while results were ranging from 92% accuracy from 5 iterations to 99.2% after 80 iterations. Also, Harish et al. developed an algorithmic DL/ML based approach for TO for getting the optimized structure with a given condition of the structure and for that purpose, they trained a CNN model variant of DL with a decoder, encoder structure with decent results [160]. In another research, which was concerning the application of 3D cantilever beams, Banga et al. [103] reached the binary accuracy of 96%. This indicated that with significantly less time TO could be done with the same quality. Furthermore, higher resolution TO was used effectively in the practice phase therefore, leading to better quality outputs and finally, higher complexity was achieved leading to optimized structure without supports [161].

2.1.2 Design Feature Recommendation

Design feature recommendation is the very foundation of a successful AM process, as it is indicative of how efficient the print process would be in terms of cost, preciseness, amount of post-processing and usage of support structure [122]. ML approaches also have the history of being used to determine how complex or simple the process of manufacturing of a computer-aided design (CAD) model would be, based on its features, such as multi-scale clustering and heat kernel signature methods. This capability is very helpful in order to prevent futile designs early on and also in setting the proper build orientation. CNN, has shown

significantly better accuracy in part mass estimation and build time forecasting than conventional linear regression modeling approaches [162, 163]. In a work done by Yao et al. [164], a method of hybrid approach was presented in order to come up with the best design features, using unsupervised and supervised techniques as the form of Hierarchical clustering (HC) and SVM, in a way that initial AM design features and targeted parts and components are coded and thereafter, HC method is applied on the coded design features resulting in an initial plotting, then the SVM classification is applied to iteratively optimize the plotting made by HC. the byproduct of the hybrid ML approach contains the recommended design features. In order to proceed with the proposed hybrid ML approach, four general steps were considered. These general steps contain a route to fully use unsupervised learning clustering and classification made by supervised learning. The first step is to code the design features and targeted components to be stored and classified in a referable dataset. Then, the second step would be to execute HC to all design features and targeted components within the database, resulting in plotting of hierarchical tree structure. The third step is to commence SVM classification by training on real industrial data, and in the fourth step, the classifier that was trained in the previous step is employed to form an algorithm capable of identification of recommended design features via cutting and selection of branches formed on the hierarchical tree shaped in the second step. The fundamental step toward the proposed approach is the multi-categorial coding which grants better intuition as to how the HC and SVM would function. The authors differentiated 3 distinct categories for initial coding of target components and design features, the "loading'' category, "objectives'' category and "properties'' category. Moreover, these 3 categories are found to be co-related, such that either a target component or an AM design feature which is under a static tension load might be having resisting linear distortion as design objective, while Young's modulus and tensile strength are the important properties. The coding considerations are shown in Table 3 and the complete mapping of the aforementioned 4 steps is depicted in the Fig. 27 [164].

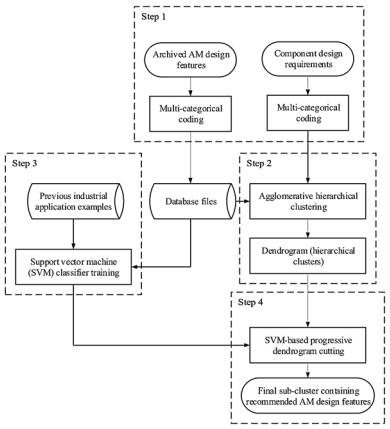

Fig. 27 Process steps to hybrid ML design [164]

2.1.3 Geometric and Shape Deviation

There exist many aspects leading to geometry and shape deviation. In the process of converting the CAD model to standard input files, numerous inaccuracies and geometric deviations occur. Also, errors of the machine would result in shape and geometric inaccuracies and shape shrinkage. For getting into more specifications of this issue, Huang et al. [165] achieved optimal shape dimensions for 3D printed objects of polygon and cylindrical shapes, a new statistical

Table 3 Categories in functionality-centric design, coding based on expert knowledge of experienced operators and their archived design features which are coded and could be extracted. matching each archived design feature to target components is the basis of design feature recommendation [164]

Initial coding step	Type of coding	Type of input	Type of classification in database
Loadings	Binary pattern, the digit "1" indicates that the corresponding loading will be applied on the design feature or the target component, digit "0" indicates that the corresponding loading is non-existent	Physical inputs, including mechanical loadings, fluid and heat flux and electromagnetic loadings	As a vector $\mathrm{L} = \left[l_1, l_2, \ldots, l_3\right]^T \left(l_i \in \{0, 1\}\right)$
Objectives	Coded with numerical ratings from 1 to 3, indicating levels of relevance	List of design purposes of AM design features and target components such as aesthetics, ergonomic factors, weight, instant assembly, etc.…	As a vector $\mathrm{O} = \left[o_1, o_2, \ldots, o_3\right]^T \left(o_i \in \{1, 2, 3\}\right)$
Properties	Coded with numerical ratings of importance	A list of key properties, including mechanical, chemical, thermal and electromagnetic properties	As a vector $\mathrm{P} = \left[p_1, p, \ldots, p_3\right]^T \left(p_i \in \{1, 2, 3\}\right)$

model was established and their model delivered promising results in shape prediction where it was capable of compensation and prediction of 75% of deviations of a dodecagon shape deviations based on statistical approaches. In another research, a deviation modeling method was suggested by Zhu et al. [166] for making accurate forecasting of the shape and geometric deviation trends in AM. For realizing this purpose, Bayesian inference was used. Based on the data from different shapes, the models perform and thus, more accurate tolerancing of AM parts would be achieved.

Furthermore, in a study by Ghadai et al. [167] DL is used to learn from 3D CAD models and make better suggestions on DFAM, without the need for additional shape information. The layer-wise stacking process in AM and the fact that materials undergo repeated thermal expansion and shrinkage causes some issues in preciseness of the shape and geometry, causing the influence of deviations to be existent inside each layer or in between each layer. Nonetheless, other factors such as errors due to geometrical approximation, mostly because of converting the 3D CAD model to the standard file input, should be accounted for. In The approach by Huang et al. [165], the mathematical expression to address deviations is in 2D domain, due to negligible width of each layer is presumed. thus, resulting in an expression based on the original objective dimensions comparing with the shape that was attained after the process. In a 2D layer, the axes in which deviations could occur, based on the cartesian coordinate system are in the X, Y and the rotational expression with respect to the original shape. These expressions are used to make transformational expressions. However, the aforementioned expression could only account for overall in-plain shape deviations and not the more complex error sources such as location-dependent surfaces along the shape boundary. The authors assume that such complexity, which could not be expressed by parametric function, could be related to the uniqueness of the shape. As a result, the need to apply a data-driven model comes from the complexity of this multifaceted error source, and the multi-task Gaussian process (GP) was chosen to learn, characterize, and predict the deviations. GP is a supervised learning ML technique. This method is known for its probabilistic predictions and its capabilities in real-life applications. The more the number of training points increases, complexity in computations gets updated, and predictions improve [168]. Supposing that our objective is to model the deviations of M number shapes, formula (6) that expresses GP is as follows;

$$y_l(\theta) = f_l\left(\theta;\psi_l\right) + g_l(\theta) \tag{6}$$

where M is the index of the shape, l = 1, 2, 3…M. $f_l\left(\theta;\psi_l\right)$ = the parametric function for expressing systematic deviation of shape l. where $g_l(\theta)$ is a zero-mean and GP models the local variation of shape 'l'. Eventually, random noise is learned while all M shapes are accessed via multi-task learning algorithm.

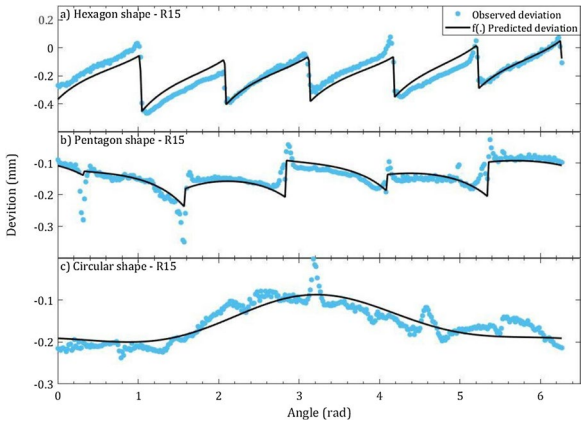

Fig. 28 Accuracy of the prediction in deviation forecasting compared to real observed deviation [166]

Overall, the relationship between occurring errors to shape and geometry deviations are far too non-linear to be modeled empirically from a set of samples. Therefore using data-driven ML techniques has proven to be a proper choice, as the results are shown in Fig. 28 [166].

2.1.4 Materials in AM

In AM, specific manufacturing techniques are used for each type of material. Material types in AM could vary depending on the material scale (at mesoscale, macro-scale, or nano), type of material, which could be metallic, ceramic, polymer. Also, process parameters for printing the material are very influential when it comes to material quality. One of the reasons which makes AM unique compared to previous manufacturing methods like subtractive manufacturing is the fact that material inheritance is kept intact and unaffected. For example, in machining, only a block of material is subtracted and shaped to the manufacturer's desire. Therefore, this is only physical manipulation of the shape of the aforesaid block that is happening. On the other hand, in AM, the material is being transformed by a chemical or thermal process all the while geometry of the manufactured part is being established. The very materials implemented, such as powder or polymers, are quite influential. However, process parameters, such as printing speed, printing scalability and printing resolution, also play a significant role in material characteristics [169, 170]. Owning to this new niche in material manufacturing in AM, a large number of variables for material analytics are generated, and storing, clustering, and gaining insight from such vast amount of data is a cumbersome task. For example, in a case of powder chemistry of a certain metal or alloy, such as the case of Ti-6Al-4 V alloy powder, the chemistry could vary drastically because of the

impurities like oxygen, carbon, iron, or nitrogen. This variation can affect the tensile properties, which could alter the configuration of each set [171]. As a result, ML methods can be used for better material composition and the usage of sensors such as pyrometers or acoustic sensors [172, 173]. In general, this study overlaps with the material science aspect, so it would be helpful to mention the most prominent ML method used in material science (Table 4).

In a case study in bone tissue engineering, conducted by Guo et al. [174], it was shown that the microstructure of the required porous geometry could be further improved by the control which would bring about possibilities such as precision in intricate micro and macro porous parts for printing bone tissues. These can be realized only via 3D printing (Fig. 29). They studied a case of printing Ti6Al4V titanium alloy and concluded that ML method could immensely aid in the following aspects of bone tissue printing:

- Gradually updating the process-microstructure performance relationship based on repeated training
- Providing guidance for process parameter selection for a higher quality of printed material
- Minimizing the unwanted porosity caused by measly hole instability
- Reduction in fusion defects due to inadequate overlapping of adjacent scanning routes

In another attempt to construct a Bayesian framework based on GPR and Bayesian optimization approach, unification of nanocomposite design and part construction was done by Liu et al. [175]. The researchers combined the decent surface quality forecast and process parameter optimization to gain improved surface roughness. It was reported that GPR performed better than other targeted benchmark methods in terms of convergence with the highest coefficient of determination (R^2) value ($R^2 = 0.84$), and the model accuracy with the smallest mean absolute percentage error value (MAPE = 0.13) and root mean square error value (RMSE = 2.66). It can be stated that the type of material and complexity of the respected material is a challenge. To tackle this issue, an unsupervised method was suggested to reduce the amount of vast data generated from metallic material for the AM process [176].

2.1.5 Product Cost Estimation

In general, to determine whether a product development would result in financial gains, the product should neither be overpriced nor undervalued. The determination of such quality of products for manufacturing is product cost estimation related to many factors, which will be addressed in the following section. In a paper by Busachi et al. [177], three general approaches for product cost estimation were distinguished, "Intuitive Techniques", "Analytical Techniques" and "Analogical Techniques". In intuitive techniques the past successful designs are used as data for applying to new designs. In analytical approach, the cost of each product is estimated based on the features that the product is set to have, namely complexity of design, mass of the object or certain objective standards which the product should have. This approach has little flexibility and is better suited for the final stages of the design and the analogical techniques. In this technique, the most indicative factor is the amount of data, as the robustness of the historical data set indicates the accuracy of the analysis. Regression techniques are used to predict the cost of the novel designs. Well-structured mathematical relationships and background are very deterministic in this approach, and the weight each variable might have in the overall cost is derived. ANN modeling has proven to be very effective in cost estimation even without a comprehensive dataset. It can investigate in non-linear environments, and they are insightful tools for the early stages of the process [178, 179]. At large, ML algorithms are used for monitoring and system diagnosis and machine condition monitoring. In the coming years, owing to the rise in computational power and advancement in hardware, ML approaches have grown even faster as DL approaches are capable of making calculations on millions of parameters [180]. Methods such as least square SVM were used by Deng and Yeh et al. [181] to predict the production cost. Least squares support vector machines for the airframe structures manufacturing cost estimation, and K-nearest neighbors and meteorological parameter section for assembly of cost features in the form of vectors [182] are also used. In a suggested framework proposed by Chan et al. [183], maintaining consistent cost estimation is directly linked to processing the related feature extraction form the proposed model to the analysis of dynamical clustering. Also, in the proposed framework, the extracted features are considered to be the main factor in the amount of processing time and complexity of the design. For instance, in injection molding, features are size and number of cavities, venting system, surface quality, and the overall dimension of the objective part the material of choice and etc. However, in this approach, the method of choice is FDM (FFF). From a stereolithography format file (STL). Features that determine the cost could be obtained, such as print path length, printing duration, the volume and number of prints made and so on. The aforementioned features extracted from the 3D model are crucial in the overall print cost and are assembled in the form of feature vectors. The process of cost estimation is depicted in Fig. 30. The next phase is to process the extracted vectors and coding. the information will be in a G-code format, regardless of being geometry-related or non-geometric. The generated data will be stored in the Cassandra storage system. Afterward, in order to increase the preciseness of the cost forecasting, the

Table 4 Prominent ML method used in material science [69]

Class of algorithm	Cases	Bids	Advantages	Shortcomings
Weighted neighborhood clustering	Decision trees, random forest, k-nearest neighbor	Regression, classification, clustering and similarity	Robust against uncertainty in data sets	Vulnerable to classification bias toward descriptors with more data
Nonlinear dimensionality reduction	t-Distributed stochastic neighbor embedding, kernel ridge regression, multidimensional metric scaling	Experimental design, model dimensionality reduction, model or experimental input/output visualization, descriptor analysis, regression	Algorithms strong against nonlinear input/output relations and can aid visualize resemblance in vast dimensional relationships	Interpretation the reasons of the relationship found via the algorithms is difficult. Global relationships can also be vanished when nonlinear dimensionality reduction outcomes are probable onto lower-dimensional spaces
Search algorithms	Genetic algorithms, evolutionary algorithms	Topology and model optimization, alloy design	Search algorithms are innate for material characteristics that can be described geometrically, finding local maxima of quality in multidimensional design spaces	Success of such algorithms is highly reliant on choice and mutation conditions
Neural networks and computer vision	ANN, CNN, general adversarial networks	Process control and feedback control, regression and classification analysis, feature detection in imagery, atomic potential simulation and transfer learning	Networks have successfully modeled processing and image data, and abundance in studying ANN algorithms	Demand for large datasets for better convergence and results even tough transfer learning could be used for small datasets
Linear dimensionality reduction	PCA, SVR, nonnegative matrix factorization (NMF)	Experimental design, model dimensionality reduction, model or experimental input/output visualization, descriptor analysis, regression	Algorithm capable of producing orthogonal basis sets for training data space reproduction, fast regression analysis	Bias susceptibility in the case of different descriptors is scaled in a different manner, the relationship under analysis cannot be non-linear

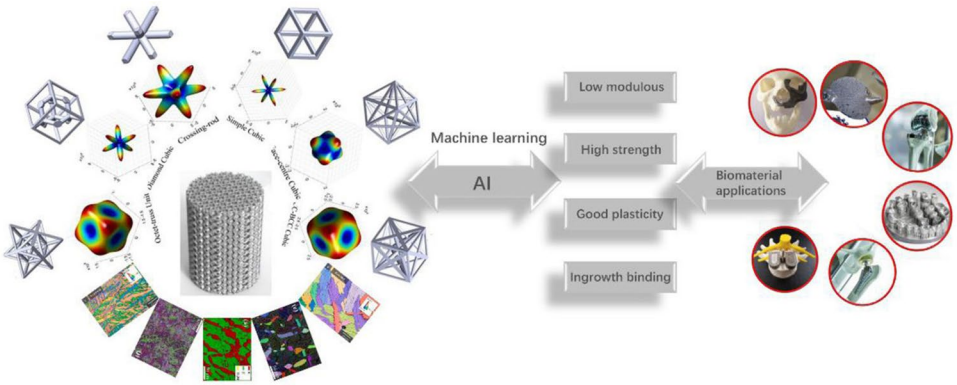

Fig. 29 A wide-ranging deception of paring ML in printing bio-engineered materials [174]

data are first grouped based on their similarities, and regression models are embedded within each cluster that is constructed dynamically as a method to reduce variance. while prediction is ongoing, a cluster which shares the most similarity with the new generated model is imported. afterwards, two methods of regression known as least absolute square shrinkage (LASSO) and elastic net (EN). These regression models work well in high dimensional spaces while input variables are highly dependent upon one another. They show high selectivity towards correlations between inputs and outlier data. This suggested forecasting method to determine production cost estimation, collects a comprehensive data set for more accurate results to make cost predictions regarding a new task based on the history of previous tasks of similar merit. it is elucidated that G-codes generated could be a means to make cost estimation while geometry features could be extracted from the G-codes. geometrical features, non-geometrical features such as temperature settings could also be accessed, however, other features such as labor cost, print machine selection and type are decided by technicians [183].

2.2 Process Parameters and Performance Optimization

Different ML models have different sets of parameters that rule the process of printing. After tuning the geometrical parameters, the next step is the selection of suitable process parameters. Different ML models have different sets of parameters that rule the process of printing. Process parameter optimization is studied in cases where either new materials or a novel approach is considered to be implemented [122]. Determining process parameters has a very big impact on AM products [184]. The relationship between process parameters are highly complicated, none-linear, vast dimensional space and even non-convex at times [185]. In an attempt by Rosen et al. a modeling framework for process-structure properties has been presented, shown in Fig. 31 [186]. In the following section, extensive case studies of process parameters and performance optimization-based application of aforesaid optimization approach on specific AM method is discussed in details.

2.2.1 Implementation of Genetic Algorithm for Process Parameter Optimization

Typically, FDM consists of polymers extruded through the nozzle layer after layer. In this method, parameters such as layer height, printing speed and material flow from the cartridge cartilage are critical and choosing proper parameters with correct values could tremendously optimize the AM design (Fig. 32) [187]. In Table 5, proper parameter selection in FDM and applied ML approach is shown. in laser fused AM methods which are somewhat similar to FDM in terms of being layer-based, parameters such as laser scanning strategy, laser power, and laser speed are pretty influential as is shown in Table 6. overall, It has been found that genetic algorithms (GA) [188] used in ML modeling can influence the quality of 3D printed parts. Through a criterion known as fitness function, the first set of parameters also known as parent generation set is accessed. However, if the target is not reached, the process keeps repeating until the optimal results are generated and the objective is fulfilled. An instance of the implementation of GA is with the design of experiments (DOE) [189]. The objective is to find the optimal combination of process parameters that could potentially minimize the surface roughness and porosity of the manufactured objects. In this case, the parts were created by FDM method, the material used in the process was acrylonitrile butadiene styrene (ABS) and the process parameters of the study were slice thickness, road width, nozzle temperature, and air gap. At the beginning of the process, DOE operation was set to achieve the porosity the roughness of surface from a number of combinations of abovementioned parameters. Then, based on the obtained results and in order to get fitness function, a methodology known as response surface method (RSM) was applied. This method is

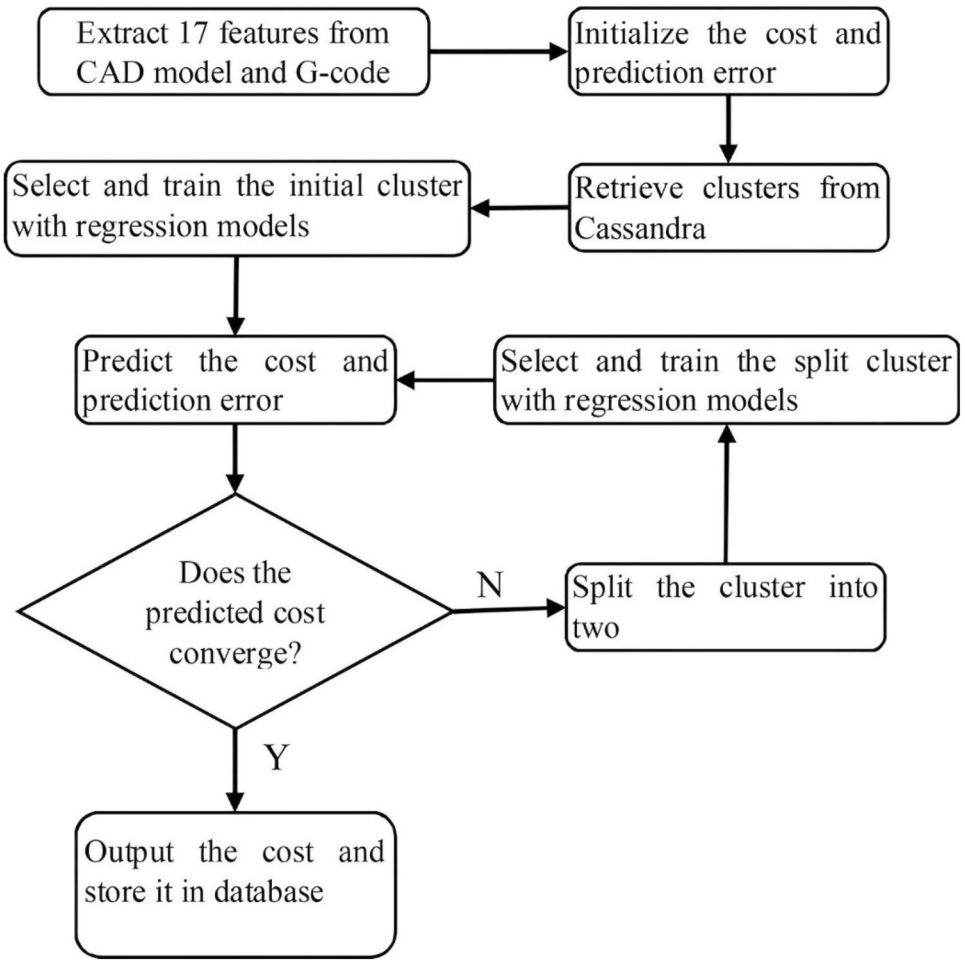

Fig. 30 Process steps to proposed cost estimation approach [183]

basically a selection of statistical and mathematical technical approaches applied for both approximation and optimization of stochastic modelling in manufacturing [190] extracted as a second-degree polynomial equation of the set of process parameters. Then, GA was used to forecast the optimal process parameter sets. Finally, it was concluded that minimal surface roughness was obtained at the smallest determined slice thickness, road width and air gap with an intermediate nozzle temperature, which was consistent with both experimental and GA model[188].

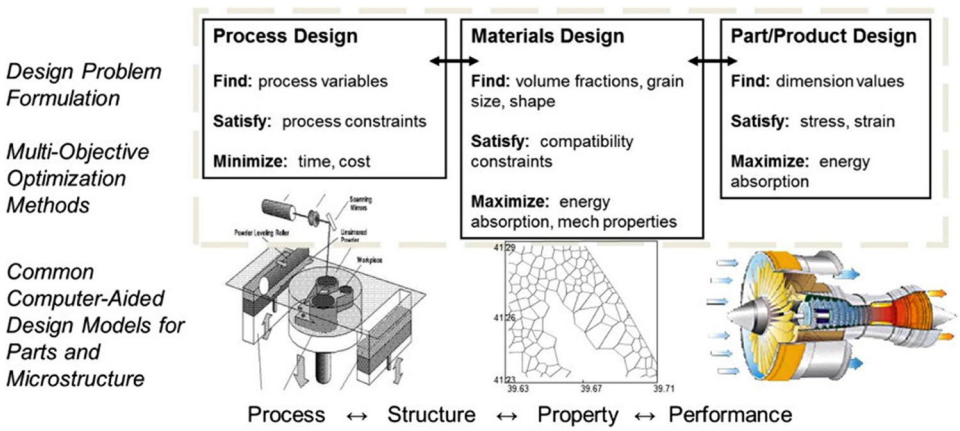

Fig. 31 Process structure property problem framework [186]

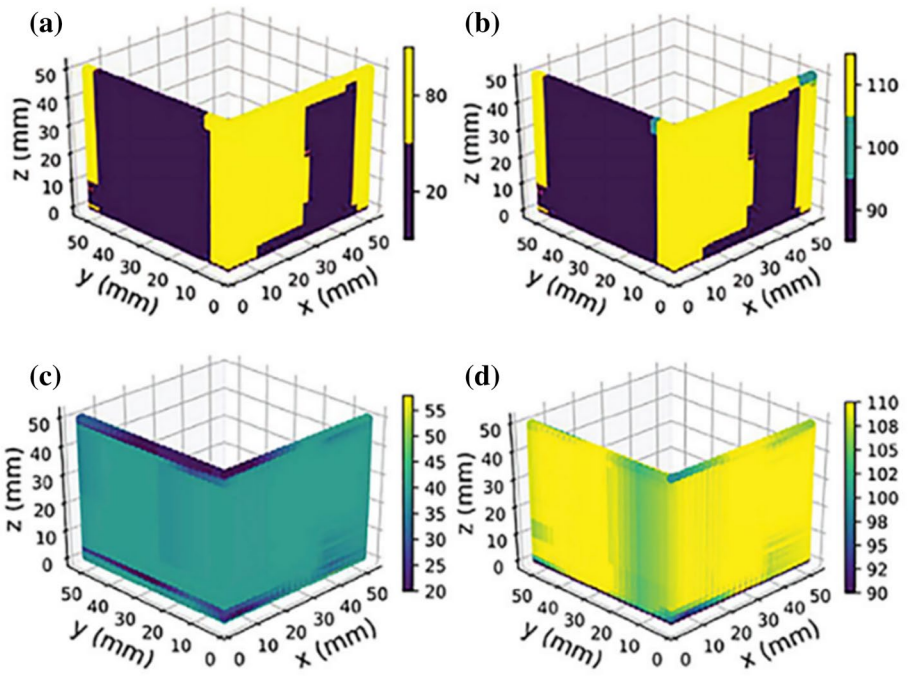

Fig. 32 Optimization of process parameters suited for thin walled applications **a** The original setting of printing speed, **b** The original setting of extrusion multiplier, **c** Printing speed with an optimized setting, and **d** Optimized settings for extrusion multiplier to preform according to optimized process parameters [187]

Table 5 Most indicative process parameters in FDM, based on the information extracted from numerous references, multi-layer perceptron (MLP) is the most prominent ML method implemented [191–197]

Material	ML method	Inputs	Outputs	Objective
Poly carbonate-ABS	MLP	Layer thickness, air gap, raster angle, build orientation, road width, number of contours	Creep and recoverable compliance	To optimize process parameters and improve viscoelastic responses
PLA	MLP	Print speed, cooling fan speed, print temperature	Printable bridge length	To predict maximal printable bridge length and minimize support waste
PC-ABS	MLP	Layer thickness, air gap, raster angle, build orientation, road width, No. of contours	Dynamic modulus of elasticity	To predict dynamic modulus of elasticity for load-carrying parts under dynamic and cyclic conditions
Polylactic acid	MLP	Temperature, layer thickness, raster angle	Tensile strength	To generate a mathematical model to predict tensile strength corresponding to three raster patterns
ABS	MLP	Layer thickness, orientation, raster angle, road width, air gap	Sliding wear value	To optimize parameters and improve wear resistance
ABS	MLP	Layer thickness, part orientation, raster angle, road width, air gap	Compressive strength	optimizing process parameters and to improve compressive strength
PC-ABS	ANN-GA	Extruder temperature, infill percentage, layer thickness	Part thickness, and production cost	To boost toughness and reduction in production cost

2.2.2 Implementation of ANN for Process Parameter Optimization

Setting the process parameters could be better performed by using ANN models (Fig. 33) [203]. In general, there are two levels of quality indication in ML models which are related to the main process parameters of interest. The first one is related to mechanical properties which is at macroscale level and the other scope of analysis is at mesoscale which is linked to melt pool geometries, relative density and pores. Furthermore, in order to better identify the process, ML is used to lay down mapping of processes which is a helpful visualization tool [202]. Figure 34 shows a few of such instances [201].

In a study on DED with Ti-6A1-4 V which is an alloy with remarkable strength, resistance corrosive agents and remarkable fracture toughness [204]. There exist reports regarding experiments on process parameters in SLM laser

Table 6 An example of process parameters and applied ML models in PBF method [198–202]

AM process	Materials	Inputs	ML methods	Outputs	Purposes
Selective laser melting (SLM)	SS316L	Laser power, scan speed, layer thickness, post-processing temperature, tensile properties	Adaptive-network-based fuzzy inference system	High cycle fatigue life	To predict high cycle fatigue life with 'process-based' and 'property-based' models
SLM	Bronze	Laser power, scan speed, hatch distance	Multi-layer perceptron (MLP)	Relative density, microhardness	To predict porosity and microhardness
SLM	SS316L	Laser power scan speed	Gaussian process-based (GP)	Melt pool depth	To construct a process map and predict melt pool depth
SLM	SS17-4 PH	Laser power scan speed	GP	Porosity	To model and predict porosity at any combination of process parameters from a small dataset
SLM	IN718	Part-orientation and part position fraction of recycled powder	Random forest (RF)	Porosity, median pore diameter and spacing	To connect the process parameters to pore formation
SLM	Ti-6Al-4 V	Spreader translation and rotation speed	MLP	Powder bed surface roughness, spread speed	To construct a spreading process map to optimize surface roughness and spreading efficiency for powder bed
Electron beam melting (EBM)	CoCr	Beam current, scan speed	Support vector machine (SVM)	Energy density	To construct a process map from a small dataset
EBM	–	Presence of core support, support density and angle	Decision trees, Bayes classifier	Classification of part quality	To investigate the influence of support structure parameters on part quality
Selective laser sintering (SLS)	PLA	Layer thickness, laser power, feed rate	MLP SVM	Open porosity	To predict open porosity
SLS	58 wt% HA + 42 wt% PA mixture	Layer thickness, laser power, scan speed	Ensemble-based multi-gene genetic programming	Open porosity	To achieve desired open porosity values by regulating process parameters

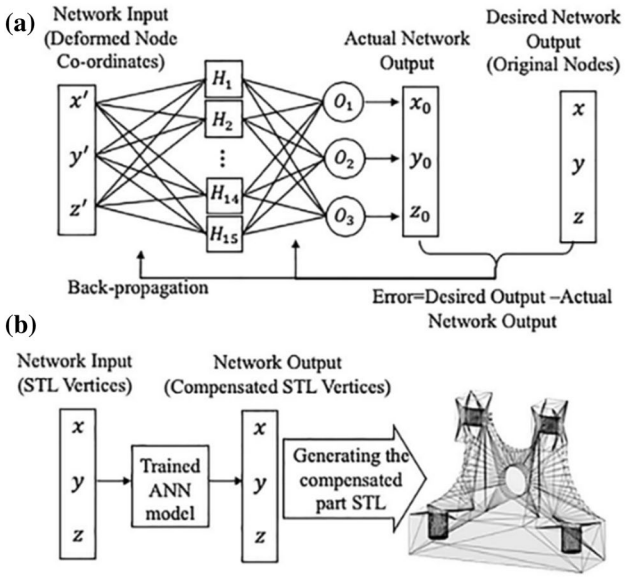

Fig. 33 **A** Illustration of ANN model trained based on geometric rewards received based on error elimination [203], **B** The stereolithography method generated via a proficient ANN model [203]

PBF and PBF technologies that are indicative of aforementioned occurrences [205–208]. Conversely, there are not many reports regarding alterations in part quality related to process parameters. It is a daunting task to select the proper process parameters while refraining from the costs experimentations could result to. thus, researchers are resorting to statistical approaches, namely Taguohi design approaches to design experiments for AM methods [209, 210]. Today, ML methods are used in many aspects of AM, such as melt pool signature, and overall defect generation. The primary objective of these methods is to reach a state capable of mutually corelating dependent factors at parameters and the overall generalization of complex problems between parameters to function as a map for conducting real experiments [211]. In this case study, for the purpose of mapping the indicted input into objective output, an ANN model has been developed. The major inputs of study are laser power, scan speed, rate of powder feed and layer thickness, and the density of the alloy material and the build height are designated to be the outputs. Based on trial and error and model tuning, minimized prediction error is understood and thereafter, the number of neurons and hidden layers are better determined. The general depiction of the model implemented in this study is shown in Fig. 35.

The steps to completion of ANN model begins with synchronizing the empirical values with an ANN model, resulting in minimum amount of error in the developed model [212]. For training stage, sigmoid back propagation algorithm was activated. The main objectives to be reached are the least amount of mean square error and average prediction error, that are expressed in (7) and (8) formulas,

$$MSE = \frac{1}{p}\sum_{p}\sum_{i}\left(t_{ip} - o_{ip}\right)^2 \tag{7}$$

$$E_{tr}(y) = \frac{1}{N}\sum_{i=1}^{N}\left|T_i(y) - o_j(y)\right| \tag{8}$$

where $E_{tr}(y)$ is the mean error in output prediction (related to parameter y), N is the number of data sets, $T_i(y)$ is targeted output and $o_j(y)$ is processed output. In the case of the ongoing ANN model, pattern and variations in occurrences of errors and defects dictate the number of neurons and hidden layers. The model is set to have 2 hidden layers with 2–15 neurons in hidden layers. Figure 36 shows the value of mean square error and mean error in the output, on par with variations of these values while using one and two hidden layers. Furthermore, it was observed that by increasing the number of hidden neurons, mean error value was decreased. Ultimately, the 15-neuron ANN structure delivered the lowest overall error. The next step in the development of the model is to optimize the number of instances for iterations. Based on the results depicted in Fig. 41c, the initial number of iterations started from a range of 500–25,000. Nonetheless, when the number of iterations reached 18,000, the error values (MSE = 0.000001 and E_{tr} = 0.001124) were fixed when model was trained again. ANN hyperparameters such as momentum (α) and learning rate (η) both ranged from 0.1 to 0.9 and when momentum was set at 0.9, the minimum error value was reached (Fig. 35). An observation made at a momentum of 0.6 was a drastic shooting of error value which was a sign of overfitting. Similarly, in a case reported by Reddy et al. [212], it was shown that high learning rate could also lead to overfitting. At last, an ANN model of two hidden layers, 15 neurons, trained for 18,000 iterations with hyperparameters of 0.9 for momentum and learning rate of 0.7 was recognized as the optimal model for the estimation of process parameters related to DED AM.

In order to investigate the effects of process parameters, especially build height and density, as indicated in Figs. 37a and b, the areas shown in red indicate poor densities and unbalanced build heights, which are in proportion to scan speed and power. However, some process parameters such as thickness of layer (0.3 mm) and the fed rate of powder (2 g/min) were kept constant. Overall, it was construed that depending on the type of material and fabricability, in the case of specific alloy which is used in particular, it is most suitable to keep the power for deposition at a high output while keeping the scan speed at a low pace for avoiding lack of fusion defects [204]. Generally, scan speed and

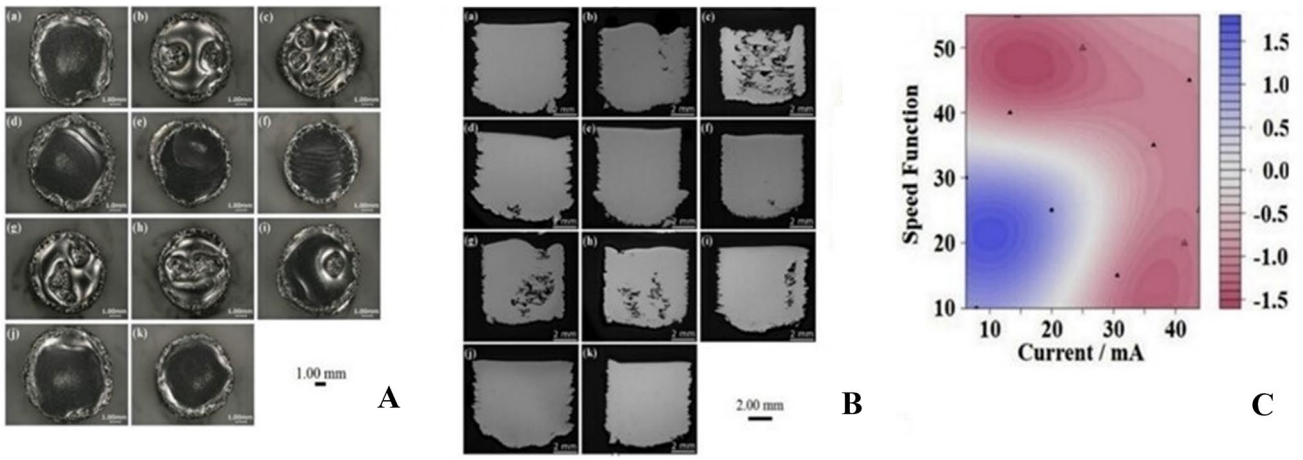

Fig. 34 **A** Support vector machines used for the prediction of macro scale properties of electron beam melting built products, **B** The cross-section views of defects, **C** Pores in the form of black spaces and the optimization process mapping on the right [201]

temperature gradient dictate laser power density, which consequently alters the build height of deposited material. Based on the results of this study, the best combination values of process parameters are for laser power and scan speed to be in the ranges of 320–400 w and 0.75–1.2 m/min, respectively. Other combinations that could lead to relatively optimal results are illustrated within the bounds of green area in Fig. 37. Additionally, high feed rate results in low layer thickness and conversely low feed rate and low layer thickness leads to increase in build height, whereas combination of low feeding rate /layer thickness will transfer the heat to the previous layers and reheats them. Also, regardless of layer thickness of as high as 0.3 mm, build height decreases owning to its insufficient energy expansion, further hindering the precision of the design. The green region also shows the best build height values. In summary, ANN model is evolved such that it can find proper density and build height for Ti-6AI-4v alloy, by DED and AM methods and the suggested set of parameters led to high quality printed products [211].

In a research conducted by lang et al. [213], a method called multi-material jetting (MMJ) was evaluated for a multi-stage ceramic material application and related issues to shape deviations, unwanted mechanical anisotropy, and residual stresses were discussed. The authors deduce that the reason for this shortcoming, aside from the fact that AM is still an evolving field, is due to the tendency to opt for empirical data gathering, which comes at a high cost and is generally slow to build up. Therefore, since the parts are printed drop by drop, there is a good possibility to parameterize each droplet being desposited. Some defining parameters for each drop are volume, height of droplet discharge to form specific geometry, and the diameter of droplet. The main objective is to assemble a data managing system to keep a record of the most influential data. By keeping track of manufacturing components and material behavior. It is possible to assign the most infeluntial data to their unique identifiers in the form of a parameter within the database. By implementing a DNN model, an object recognition for droplets is defined. By means of proper training on multiple training sets and image recognition algorithms, the automation of drop exertion was realized. What affects the model's efficiency is that each drop is given its own identifier and related traceability based on the defined target value. The

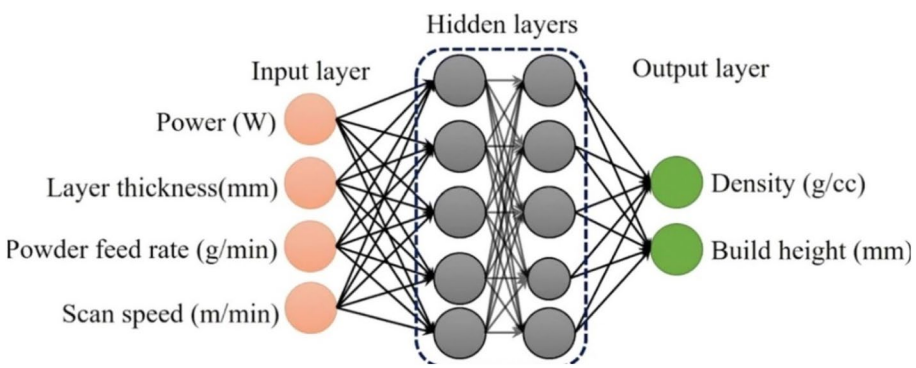

Fig. 35 The proposed ANN model with indicated input, hidden, and output layers [211]

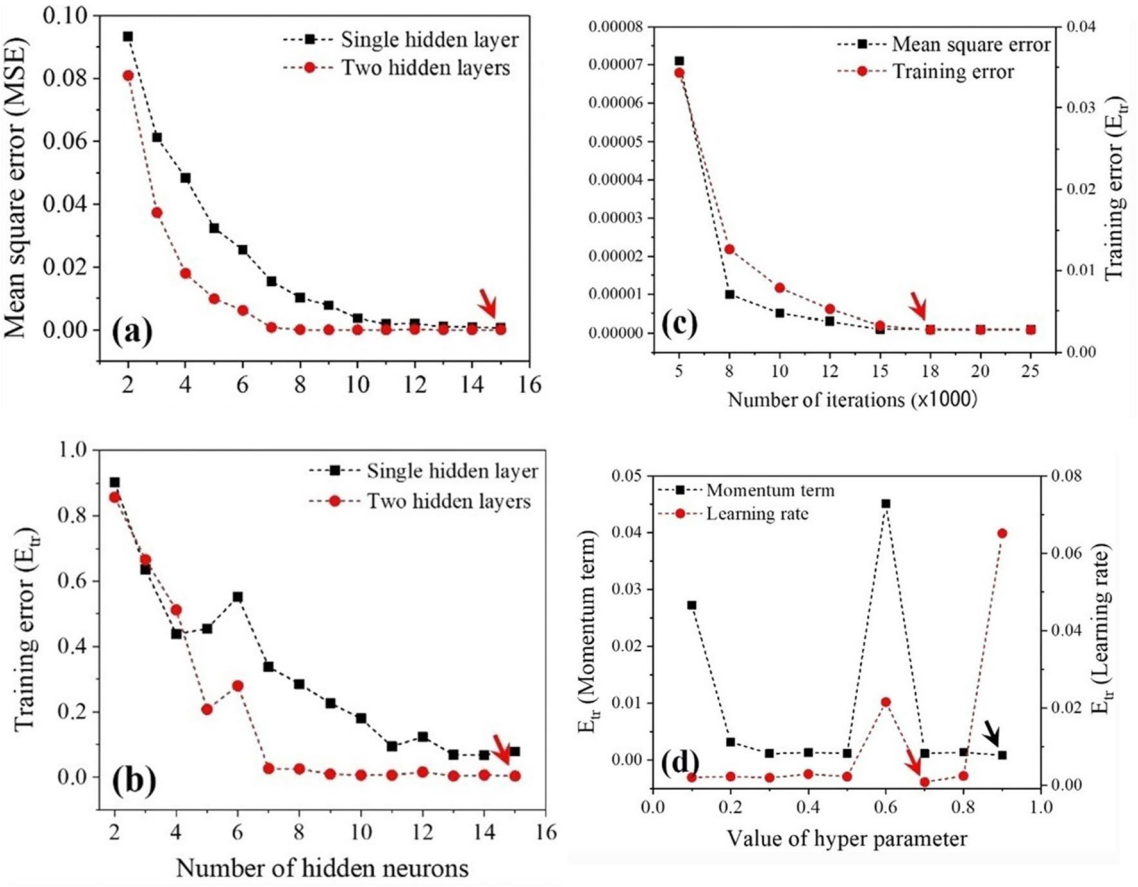

Fig. 36 Process of plotting the evolution of ANN model, **a** The optimal number of hidden neurons with respect to error value, **b** Number of hidden neurons with respect to error value, **c** Number of iterations and **d** Number of iterations and learning rate respectively [211]

most influential target values were the particles in ambient environment while printing, drop circularity, drop height, and standard deviation of each droplet. In conclusion, the detection of significant factors in droplet generation and their introduction in the form of process parameters made for more control and regulating the influential parameters such as droplet height, leading to more process control and optimization. As Fig. 38 shows, drop geometry and drop height are much better tuned [213].

2.2.3 Process Parameter Optimization using Gaussian Regression

Laser powder bed fusion (LPBF) highly relies on the parameters related to operating laser [214] and there are lots of underlying parameters involved that are yet unstudied. These process parameters do not necessarily manifest themselves in one process step because of the iterative approach of AM methods. Needless to say, process parameters have relatively high dimensions and magnitudes. A tabular data (Table 7) showing the most important process parameters in a LBPF process is presented in [23]. Sophisticated chemical and physical factors need to be considered in LPBF and all subbranch methods. an existing microstructure-property relationship should be defined for different materials that are chosen in AM process [215]. The perception and indemnity of right optimized LPBF processing parameters often rely on an expensive empirical process to be experimented for multiple times. When the alloy or metal selected for LPBF is newly introduced, this procedure becomes even more complicated. Furthermore, most of the current ML methods are far more limited in terms of the number of processing parameters suitable for fabricating (Fig. 39) [216]. As suggested by Kamath and Fan [217], since only a few parameters need to be processed, Gaussian process regression (GPR) is selected as the most suitable method because other methods like NN and support vector machines (SVM) deal with a considerable number of parameters and require unnecessary computational burden One of the unique attributes of this regression is its ability to indicate how uncertain a prediction could be. GPR acts as a link between the density of fabricated objects and process parameters, i.e., laser power and scan speed [218]. Also, some important

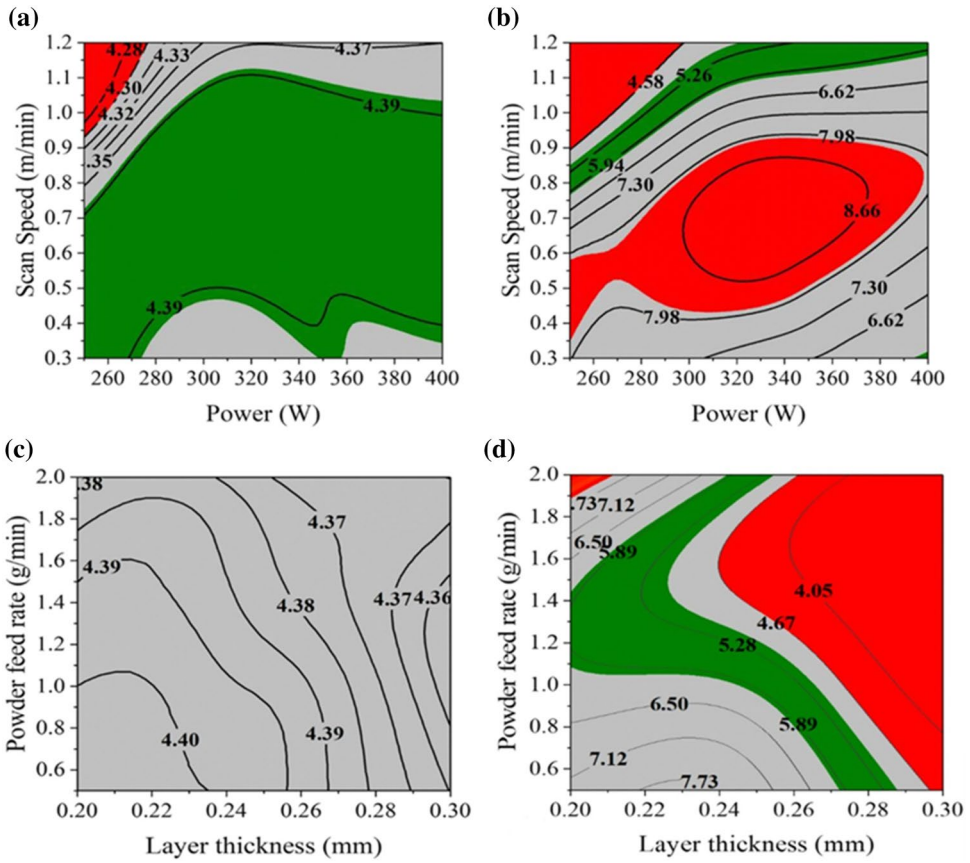

Fig. 37 Process parameters plotted based on ANN predictions and green boundaries are shown as the areas where the combination of process parameters had optimal results. **a** shows density while **b** indicates build height of DED Ti-6Al-4V alloy based on considering power and scan speed, **c** shows density plot of and as powder feed rate and layer thickness **d** build hight related to process parameters such as powder feed rate and layer thickness [211]

mechanical properties, namely fracture toughness, fatigue resistance, and tensile properties, need to be accounted for [219].

Overall, using ML methods and GPR in the aforementioned process, it was found that this new and significantly larger optimized LPBF prospect was never tested for manufacturing fully dense AlSi10Mg samples (i.e., relative density $\geq 99\%$). The newly determined optimized processing parameters (e.g., laser power and scan speed) have made it possible to achieve previously unattainable high strength and ductility. The obtained results revealed that even though AlSi10Mg exhibited similar Al-Si eutectic microstructures (e.g., cell quality in fine and coarse grains), large differences were revealed in their mechanical properties including hardness (118–137 HV 10), ultimate tensile strength (297–389 MPa), elongation to failure (6.3–10.3%), and fracture toughness (9.9–12.7 kJ/m^2). The underlying explanation was attributed to the subtle microstructural differences known using two newly defined morphology indices (i.e. dimensional-scale index Id and shape index Is) based on several key microstructural features retrieved from scanning electron microscopy imaging [220].

2.3 In-Situ Anomaly Detection

Human examination with naked eyes could always be prone to flaws and inconsistencies. An accurate defect detection is an integral part of AM process [221]. An instance of such are delays happening in defect detection which even when executed by an experienced human operator, a flawless detection could still not be achieved. Supervision, while the printing process is ongoing, is paramount because precise detection could identify potential defects stemming from poor parameter setting. In order to address the issues with acquiring through data from the in-situ spatial domain, Jin et al. [222] proposed an ML algorithm in order to deal with over and under-extrusion occurring at in-plane directions, on global and local scope. As a result, their approach resulted in synchronized defect detection without latency and real-time defect detection. Also, in order to address the issue of efficiency of data processing and modeling, and in an attempt to implement unsupervised component analysis to aid in fusing features extracted from sensing data, Wang et al. [223] made an effective effort towards better defect detection. In another work by Ye et al. [224] the issue of inability of detecting layer surface variations and small process shifts was put under scope, and the authors argued that this shortcoming requires development of a framework which

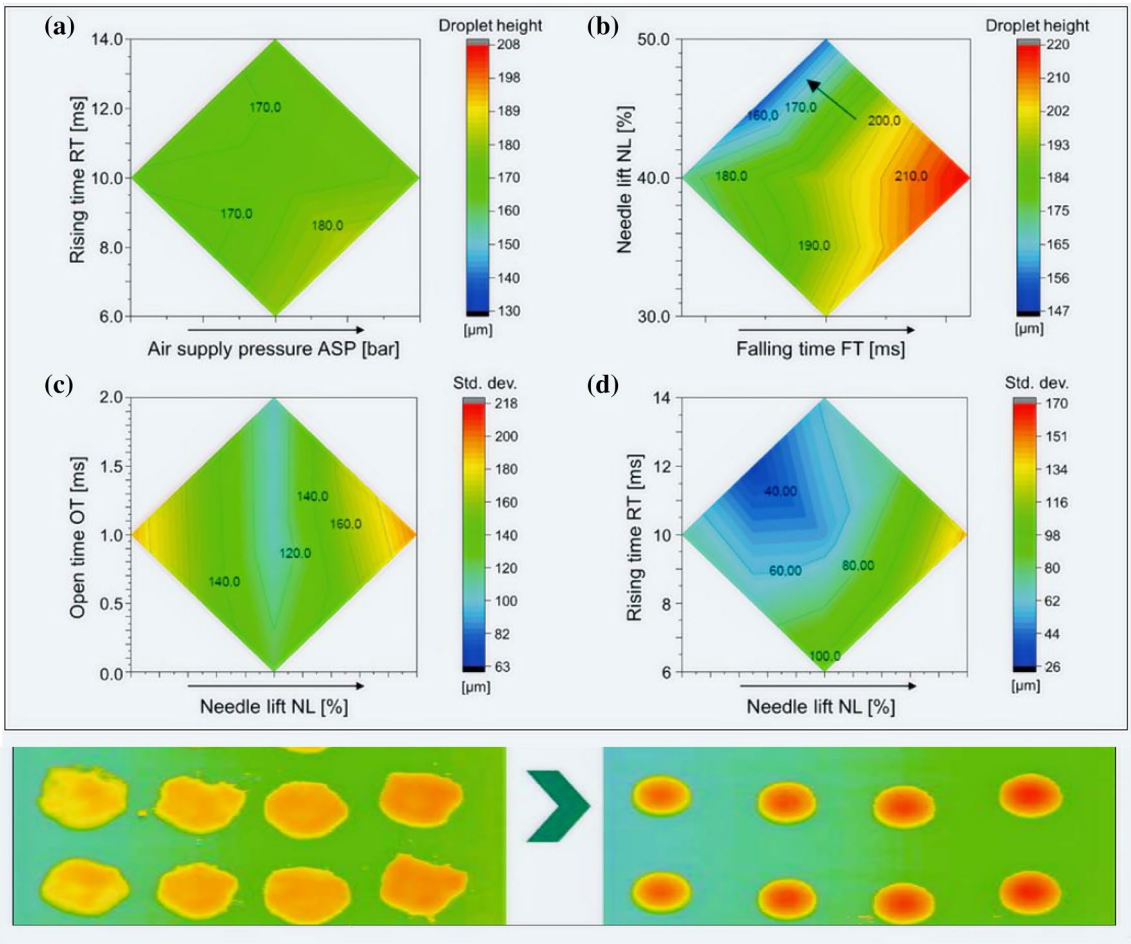

Fig. 38 Plotting droplet hights and related standard deviations as functions of process parameters and comparison of droplet accuracy before and after ambient particle accuracy regulation. **a** relation between raising time and air supply pressure to height of droplets, **b** percentage of drop exerting needle lift with respect to droplet falling time, **c** influential parameters such as droplet open time and needle lift on standard devieation of droplet hights, **d** Rasing time and needle lift on standard devieation of droplet hights [213]

Table 7 Considered process parameters for a LPBF process [23]

Manufacture parameter	Symbol	Value range	Unit	Value used
Build mass	m_b	4–12	kg	Pre-determined
Build Height	h_b	80–90	mm	Pre-determined
Build Time	t_b	30–120	hour	Pre-determined
Part volume	v_p	14,200–15,900	mm^3	Pre-determined
Post chamber- pressure drop	Δ_p	45–175	mbar	Maximum
Powder PSD D10	PSD_{D10}	10–25	um	Measurement
Powder PSD D50	PSD_{D50}	25–40	um	Measurement
Powder PSD D90	PSD_{D90}	40–60	um	Measurement
Powder hall flow	t_{hall}	10–20	second	Measurement
Powder apparent density	$\rho_{apparent}$	4.3–4.5	g/cm^3	Measurement
Sample location X axis	X_{loc}	−130–130	mm	Pre-determined
Sample location Y axis	Y_{loc}	−240–240	mm	Pre-determined
Temperature in chamber	T_c	45–70	C^0	Mean
Temperature of process gas	T_g	30–70	C^0	Mean

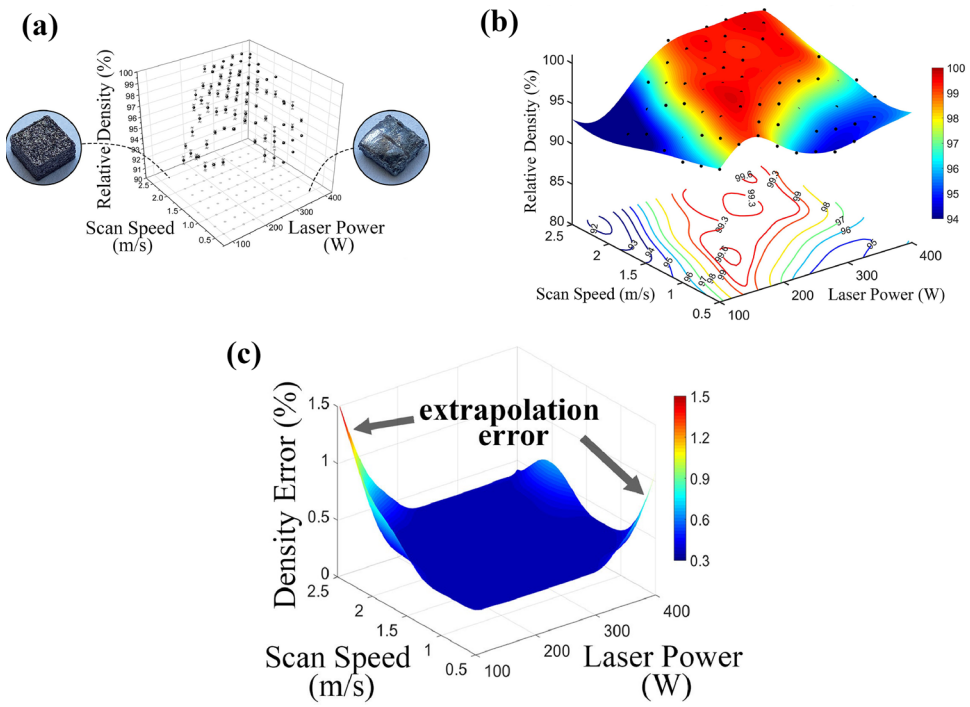

Fig. 39 Image of GPR results as an indication of the training data for the average and standard deviation. **a** Showing two sample specimen from two selected points of the domain, **b** Relative density at discrete parameters of laser power and scan speed, **c** Extrapolated error from scan speed and laser power [216]

has layer wise monitoring ability. Furthermore, the authors claim that their approach is among the first attempts to fully take advantage of 3D scanning for in-situ monitoring. This novel approach resulted in better defining of morphological changes within the printed layers, regardless of shape and size. Overall, results show better recognition of miniature shifts that bring about deviations that are not conspicuous but shape-altering, impeding the overall part quality. This issue is mostly stemmed from poor parameter setting. An example is shown in Fig. 40 [225].

In order to address this challenge while executing in-situ monitoring, proper in-situ monitoring systems and image processing installments are necessary. Aside from image-based or real-time monitoring, there are other clues in the form of signals, that could be detected and analyzed in order to perform the anomaly detection task. Namely, useful information could be achieved by the application of signal-based methods, where the acoustic signals emitted are used while the operation is ongoing. Acoustic signal detection, optical emission, infrared signal emission, and multi-sensory signal installments [226] are some methods that will be explained in the following section. Having these provisions could go a long way in producing high-quality printing parts. Numerous efforts have been recorded to achieve the abovementioned objective, namely, novelty simulating methodologies, better developed experimental setups, and more optimized computer vision. In the following, we further expand the accuracy of Image processing methods via ML models.

2.3.1 Real-Time Anomaly Detection

The capability of these anomaly detection systems is determined by the direct feedbacks they receive from the system in real-time. One of application cases of this method is the use of a camera known as DIC camera [227], which performs image correlating tasks. DIC is a state-of-the-art camera imaging reconstruction system, performing the task of monitoring the surface geometry of printed parts. In our particular case, this installment is used while a fused filament fabrication (FFF) was ongoing. The system was capable of correlating stereoscopic images. An algorithm known as random sample consensus (RANSAC) [228] was set to the task of cloud alignment of different points and eliminated potential outliers in the process of data correlation. Results of this effort showed that defects such as porosity within the printed parts were detected. The detection was accurate enough to identify a porosity at the resolution of 0.0202 mille-meters and this revealed the efficiency of coupling DIC with 3D printing process in in-situ detection. This finding could also be used in other fields such as LPBF [229–231], where porosity detection could be a hefty work. There are records of other capable algorithms to address different types of reoccurring defects in fabrication stage, such as image segmentation methods established with high-quality imaging systems to set the precision of in-situ geometrical documentation of images taken from each layer of LPBF process. One of these methods is active contours without edges (ACWE) [232]. Another method is

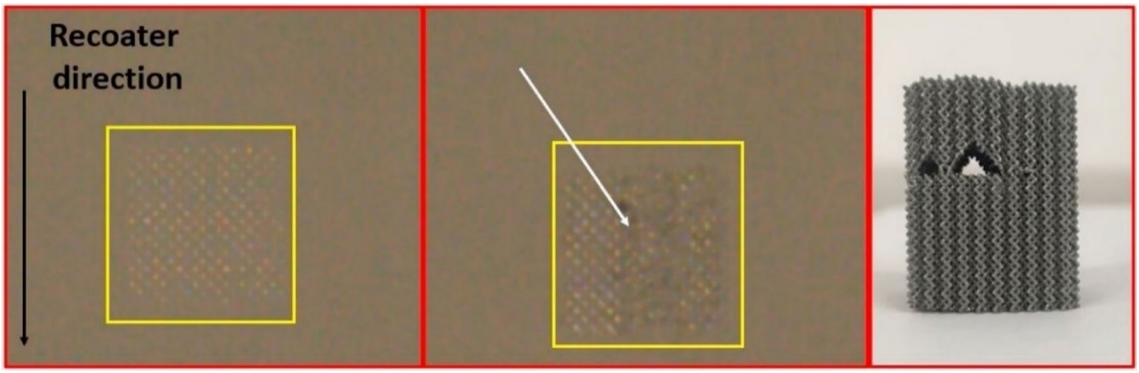

Fig. 40 An instance of poor parameter setting in LPBF where build up direction is from bottom to top which resulted in obvious voids within the printed part [225]

based upon level-set methods with bias field approximation (LSM-BFM), which has been applied for the creation of boundary charting. Layer-wise nature of the geometry of the printed part is also analyzed and finally, were compared with ground truth that was captured in optical microscopy images. A number of different parameters such as lighting conditions, printing geometries, and different directions of laser scanning were also considered. Overall, the conclusion was that the dark illuminated spots while performing in-situ anomaly detection using ML showed promising outcomes in in-situ anomaly detection.

Nevertheless, the abovementioned methods do not have all-inclusive methodology of ML models in terms of detecting different categories of imperfections at the same time. One of the most notable and fitting accomplishments of ML is revealing underlying patterns that could not be seen. This accomplishment of ML is advantageous in processes such as 3D printing since it is a multi-physics process with many variables. Therefore, imaging systems to monitor fabrication process, ML algorithms and computer vision are decisive in comprehending and categorizing different defects of a 3D printing process. In a case study, the process was recorded via the attachment of a USB (universal serial bus) camera to the printing nozzle resulting in a sable recording of printing process while the print nozzle was changing its plane, the setting of the camera proven stable and unchanged. An example of this installment is shown in Fig. 41 [222].

A CNN was trained to analyze the recorded real-time images to predict status of in-situ printing. Another method is known as delamination, where the primary parameter was nozzle height which needed vigilant monitoring. In this case, the model was trained based on input images having four different nozzle height adjustments. Overall, it was revealed that the accuracy of the two models was 98% for defects within planes and 91% for the lack of lamination. In this process, a modification of an automation technique that operates in a closed-loop correction structure was established. This establishment analyses and modifies process parameters in accordance with the prediction made by ML model and the obtained results have shown that ML generally functions much better than a well-experienced operator. Another example of an in-situ anomaly is the application of clustering techniques in an unrevised manner. This showed an astonishing accuracy of finding seven anomalies and with overall 98% accuracy in one case, and also 95% accuracy in the classification of six other anomalies. To achieve this accuracy, six types of common anomalies were considered including incomplete spreading, part failure, debris, superelevation, recoater streaking, and recoater hopping. The model operates with applying a filter bank to the first response images and gathered a database grounded on clustering techniques and feedbacks from the filters in site. Each image is processed and archived base on fitting its histogram or assigned fingerprint to the ones in the baseline and their matching degree. This process is repeated for each new input image and the images are classified in accordance with the gathered database and that the defects and errors are traced via the comparison of the fingerprint of new images to baseline data images. Furthermore, this method has the potential to be applied to many other manufacturing methods and is not limited to AM procedures [134].

2.3.2 Image-Based Anomaly Detection

In-situ anomaly detection using Siamese network, as is mentioned in Sect. 3 of the paper, fall in a category of AM (VATP) which has seldom been paired with ML techniques and data-driven approaches. Therefore, there are limited available data. Thus, it is a challenge to apply ML models and get a decent accuracy in results. In order to overcome this hindrance, a specific type of ML/DL model known as Siamese network, is chosen. This network was first used for identifying different handwritten signatures but has proven

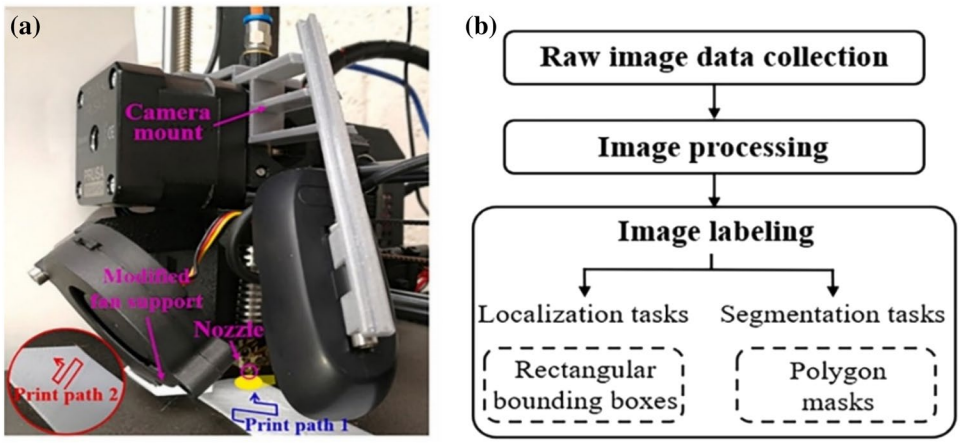

Fig. 41 **a** A trial anomaly detection set up mounted by a USB camera. The camera records the process with a 30-degree slope downward to the horizontal axis. Blue and red arrows show even numbered or odd numbered layers, respectively. **b** The flow diagram of preparation of data set images [222]. (Color figure online)

to work well with limited data. A general two-layer Siamese network is shown in Fig. 42 [233].

In addition, the use of synthesized data was considered to be evaluated with respect to available experimental data. The synthesized data were governed by a developed theoretical model shown in Eqs. (9) and (10) [234, 235].

$$\{F_{separation}\} \subset [F_{0,F_1}], \text{ success} \tag{9}$$

$$\{F_{Separation}\} \not\subset [F_{0,F_1}], \textit{failure} \tag{10}$$

where $F_{separation}$ indicates the maximum measure of a force of separation that each layer might have, and $F_0 and F_1$ indicate the lower and upper bounds of the separation force denoted to each printed layer. Also, based on the previous works which are modeled after the separation force of a constrained smooth surface and the drop in pressure for a constrained textured surface. In Eqs., (11) and (12). The separation mechanism of layers and the effects of liquid filling around the separation surface are expressed as following,

$$F = \frac{3\pi.\mu V}{2.h^3.}.R^4 \tag{11}$$

$$\frac{dp}{dr} V.\pi r^2.2\eta.\frac{\left(4\pi.r + \frac{2nd}{cos\alpha} - n.w\right)^2}{(2\pi.r.h + 0.5n.w.d)^3} \tag{12}$$

where r is the radius of the part cross-section and is variable from the minimum of zero to the maximum of R, V indicates separation speed, n shows the number of grooves of a texture at micro-scale, μ represents the viscosity of resin, d and w are depth and width, respectively, and h indicates the initial gap that is oxygen layer thickness. Based on the aforementioned theoretical equations, the synthetic data are generated which help in indicating and setting the right printing speed for continuous printing to avoid further separation of the printed material. The workflow of how ML approach and an AM process could be interlinked and further exploited is depicted in Fig. 43 and Table 8 illustrating the most important process parameters [51]. In Fig. 43, a subset denoted as subset S is designated as the original DOE table set. The best ML model will be selected out of the designed experiments in the sub set S. For the purpose of comparison and setting a baseline, the outcomes by new DOE and predictions made by ML are compared to the original DOE. With respect to the theoretical model, the most effective and pragmatic parameters are chosen, which are included in Table 9. Each different quantity of these parameters results in a new set of experiments. In this study, there were 6000 simulation runs and the data were collected. For experimental data preparation, based on the parameters and desired variables to achieve, each set of process parameters are recorded and evaluated. Their results are summarized and therefore, an experimental data set is prepared. There are 180 tests and the data gathered are employed for ML models to forecast the variables of interest, which are printing speed and elevation. When data preparation reaches a satisfactory stage, the next step in the application of ML in CLIP parameter optimization is done by three different routes; i.e., ensemble models, conventional ML methods, and Siamese neural network.

ML techniques and data-driven approaches are considered as efficient ways for pore detection in order to prevent and optimize the final product [236]. The parameterization of the defects demands advanced methods to make proper inspections on pore and defect evolution. BJ is characterized by the large number of pores that are globally spread in a printed part [237, 238]. The most challenging observation in this regard is the detection of internal pores and defects. Moreover, the scope of observation (meso, macro, and micro scale) for identifying defects is very determinant in the analysis. To overcome this issue, in a work by Zhu et al. [239] on metal BJ, an inspection method was presented which was consisted of three steps,

- Micro scaale X-ray CT scan reconstruction.

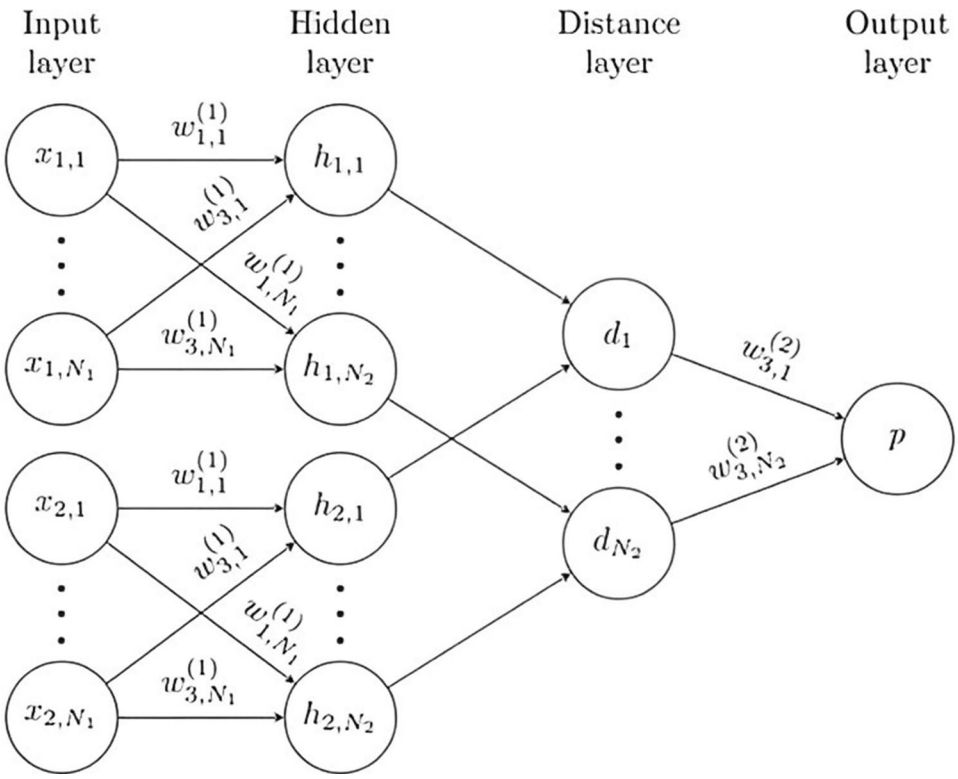

Fig. 42 A general two-layer Siamese network, as a binary classifier with the prediction 'P' [233]

- Auto 3D morphology analysis
- Big data analysis based on ML approaches

A very comprehensive and effective setting was installed taking advantage of X-ray CT scanning and computer vision connected to a substantial defect formation database monitoring on a macro-scale for a given volume. Thereafter, ML clustering and regression techniques detect patterns and qualitative results never seen or acknowledged by human eye. On a macroscopic analysis, this setting detected around 10^5 pores. Overal, AM products have a myriad of defects, such as internal cracks trapped air bubbles and pores that could be manifested in considerable numbers which are often random and homogeneous [237, 240]. These issues would result in crack and deformation propagation, especially lowering the fatigue strength and static mechanical properties, thus making the binder jetted material less reliable for engineering applications. This lack of quality demands novel quality control provisions to be taken into account. An accurate defect development analysis and a thorough microscopic evaluation of a printed part is of paramount importance [241–243]. Typically, the initial challenge ahead is defect information from a microscopic analysis, because the defects are not clustered by the same pattern in every part of the binder jetted part and they are randomly dispersed. Traditional techniques are not very efficient and as a result, in order to tackle this issue, the use of x-ray ct (XCT) scanning has proven to be very effective. XCT generates a very extensive data set from the captured images of the specimen of interest. The broad database generated was in the range of 2–15 GB of data in the form of images captured from defect morphosis in 3D. However, these images need to be compatible with 3D morphological algorithms [244, 245]. These algorithms are able to decipher data related to defects, their position, the fraction of porosity, pore per volume area in 2D [245] and slices or 3D [246]. The issue lies in the fact that these methods are not conditioned to work well with binder jetted samples. This hurdle was passed by using computer vision-based auto inspection, especially DL approaches, for they function based on real examplifiction in numerious interations, rather than being rule or algorithm based [247, 248]. The complex and coincidental shapes the defects might pose a challenge since it is very important to accurately quantify the changes and developments of the shapes of pores and defects during or after print process. At the time, this research consders only a single criterion which is the volume fraction of the pores (porosity) [249]. This criterion cannot indicate anything regarding other properties a printed part might have including fracture toughness, anisotropic elasticity, permeability, etc. [250], which are proportional to pore orientation, sparsity in the printed part and the geometry of pore. Therefore, understanding the vast dataset containing such information is very necessary. As a result, quantitative big data analysis is preposed to not only overcome the challenge but also to eventually provide new physical insight [239]. These obsticles are dealt with

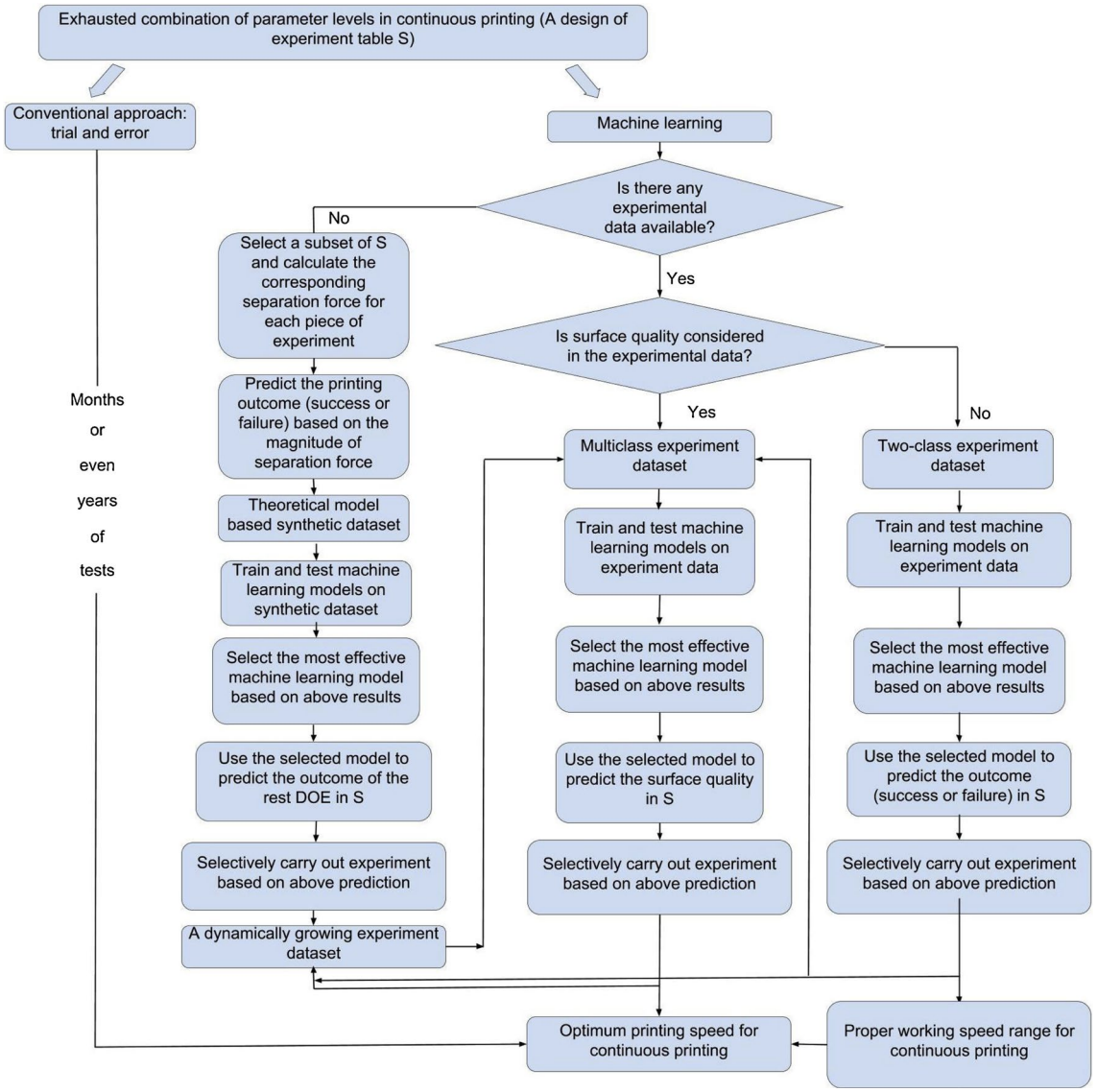

Fig. 43 The workflow and the planning for applying ML with experimental and synthetic data [51]

Table 8 Different quantities of important process parameters [51]

Resin viscosity (Pa. s)	0.09	0.12	0.14
PDMS thickness (mm)	1	2	4
Manufacturing velocity (mm's)	0.052	0.038	0.05
Cross section j, for data synthesis (mm^2)	3.1	12.6	55.3
Constrained surface type	Smooth	Textured	Island
Duration of frames (s)	0.5	1	1.5
Video projection time	15	20	30
Groove width (μm)	100		
Groove length (μm)	100		
Cross section sizes j_b, used for separation force of synthetic data (mm^2)	3.1, 7.1, 12.6, 19.6	28.3, 38.5, 50.3	63.6, 78.5

Table 9 Data acquired from the pores

Pore index	Centroid μm				Orientation	Principal axis length μm			Bonding box size μm			Volume μm^3	Surface area μm^3	Convex hull volume μm^3
1	x	y	z	Θ	Ø	a	b	c	x	y	z	ν	s	νhall
2	5.3	87	2.2	57.6	95.2	51.4	17.4	13.2	44.4	22.2	14.8	3.19e3	1.55e3	7.70e3
3	2.5	273	5.7	33.8	120.5	39.3	25.9	14.4	29.6	25.9	44.4	6.13e3	2.23e3	1.02e4
4	27.9	80.9	14.3	72.2	74.7	283	91	89.4	241	189	163	2.14e5	5.37e4	2.31e6
5	13	412	39	54.5	264.2	254	127	54.8	137	122	244	2.50e5	5.69e4	1.64e6
6	4.9	295	6.3	78.2	9.6	24.5	33.4	21.2	33.3	59.2	40.7	1.27e4	4.21e3	3.34e4
117.669	61	40	600	90	251.6	23.5	8.2	4.3	18.5	11.1	3.7	455.90	302.8	557.2

via implementation of the latest advanced technologies. For the first aforementioned challenge, fast XCT, another step is morphological analysis and for the final step, challengs is in ML big data analysis driven with DL methods. Images taken with XCT are used which delivered the images in a fraction of the time of a typical data gathering method would take [251]. By using ML methods [252], a large amount of data from different pore shapes, sizes and orientations are recorded, identified, and clustered resulting in a very accurate analysis. In Fig. 44, the function of the proposed approach and the application of ML at the final stages are shown.

In a research by Zhu et al. [239], copper samples were binder jetted and post-processed. The samples were shaped to spherical geometry, having a bimodal diameter distribution with peaks at 5 μm and 30 μm. Post-processing was consisted of debinding, sintering, and hot isotropic pressing In total, the XCT imaging of 3 copper samples revealed 117,669 pores in total, including 22,912 for the first sample, 54,739 for the sintered sample and 40,018 for the HIP specimen and pore parameterizaion. Table 8 presents a small portion of the results generated from parameterization. These results indicated that the prosity of the first, second and third specimens were 37.90%, 3.43% and 0.89%, respectively. The density of samples was measured via Archimedes method.

The initial step for quantitative pore evolution analysis is to derive the overall morphological indicators for pores. By deriving major morphological indicators, it is possible to have a systematic way of describing porosity with fewer dimentions and less complexity. In ML quantitative pore evolution, this practice is basically known as principle component analysis (PCA). For the purpose of implementing PCA, results in Table 10 are re-scaled to become normalized, resulting in the stability of the numerical values and variance; thus, variables with extreme quantities become ignored.

Based on the PCA process shown in Fig. 45, it is shown in the first and second principle component (PC) that a combination of volume and eccentricity are indeed very important factors, which accounted for 55% and 24% of overall variance. At the beginning, the third PC only yielded 12% of the variance. The reason is that the third PC is mostly consisted of altitude angle, showing that this feature is not very relevant compared to other morphosis criteria. Clustering is another ML task which is used for anomaly detection. Based on the reduced 4D dimensions brough about on PCA, Gaussian mixture model is used for clustering analysis. Afterward, it was shown that the identified pores in the three binder jetted copper samples were conveniently grouped into four morphological categories. In Fig. 45, the clustered groups are plotted for further classification (PC1, PC2, and PC3). Concerning the sub-space defined by each cluster, the data plotted at the center of the subset of each cluster indicates the related morphesis. Eventually, the four major groupings of related pores are presentd in Table 11.

Owning to the insight learned from the analytical results of BJ specimens, the binder penetrates between loosely packed particles, resulting in large and interlinked empty spaces. The first green specimen was measured to have a high porosity of 37.9% which is the aftermath of the aforementioned effects. The defects in group four consist of interconnected gaps which are full of twists and turns, leading to narrow regions among the particles in close contact. When densification diffusion occurs during sintering, particles that are close form neck structures at the location of contact. Neck structure pulls the particles closer along with overall pore shrinkage [253]. Furthermore, when neck structures grow, interconnected pores break up their bonds resulting in the decomposition of pores and eventually making more discontinuous pores which belong to the pores in groups 2 and 3. The reason behind increased avarage size and the number of pores in groups 2 and 3 after sintering is the fact that the overal shrinkage of pores happens at sintering. Additionally, due to the orientation of the specimen, gravity enforced to the part made the pores more existent in vertical orientation. Needless to say that these findings are consistent with 2D pore formation studies [254]. In conclusion, by taking advantage of unsupervised ML methods including

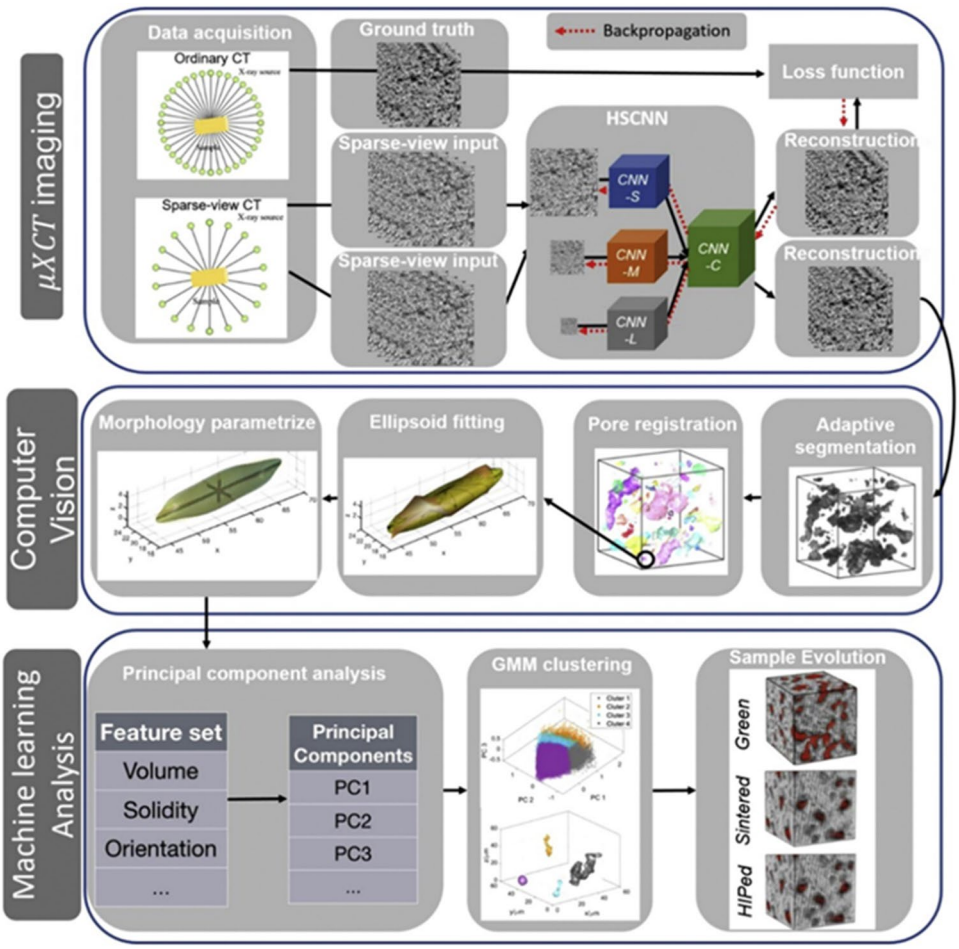

Fig. 44 μXCT imaging using hierarchical split- CNN for better grouping and at ML analysis using gausian mixture modelling, suggested to overcome the challenges regarding pore decetion of binder jetted parts using big data approach and ML unsupervised clustering [239]

Table 10 Normalization of pore attribiutes [239]

Index	Notation	Attribiute	Normalization
1	ν	Volume	$\widehat{logv}$
2	e_l	Eccentricity 1	$a/\sqrt[3]{abc}$
3	e_m	Eccentricity 2	$b/\sqrt[3]{abc}$
4	e_s	Eccentricity 3	$c/\sqrt[3]{abc}$
5	μ	compactness	$\sqrt{s}/\sqrt[3]{\nu}$
6	v	Volume ration	ν/xyz
7	s	solidity	ν/νhall
8	Θ	Altitude angle	Θ

PCA and GMM, the major factors to pore creation in binder jetted parts are discovered. The pores are comprehensively classified into four groups; therefore, this allowed the quantification of pore morphesis on the basis of describing criteria set for each type of pore which is far beyond human vision capability [239]. ML methods and data-driven modeling have contributed lots of possibilities and a new horizon to novel AM technologies such as MJ, far exceeding the experimental insight. In the forthcoming section, we present cases of novelty where data driven approaches and ML modeling were used to optimize MJ technique [213].

2.3.3 Signal-Based Anomaly Detection

The time frame in which the signals are received to gather data makes a great difference in understanding of the model behavior. In this respect, false and abnormal signals from defects can be better detected with respect to signals emitted from when process is undertaken correctly during AM process. In general, anomaly detection tasks could be optical-based, which could be real-time monitoring or image-based, as already discussed. Additionally, acoustic-based, thermal-based [255], multi-sensory approaches [226], and even generation of augmented data based on synthetic information are used to better develop the anomaly detection models [256]. Becker et al. [257] applied an acoustic-based anomaly detection approach (Fig. 46) to detect abnormal cues in the shape of emitted sound. One needs to acknowledge that in all the detected ways a 3D printing process could go wrong, not all of the signs could be detected via emitted sounds, such as aforementioned optical, thermal, multi-sensory and etc. As a result, the collection of likely errors is provided by the

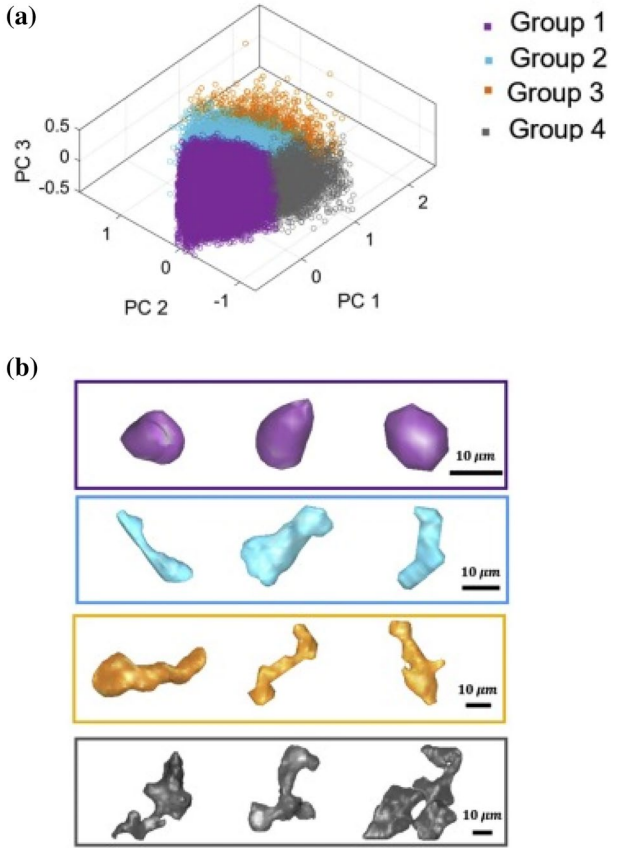

Fig. 45 **a** Plots of different pore types based and princple component anlysis, **b** Four detected groups of pores via ML analysis [239]

manufacturer of the printing device [258]. Table 12 shows the most important parameters which need vigilant detection for anomaly detection. Moreover, these will be parameters to be used in the ML model for training the model. For example, one likely fault is an incorrect adjustment of the printer's nozzle elevation. Should the nozzle move too close over the print bed and the deposited layer, it makes contact with it and leaves grinding scratches on the surface. This causes the considered heights and material flow to become inappropriate [257].

After modeling and training the model, training multiple data sets, and adding augmented data to get a better generalization within the NN, the experience brought about 96.96% accuracy and an F1- score of 86.7% for the training. This is known as a score that predicts model performance by combining recall and precision [257].

2.4 Testing, Validation and Property Prediction

The process of additively manufacturing a product is a complex and relatively novel practice. Complex geometries and lack of uniform material properties are some of the challenges in testing and validating the manufactured parts [133]. As a result, many factors must be evaluated and tested after the manufacturing of a part is done. The objective of concentration in testing and validation phase is mostly on surface metrology, and defect detection and classifications using ex-situ techniques. An example of the application of ML in optimizing the influence of ex-situ measures is presented by Datsiou et al. [259], as shown in Fig. 47, where feedstock of a type of glass material, soda-lime-silica glass, was considered for the process of LPBF. The aftermath was geometrically complex products. However, surface was rather opaque and geometrical dimensions were slightly changed with respect to the initial standards, as given in Tables 13 and 14 [259]. This aforementioned dimensional change is mostly due to particles stuck to the walls of the surface. This issue is common in methods involving powder and is often optimized by post-processing measures [259, 260].

Moreover, the measurement of a new build is extremely critical. One tactic is to use industrial computed tomography scanning (CT), which is a competent tool, particularly for the validation and generation of a plot from the internal geometry of the printed part. A notable advantage of this scanning method is that no physically enforced measures

Table 11 Four major groups detected by ML analysis [239]

Groups of pores	Shape	Volume	Solidity	Description
Group 1	Quasi-spherical pores	Small volume (0.32 ± 0.39*10^4*μ_m^3) High volume ratio (0.35 ± 0.13)	High (0.76 ± 0.13)	Absence of sharp edges or extrusions, most pores in detected samples
Group 2	Small elongated pores	Volume (0.97 ± 0.41*10^4*μ_m^3)	High (0.51 ± 0.13)	Pores are characterized by eccentric structures, without significant extrusions
Group 3	Large elongate pores	Volume (3.61 ± 0.52*10^4*μ_m^3)	Low (0.36 ± 0.12)	Elongated pores, a lot of extrusions and necking that result in low solidity
Group 4	Reticulated defects, tortuous, network	Volume (5.56 ± 1.58*10^4*μ_m^3)	(0.33 ± 0.12)	Defects have large packing interconnected voids. Average volume of defects is larger than that in previous groups

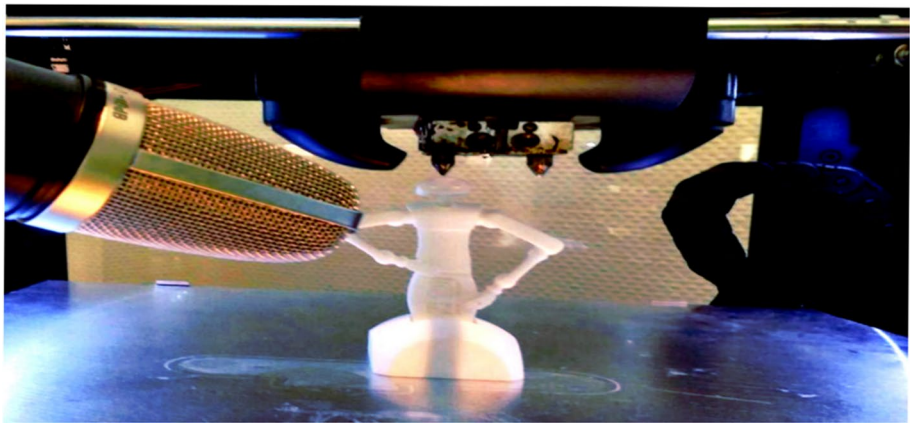

Fig. 46 A picture of the signal based (acoustic) anomaly detection setting [257]

Table 12 Selected parameters based on importance in acoustic anomaly detection to train the NN model [257]

Number of parameters in NN modeling	Parameter name
0	Fan noise
1	Printing process
2	Door opening
3	Door closing
4	Movement in the Z direction
5	Faulty Nozzle Height

need to be taken, keeping the part's physical shape, form and texture intact. Another technique of CT scanning that has proven to show accurate results in identifying flaws and defects in AM parts is X-ray computed tomography (XCT). Even though CT scanning is an ensured method of flaw detection after the build is completed, the process of scanning comes at a hefty price, resulting in more expensive testing process [134]. One ideology to tackle this issue is the use of data generated from the monitoring devices installed in-situ to detect the flaws instantaneously. With this approach, expensive CT scanning procedures are no longer needed and the concept of generalizability, meaning the ability to apply generalization based on the baseline drawn by ML regression analysis from in-situ imaging of defects to parts manufactured by AM builds, results in keeping quality of the performance at a satisfactionary level [261]. Another issue that ML handles thoroughly is the detection of errors at micro scale out of terabytes of data generated from the installed sensors [255, 262–264]. Even though 3D printing allows for freedom in geometrical shape, build quality in static or dynamic mechanical operations is a cause of concern. Scatter in fatigue properties is one example of prominent issues, which generally leads to failings within the solid such as gas porosity, keyhole pores, and lack-of-fusion [265–267]. Among aforementioned failings, lack of fusion pores is the most challenging because they turn out to be bigger in dimensions compared to gas porosity and keyhole pores (gas and keyhole pores being ~ 50 µm or smaller). Keyhole pores are more critical since their size and irregularity are more likely to lead to crack development

Table 13 Set dimensions [259]

Design limits	Wall thickness (x)	Wall thickness (y)	Wall thickness (z)
Set values(mm)	0.2	0.3	0.4
Minimum internal design diameter Din(mm)	1.1	1.7	2.0
Maximum length, L (mm)	14	14	8

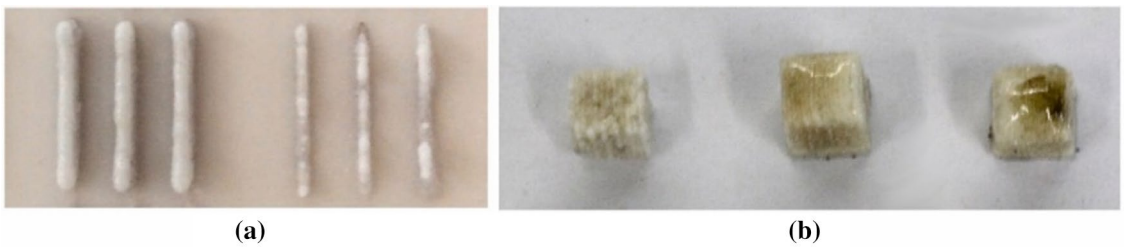

Fig. 47 LPBF of glass: **a** Thin-walled structures with good (left) and poor (right) consolidation; **b** Cubic structures having poor (left) and good (middle) consolidation and balling (right) [42]

Table 14 Comparison of resulting dimensions [259]

Designed wall thickness tw (μm)	Measured features	Results (μm)	Difference in percentage
200	Max wall thickness	688.5	244.2
	Min wall thickness	533.1	166.6
	Mean wall thickness	619.6	209.8
	Standard deviation	51.04	
	Coefficient of variation cv%	8.3	
300	Max wall thickness	1080.4	206.1
	Min wall thickness	901.4	200.5
	Mean wall thickness	978.8	226.3
	Standard deviation	78.7	
	Coefficient of variation cv%	8.0	
400	Max wall thickness	1247.6	211.9
	Min wall thickness	1076.8	169.2
	Mean wall thickness	1168.0	192.0
	Standard deviation	94.2	
	Coefficient of variation cv%	8.1	

and propagation. One of the possible reasons leading to this defect is the presence of spattered particles in build environment. Needless to say, this matter depends heavily on AM method, LPBF method undertaken by the following papers [267, 268]. An example of lack of fusion is shown in Fig. 48 [268].

In the case of LPBF, using an automated defect recognition (ADR) algorithm[269]. ADR helps in analysis of raw XCT imaging data by identification of deviations in the images using 3D, zero-sum, Gaussian convolution kernels techniques. Thereafter, the next step is to register the data gathered from XCT and the ADR algorithm within the layer wise image domain(Fig. 49) [261]. With methods explained in [270]. Eventually, data is prepared to be fed to CNN and NN models along images of both XCT scanning and in-situ imaging installments (a combination). part quality was validated and decent results were obtained [261]. Regarding multiple trained networks in this case study, classifiers with more diversity in datasets manifested more accurate results and were more generalizable. The accuracy of results had little to no relation to the data size as long as the generated data was from different parts and components of any given build. The data gathered via sensory systems related to post-scanning proved to be more detrimental in flaw detection and validation compared to post-recoating images. Nonetheless, they were used for improving information for post-scan modalities since they contained applicable information. Eventually, the presence of spatter particles to printing bed from the previous operations was considered as the main reason for the development of flaws related to lack of fusion. a 3D voxelated presentation of pores is presented in Fig. 50.

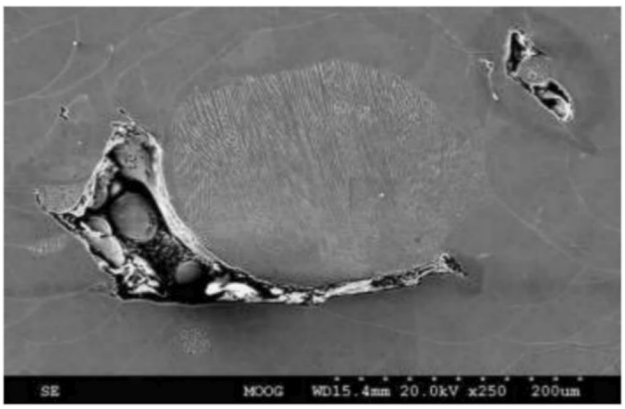

Fig. 48 An example of lack of fusion in a laser PBF process [268]

In general, to obtain a clear notion of part quality and validity, the mechanisms leading to pore development, which are mostly due to bubbles trapped during solidification of the solid manufactured parts, are very important to monitor and are essential to testing and validation in general [271]. The word prediction in ML refers to the output of a trained model, representing the most likely value that will be obtained for a given input In this study, the property of choice for prediction is the quality of the printed part, which in the following figure is a prediction of glass formation (Fig. 51) [272].

The model is trained with historical data and then predicts a selected property of the data for new inputs. This approach is also called forward modeling. Contrariwise, suggestion based on process parameters when given target properties is known as reversed modeling. In a study by Gou dong et al. a specific variation of MJ referred to as polyjet, was

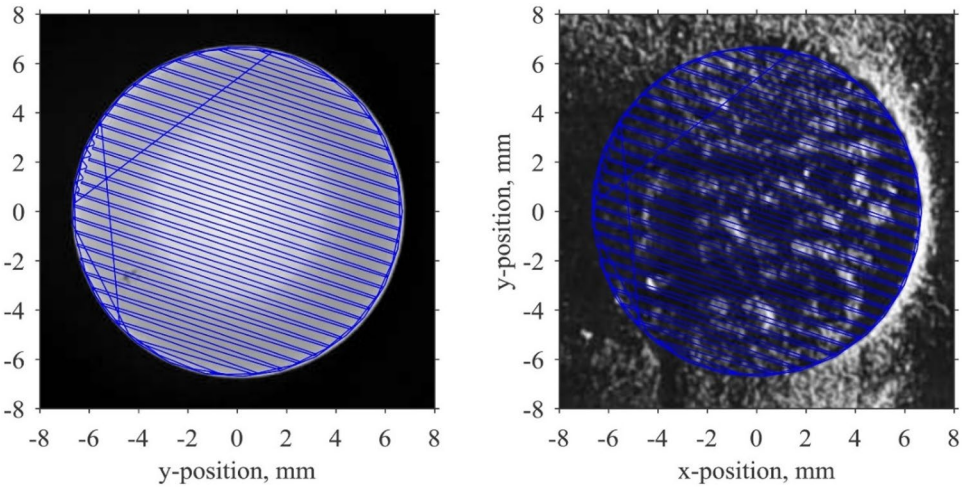

Fig. 49 Comparison of images taken via XCT(left) and in site screening using ADR algorithm (right) [261]

used in order to print patient-specific anatomical replicas, as this method has proven to be much cheaper than conventional methods, with the ability to fabricate without the need for tooling and capability to print multiple materials. In their approach, they used composite layering to construct their structure and used the following materials with their respected mechanical properties; TangoPlus (with an elastic modulus of 0.45 MPa and shore hardness of 26A) and Verowhite (having elastic modulus of 2500 MPa and shore hardness of 86 shore D scale). In their work, they derived formulas to predict the shore hardness and compressive modulus. Their ML approach outperformed conventional surface method response by 3.5%, and their multi-layer model was able to mimic human tissue material properties from the durometer of Shore 20A to 65A [273]. In the case of weld bead height (h) and width (w) estimation, an ANN model is constructed which is made of 3 input layers that are V (voltage), F (feed rate) and welding speed (S). In the

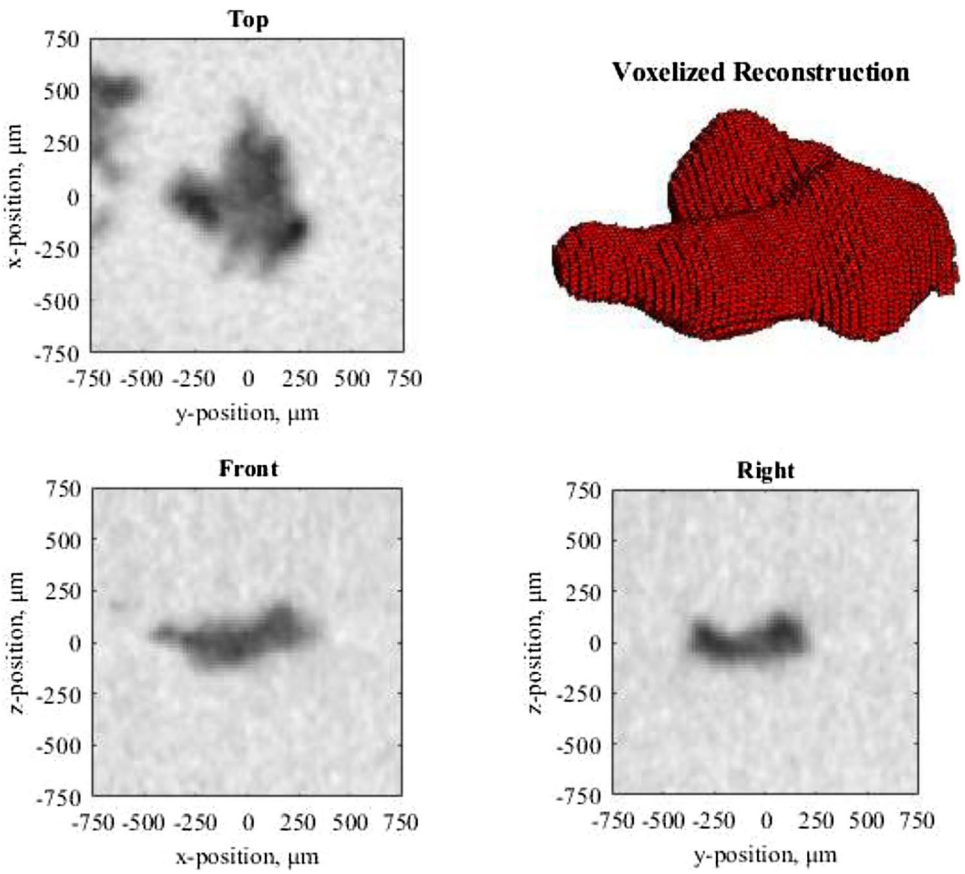

Fig. 50 Image taken of a pore from different angles and its voxelated reconstruction [261]

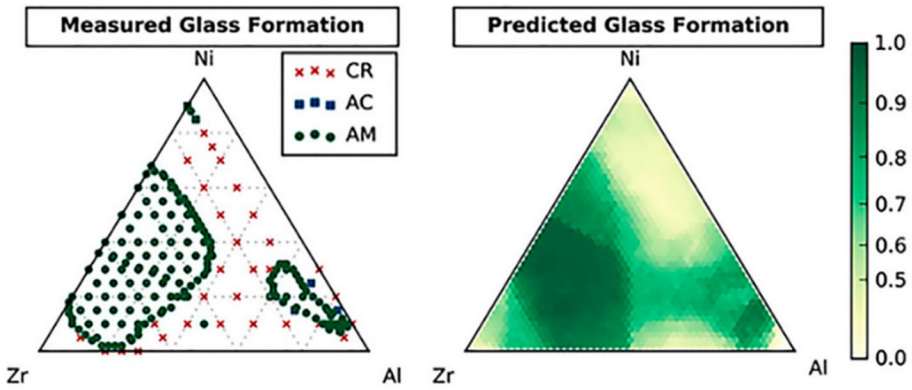

Fig. 51 The capability of glass formation within Ni—Al—Zr ternary realized via ML forecasting and computer generation [272]

case of the forward model, two hidden layers are included that each layer has 10 and 4 neurons respectively and the reverse modeling considered to be the exact opposite but only difference in the reverse model is that the two hidden layers have 12 and 10 neurons because of the results achieved after 1034 epochs and reaching a mean square error of $6.1216e^{-16}$ and $2.0072e^{-16}$ of mean square error for the reverse model after 4311 epochs. Figure 52 [274] illustrates this process. In order to hit multiple target properties, a problem should be formulated in a way to cover a multi-objective task optimally. An example is formulating the problem as a multi-objective optimization process. This approach seeks multi-dimensional optimization within a property space. It is worth mentioning that because common gradient-based methods are not exactly suited for this problem, an algorithm known as multi-objective genetic algorithm was applied to simultaneously optimize trained Navier Bayes models or any given parameter. GA implements principles from evolutionary biology and maximizes the fitness of a batch of parameters [275, 276].

Moreover, in a study carried out by Singh et al. [277] regarding the laser direct metal deposition, also known as DMD [278], another case of forward and backward modeling was exercised. In this study, the forward modeling was used for estimating the width and height of the deposited beads, and the reverse model revealed the pragmatism of input parameters such as laser power, scanning speed and powder flow rate. To fulfill the aforesaid objectives set, three different NN models were organized; RNN, multi-layer feed forward neural network (MLFFNN), and radial basis function neural network (RBFNN). RNN outperformed the two latter models in forward modeling since hidden layers in RNN are fed with internal processed inputs, which aid in maintaining previous information [277]. Numerical and analytical modeling methods have long been applied to indicate melt pool temperature. However, these methods do not provide the best results, as temperature distribution in real-time is not taken into account. For this issue to be dealt with, a data-driven predictive method was proposed using ML techniques to estimate melt pool temperature while DED was in process with high precision. In this scenario, based on the number and value of the parameters involved, two ML algorithms are chosen; extreme gradient boosting (XGBoost) and long short-term memory [220]. One of the main factors for choosing XGBoost is that it is easy to interpret and visualize and computationally cheaper because it is a decision tree-based model [279]. First proposed by Chen and Guestrin [280], it has earned its popularity in ML applications because of its speed and efficiency. This method creates decision trees in each step and each tree can fit the residual of previous trees. A scalable model achieves excellent property feats in many aspects. Different from random forest (RF) which is a parallel ensemble-based method, XGBoost model is based upon the notion of "boosting," which accounts for all predictions of "weak" learners for further improving more competent learner through step-by-step training routines [281]. Long-short term memory (LSTM) is an algorithm that has the capability to learn long-lasting dependencies, a form of a RNN model. LSTM (Fig. 53) [282] has both forward and backward loops. This model efficiently performs classification, storage, and forecasting of time series information because this model uses a time delay in some spans separating crucial data in a time series. Unlike novel feed-forward NNs, LSTM goes in both forward and backward loops; thus, functions well in addressing deviations such as explosion and losing gradients. LSTM algorithm was first presented by Hochreiter and Schmidhuber, in 1997 [283].

These two methods (XGboost and LSTM) were used to improve the accuracy of melt pool temperature predictions. However, XGBoost is more efficient in terms of computational load. On the other hand, LSTM is more accurate and has more robustness. While DED is a decent choice amongst other AM methods, it has its own disadvantages. Due to the assumptions of entrapped gas, powder melting incompletion, lack of fusion and rapid solidification, no porosity and cracks are formed in the manufactured product [284]. Both algorithms have predicted melt pool temperature with particularly high accuracy. For the cases with large fluctuations

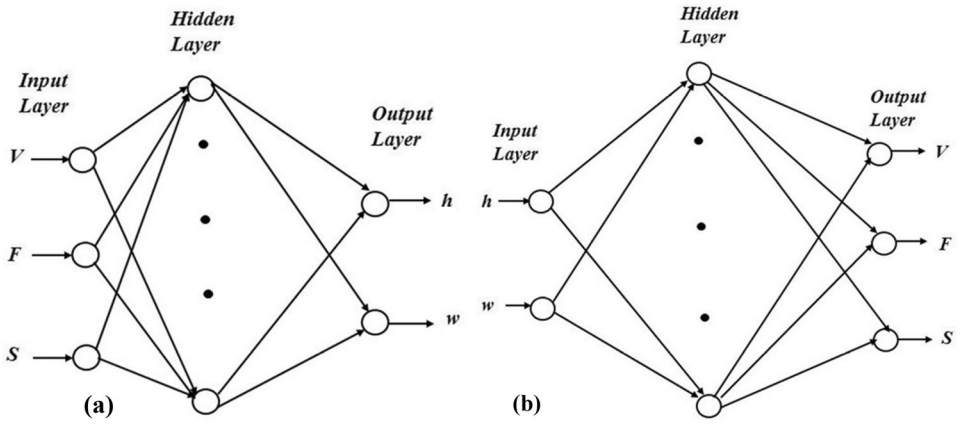

Fig. 52 An example of usage of forward (**a**) and inverse (**b**) modelling for property prediction in an ANN model, where parameters and variables could be swapped to gain different perspective and prediction on parameters [274]

of melt pool temperature, the performance of XGBoost is not far superior to that of LSTM. When melt pool temperature fluctuations are not substantial, LSTM outperformed XGBoost. The computational efficiency of XGBoost, however, is much better than LSTM. The comparison of the performance of XGBoost and LSTM with ridge regression algorithm, which is a linear regression model, revealed that LSTM performed 400 times slower than XGBoost. In future studies, the relationship between melt pool temperature and porosity in DED-fabricated parts using ML techniques should be further investigated [220].

3 Outlook for AM and AI in Industry 4.0

3.1 AM Outlook

AM is regarded as a promising new manufacturing approach compared to the conventional processes. Aside from the precision and freedom in geometry that is brought about via

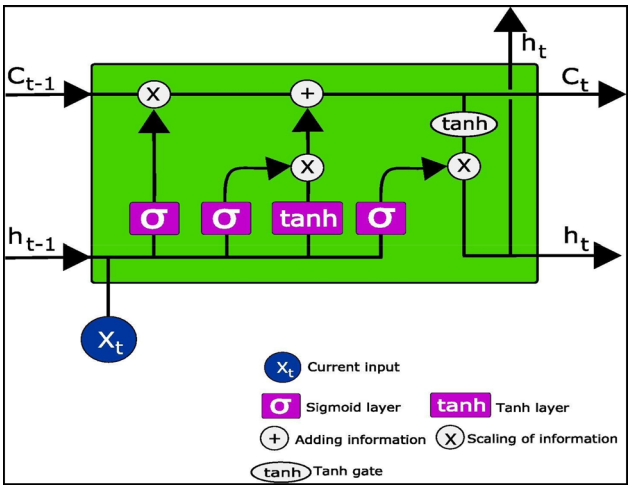

Fig. 53 The operation mechanism of LSTM [282]

AM, the flexibility of the process for initiation, less needed space for the AM installment, and the fact that it is more environmentally friendly make up for a rapidly increasing application in the industry [285]. Moreover, with the vast quantity of data that is generated from each AM process and the aid of AI driven approaches such as ML and DL, AM can be an integral part of the forth industrial evolution [286], as is shown in Fig. 54. 3D printing, ML, DL, and AI approaches are common Information and Communications Technologies (ICT) topics that are of outmost importance.

An example of one of the methods, which is greatly beneficial, is a state-of-the-art method referred to as wire arc additive manufacturing (WAAM)[285, 288]. This method has excellent capability for mass production and the ability to process all materials used in a welding process. However, it is not yet mature and many process parameters are still not optimized, which are amended and more understood via ML approaches. An example is using Gaussian process regressor in a work by Barrionuevo et al. [289]. Moreover, as image processing machinery is advancing in defect detection and general computer vision, better understanding and the underlaying patterns are being realized. An instance of benefits of computer vision is WAAM that is being understood and used with better understanding and with a higher output. As reported in a work done by Li et al. [290], defects owning to voids and lack of fusion are instantly detected after each layer deposition. The current trend of pattern or defect detection and optimization of process parameters is a reoccurring trend that predominantly give more insight to any AM process for any purpose, any type of material, and any type of application or quantity of production. Moreover, with more experience and investment in AM, a myriad of other methods and approaches in AM are arising, such as nano-scale AM [291, 292], Hybrid AM, where AM is used to compliment subtractive manufacturing [293], AM with a printing nozzle of 5 degrees of freedom being capable of printing curves instead of just flat layers [294, 295], electrically assisted 3D printing [296] and responsive material AM

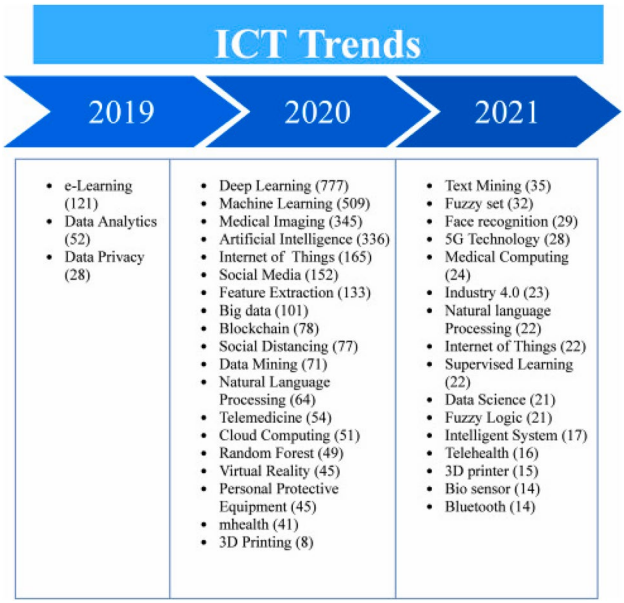

Fig. 54 Common trends in information and communications technologies (ICT) in the last three years [287]

or 4D printing [297]. Overall, over the past 20 years, the 3D printing market has been growing rapidly where worldwide revenue rose 21% from 2017 to 2018, reaching 7 billion USD in 2018. It has become a 10.6 billion USD industry in 2021 and is projected to spike up to 50 billion USD [298]. Ultimately, with the growth of the AM industry in the coming years, health and maintenance of AM machines should be considered. As a result, Analatom, Applied Research Laboratory of Penn State University, and University of California suggest to apply contemporary concepts inspired from simulation runs, corrosion modeling, and control theory merged with PHM in the development of AM materials evaluation in order to understand AM machine health and Manufacturing quality [299] and in another paper by Liu et al. [300], the concept of condition monitoring and fault detection based on machine vision for maintenance of tools and tool health and ability to operate is recognized as a vital measure.

3.2 Self-explanatory ML Systems and More

There are much room for the improvement of AI approaches in general, and particularly, its applications in AM. An instance is self-explanatory ML approaches. The most significant advantage of self-explanatory ML, as the name suggests, is the ability to depict what process takes place for the ML models to decide and make the conclusions the way they did. As crucial as precision is for an ML model, the ability to explain is also as important [301, 302]. Also, it needs to be acknowledged that such models are clustered into two main groups of data-driven and model-driven interpretation. Figure 55 shows the classification of various interpretable methods. The best way of explaining the main difference is that data-driven models work with interpretations of inputs that were given to them and do not require explicit modeling. One case of successful usage of the self-explanatory ML method in AM known as Shapley additive explanations (SHAP) [303].

Besides the great benefits of self-explanatory ML methods, there are other fascinating routes of progression which can help ML and its application in AM, such as the quantum ML methods for maintenance of AM devices [25]. Also, ML methods that require no direct coding, known as no-code ML [304], and incorporation of emerging methods such as internet of things (IOT) and AM with the aid of ML method [305] can be useful in the future of application of cutting edge ML methods in AM.

4 Summary and Outlook

In Table 15, a tabular comparison of the most recent publications reviewed in this paper is provided in detail, dedicated to ML technologies in AM and ML applications. Difficulties and potentials identified by each work are also presented.

As illustrated in the Table above, the findings, challenges, and limitations of the latest papers cited in this review are the lack of data, computational capability, the novelty of the topic of AM and challenges in production. Although some algorithms such as LSTM are very accurate, they demand high computational power and it has been noted that algorithms which are less computationally demanding lack the desired accuracy. Less demanding algorithms in terms of computation power are not yet as accurate [312]. Also, the post-production quality of AM manufactured objects is stated to be a topic that needs much optimization and research [309].

In this review, it was aimed to evaluate how the implementation of AI, especially ML and DL, could revolutionize manufacturing process by pairing this approach with AM, which is a rather new technique, and still has incapability to fully replace the conventional methods of subtractive manufacturing. These ML methods lack enough data banks to create more efficient modeling in ML. Also, gathering data could be done by either numerical or experimental methods which is very expensive for such a multi-physics process like AM and lack of simulating software for AM processes is a notable shortcoming [313]. Furthermore, ML optimized all design steps with good results. However, in topology optimization, the use of support structures hinders the quality of parts and materials and the designer should opt to self-sustaining shapes or considering using support structures that would lessen the quality of part design and needs further research. Moreover, process parameters are widely affected

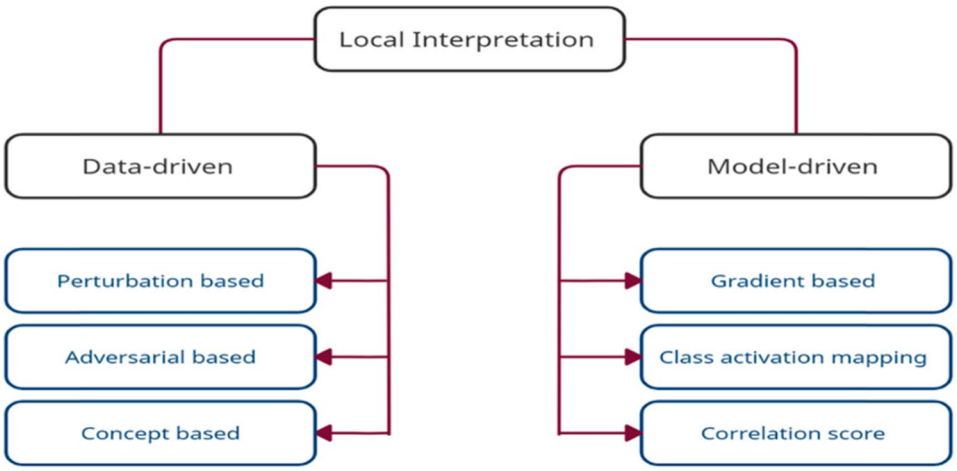

Fig. 55 Classification of various interpretable methods [303]

from device specific factors, thus for each printing device process parameters could be different and that is a challenge to get an optimal print based on the data available for each printing device. Also, in the case of anomaly detection, some improvement could be made to supplement the precision of the techniques used, namely the scope of defect detection, because based on latest efforts only above ηm levels are detected. as a result, there are no imaging of such defects in ML data base to recognize the shape and boundaries of such pores, also the data accusation time is a factor that faster and more optimal algorithms should be developed to overcome this hurdle. The most commonly used methods of AM which have been paired with ML are PBF, DED, and ME. This shows that, since 3D printing is a relatively new branch of manufacturing, many other techniques have not been put to test and experimented with ML techniques. Therefore, further experimentation and investigation using other methods such as Stereolithography and BJ are required as they demand low energy input and have the ability to continuously print, therefore resulting in a faster production rate and substantial time and cost saving.

Furthermore, there is not enough data gathered to better tune and train ML algorithms. Much more effort to collect a better and more extensive data set is required to fully exploit the potential of ML and data driven approaches in AM and more large-scale productions. Overall, AM is still not used for mass production, choice of material is still limited, and, based on the installments and devices that perform AM, production of dimensionally large parts is still challenging and as a result not enough data are generated on dimensionally large-scale AM. Due to these limitations and essence of novelty in AM, statically classified data are very much needed for ML procedures and these data sets are still missing and most ML algorithms are only as good as the data they are being fed.

Declarations

Conflict of interest The authors declare that they have no conflict of interest.

Table 15 A summary of recent works in the application of ML in AM processes

Subject of study	Application	ML/statistical method	Achievements, problems future work	References
Fused deposition modelling (FDM)	Application of a new infill pattern, the lattice infill to improve material proficiency and corrections to shape deviations of 3D prints, paired with ML	The neural network (NN) chosen to deal with a vast amount of data	The suggested strategy saves 45.9–61.3% of the material applied Additional research on the efficiency of material usage should be carried out requirement for data collection and more comprehensive database	[306]
Advancement in the mechanistic models of AM	Numerical modeling of heat transference, fluid movement and mass transference	Implementations of a heat transfer and fluid flow model, shrinking process parameter space	Providing an intuition of the development of many common flaws in 3D prints, and ways to lessen them More research should be performed to develop the beneficial applications of ML and big data in AM, from 5500 available commercial alloys, only a few are now used for AM	[307]
Parameters of (FDM) technology	Finished parts made from polyether ether ketone (PEEK)	3D printed PEEK implants were obtained using Pubmed and search engines such as google scholar	The printing of reproducible tiny-sized PEEK parts with high accuracy has proved to be possible. Consensus on a suitable printing parameter combination has not been reached, optimized parameters for printing worth pursuing	[308]
Prototyping multi-functional and multi-material designs	Geometrical design, process parameter configuration, and in situ anomaly detection	Implementing algorithms to detect imperfections and modulate printing parameters in real time	Proposed algorithms showing efficiency in product design and production still mismatched material properties, lack of build reliability, and prevalent inadequacies in the printed part could be reduced	[134]
Direct energy deposition (DED), melt pool prediction	Estimating the microstructure, porosity, and mechanical properties of DED-fabricated metal parts	Data-driven predictive model using machine learning to estimate melt pool temperature during DED with high accuracy, extreme gradient boosting (XGBoost) and long short-term memory (LSTM)	Experimental results have shown that both XGBoost and LSTM can predict melt pool temperature with high accuracy XGBoost is more efficient than LSTM but not as precise, and wise versa	[220]
Optical volume elements	Information storage, spectral filtering, and imaging applications	Optimization scheme to calculate micro-scale multilayer design, beam propagation method	This approach improves performance when layer separation becomes comparable with the thickness variation of each layer. Frequency noise due to AD imperfections. More accurate forward models are computationally too heavy	[309]
Smart AM and sustainability	Production sustainability and effectiveness	Growth of framework via merging big data analytics, additive manufacturing, and sustainable smart manufacturing technologies	Better decisions for the beginning of life (BOL) stage of product life cycle energy consumption and quality of the product are adequately controlled Proposed BD-SSAM framework is applied only on the BOL stage of product life cycle due to available resources and configuration of IoT devices	[310]

Table 15 (continued)

Subject of study	Application	ML/statistical method	Achievements, problems future work	References
Specific localization and semantic segmentation uncovering of printing circumstances in fused filament fabrication	Discovery of in-plane printing conditions with over-extrusion and under-extrusion in both local–global frameworks	Principal component analysis (PCA), (SVM), (CNN)	Detection latency improved by successfully recognizing the shifts between print quality conditions within a single raster. Detection system is capable of delivering wide-ranging defect statistics for real-time valuation and has great potential for further automated controlling	[222]
In-situ monitoring for detection of layers that are defective in Ti-6Al-4 V 3D printed porous biomaterials	Application of statistical anomaly detection for the analysis of observed data gathered from an LPBF process	Statistical model, generalized extreme studentized deviate	Generalized extreme studentized deviate GESD test is an effective and computationally inexpensive method of identifying defective layers created during LPBF process	[225]
Metal AM by the aid of ML and material development	Examination of possible applications of ML methods to advanced additively manufacturing of metals	NN models, genetic algorithm methods, principal component analysis	Material informatics as a beneficial tool for optimization in AM, ML capable of carrying out data driven designs, control and feedback and flaw detection. Needless to say, there is a need for a standardize system of data sharing	[69]
Predicting microstructure-dependent mechanical properties in additively manufactured metals with machine- and deep-learning methods	Ability of ML and DL models to predict microstructure-sensitive mechanical properties in metal additive manufacturing	Ridge regression, XBGoost, and a custom 3D convolutional neural network (CNN) based on VGG-net	Among all tested data-driven models, CNN models that use crystal orientation as input (with or without auxiliary input features) provide the best predictions, require little pre-processing, and predict spatial-property maps in a matter of seconds	[96]
3-Dimensional optimization in topology	Accelerating 3D TO and determining optimal computational strategy	A 3D encoder-decoder convolutional neural network architecture	For the best performing network, we achieved about 40% reduction in overall computation time while attaining structural accuracy of 96%	[103]
Toolpath design for AM with the aid of reinforced learning	A reinforcement learning platform is proposed that dynamically learns toolpath strategies to build an arbitrary part	DL, reinforced learning deep q-network (DQN), proximal policy optimization (PPO), Soft actor critic (SAC)	The results indicate that this learning-based toolpath design approach achieves high scores, especially when a dense reward structure is present	[120]

Table 15 (continued)

Subject of study	Application	ML/statistical method	Achievements, problems future work	References
Machine learning applications in additive manufacturing	ML applications in AM. The review identifies areas in AM lifecycle, with AM design, process plan, build, post processing, and test and validation, that have been researched using ML	Supervised learning techniques such as NN and SVM, due to the availability of labeled datasets	The high dimensionality and complexity of AM data makes it well-suited for popular ML algorithms. Unsupervised learning techniques are not as widely adopted. However, with the increasing amounts of unlabeled AM datasets, these techniques are likely to become more popular. Moreover, ML models are very poor at diagnosing conditions that have not been previously encountered. This limitation puts an emphasis on collecting data for training by creating scenarios that will address a wide range of operating conditions	[133]
Real-time 3D printing remote defect detection	Identifying 3D printing defects during the printing process by analyzing video captured from the process	Deep NN (single shot detector)	Identifying defects and also with proper adjustments to the algorithm, the printer handler will be informed of high chance of occurrence of defects when there is high probability. The model achieved a precision of 0.44 and a recall of 0.69 in the test set and is not able to generalize in external datasets	[311]
Part separation technique for assembly-based design in additive part separation technique for assembly-based design	Optimization technique for part separation in assembly-based part design	Genetic algorithm, hill climbing optimization	The technique minimizes processing time by optimizing cutting planes using genetic algorithm. It can be extended to different AM technologies including the technologies where support material is required, current work also does not focus on eliminating sharp edges or vertices which can be another area of future research	[188]
ML in AM, novelty methods and potentials	AM design, process parameter tuning, flaw detection and validating	CNN, recurrent neural network, adaptive network-based fuzzy inference system, self-organizing map, deep belief network, unsupervised k-means clustering Semi-supervised, Gaussian mixture model, decision trees, random forest, supervised support vector machines, k-nearest neighbors, Bayesian network, Gaussian process multi-gene genetic programming, Hidden semi-Markova model, multi-layer perceptron	Optimizing process parameters, inspecting powder spreading and monitoring in-process defects. In the creation of AM, ML can help experts in pre-manufacturing planning, and producing quality valuation and control	[202]

Table 15 (continued)

Subject of study	Application	ML/statistical method	Achievements, problems future work	References
ML basis to forecast local strain spreading and the development of plastic anisotropy and fractures in AM	ML based framework is proposed to predict the evolution of local strain distribution, plastic anisotropy and failure during tensile deformation of AlSi10Mg aluminum alloy	ANN models	The suggested model effectively predicts the growth of local strains, plastic anisotropy and failure throughout tensile deformation. The concentration and location of strain hotspots as well as the figure of shear bands and the location of crack openings correctly foretold by the model	[229]

References

1. Dixit US, Hazarika M, Davim JP (2017) Manufacturing through ages. A brief history of mechanical engineering. Springer, Cham, pp 99–125
2. Choudhari CJ, Thakare PS, Sahu SK (2022) 3D printing of composite sandwich structures for aerospace applications. High-performance composite structures: additive manufacturing and processing. Springer, Singapore, pp 45–73
3. Whenish R, Velu R, Anand Kumar S, Ramprasath LS (2022) Additive manufacturing technologies for biomedical implants using functional biocomposites. High-performance composite structures: additive manufacturing and processing. Springer, Singapore, pp 25–44
4. Jandyal A, Chaturvedi I, Wazir I, Raina A, Ul Haq MI (2022) 3D printing—a review of processes, materials and applications in industry 4.0. Sustain Oper Comput 3:33–42. https://doi.org/10.1016/J.SUSOC.2021.09.004
5. Sandström CG (2016) The non-disruptive emergence of an ecosystem for 3D printing—insights from the hearing aid industry's transition 1989–2008. Technol Forecast Soc Change 102:160–168. https://doi.org/10.1016/j.techfore.2015.09.006
6. Jain PK, Jain PK (2021) Use of 3D printing for home applications: a new generation concept. Mater Today Proc. https://doi.org/10.1016/j.matpr.2020.12.145
7. Bi K, Lin D, Liao Y, Wu C-H, Parandoush P (2021) Additive manufacturing embraces big data. Prog Addit Manuf. https://doi.org/10.1007/s40964-021-00172-8
8. Mahamood RM, Akinlabi ET (2016) Laser additive manufacturing. 3D printing: breakthroughs in research and practice. IGI Global, Hershey, pp 154–171
9. Leary M (2019) Design for additive manufacturing. Elsevier, Amsterdam
10. Ali SF, Malik FM, Kececi EF, Bal B (2019) Optimization of additive manufacturing for layer sticking and dimensional accuracy. Additive manufacturing technologies from an optimization perspective. IGI Global, Hershey, pp 185–198
11. Rias AL, Bouchard C, Segonds F, Vayre B, Abed S (2017) Design for additive manufacturing: supporting intrinsic-motivated creativity. Emotional engineering, vol 5. Springer, Cham, pp 99–115
12. Provaggi E, Kalaskar DM (2017) 3D printing families: laser, powder, nozzle based techniques. 3D printing in medicine. Elsevier Inc, Amsterdam, pp 21–42
13. Gaisford S (2017) 3D printed pharmaceutical products. 3D printing in medicine. Elsevier Inc, Amsterdam, pp 155–166
14. Capelli C, Schievano S (2017) Computational analyses and 3D printed models: a combined approach for patient-specific studies. 3D printing in medicine. Elsevier Inc, Amsterdam, pp 73–90
15. Roopavath UK, Kalaskar DM (2017) Introduction to 3D printing in medicine. 3D printing in medicine. Elsevier Inc, Amsterdam, pp 1–20
16. Sima F, Sugioka K, Vázquez RM, Osellame R, Kelemen L, Ormos P (2018) Three-dimensional femtosecond laser processing for lab-on-a-chip applications. Nanophotonics 7:613–634. https://doi.org/10.1515/nanoph-2017-0097
17. Mishra PK, Senthil P, Adarsh S, Anoop MS (2021) An investigation to study the combined effect of different infill pattern and infill density on the impact strength of 3D printed polylactic acid parts. Compos Commun 24:100605. https://doi.org/10.1016/j.coco.2020.100605
18. Agrawaal H, Thompson JE (2021) Additive manufacturing (3D Printing) for analytical chemistry. Talanta Open. https://doi.org/10.1016/j.talo.2021.100036

19. Ngo TD, Kashani A, Imbalzano G, Nguyen KTQ, Hui D (2018) Additive manufacturing (3D printing): a review of materials, methods, applications and challenges. Compos Part B Eng 143:172–196. https://doi.org/10.1016/j.compositesb.2018.02.012
20. Pazhamannil RV, Govindan P (2021) Current state and future scope of additive manufacturing technologies via vat photopolymerization. Mater Today Proc. https://doi.org/10.1016/j.matpr.2020.11.225
21. Richter S, Wischmann Iit-Berlin S (n.d.) Additive manufacturing methods-state of development, market prospects for industrial use and ICT-specific challenges in research and development: a study within the scope of scientific assistance for the AUTONOMICS for Industry 4.0 technology programme of the Federal Ministry for Economic Affairs and Energy. www.autonomik40.de. Accessed 28 Feb 2021
22. Qi X, Chen G, Li Y, Cheng X, Li C (2019) Applying neural-network-based machine learning to additive manufacturing: current applications, challenges, and future perspectives. Engineering 5:721–729. https://doi.org/10.1016/j.eng.2019.04.012
23. Huang DJ, Li H (2021) A machine learning guided investigation of quality repeatability in metal laser powder bed fusion additive manufacturing. Mater Des 203:109606. https://doi.org/10.1016/j.matdes.2021.109606
24. Jain AK, Lad BK (2017) A novel integrated tool condition monitoring system. J Intell Manuf 30:1423–1436. https://doi.org/10.1007/S10845-017-1334-2
25. Sharma V, Gupta S, Mehta G, Lad BK (2021) A quantum-based diagnostics approach for additive manufacturing machine. IET Collab Intell Manuf 3:184–192. https://doi.org/10.1049/CIM2.12022
26. Leary M (2020) Powder bed fusion. Design for additive manufacturing. Elsevier, Amsterdam, pp 295–319
27. Vock S, Klöden B, Kirchner A, Weißgärber T, Kieback B (2019) Powders for powder bed fusion: a review. Prog Addit Manuf 4:383–397. https://doi.org/10.1007/s40964-019-00078-6
28. Goodridge R, Ziegelmeier S (2017) Powder bed fusion of polymers. Laser additive manufacturing. Elsevier, Amsterdam, pp 181–204
29. Dev Singh D, Mahender T, Raji Reddy A (2021) Powder bed fusion process: a brief review. Mater Today Proc 46:350–355. https://doi.org/10.1016/J.MATPR.2020.08.415
30. Additive Manufacturing Machines, GE Additive (n.d.) https://www.ge.com/additive/additive-manufacturing/machines. Accessed 27 Feb 2021
31. High-Quality Industrial Metal 3D Printers, SLM Solutions (n.d.) https://www.slm-solutions.com/products-and-solutions/machines/. Accessed 27 Feb 2021
32. Metal 3D printer, DMLS Printer, Additive Manufacturing Systems (n.d.) https://www.eos.info/en/additive-manufacturing/3d-printing-metal/eos-metal-systems. Accessed 27 Feb 2021
33. Narayana PL, Lee S, Choi SW, Li CL, Park CH, Yeom JT, Reddy NS, Hong JK (2019) Microstructural response of β-stabilized Ti–6Al–4V manufactured by direct energy deposition. J Alloys Compd 811:152021. https://doi.org/10.1016/J.JALLCOM.2019.152021
34. Zenou M, Grainger L (2018) Additive manufacturing of metallic materials. Addit Manuf Mater Process Quantif Appl. https://doi.org/10.1016/B978-0-12-812155-9.00003-7
35. Khan I, Kumar N (2020) Fused deposition modelling process parameters influence on the mechanical properties of ABS: a review. Mater Today Proc 44:4004–4008. https://doi.org/10.1016/j.matpr.2020.10.202
36. Piscopo G, Iuliano L (2022) Current research and industrial application of laser powder directed energy deposition. Int J Adv Manuf Technol 2022:1–25. https://doi.org/10.1007/S00170-021-08596-W
37. Gebisa AW, Lemu HG (2018) Investigating effects of fused-deposition modeling (FDM) processing parameters on flexural properties of ULTEM 9085 using designed experiment. Materials. https://doi.org/10.3390/ma11040500
38. Sai T, Pathak VK, Srivastava AK (2020) Modeling and optimization of fused deposition modeling (FDM) process through printing PLA implants using adaptive neuro-fuzzy inference system (ANFIS) model and whale optimization algorithm. J Braz Soc Mech Sci Eng 42:617. https://doi.org/10.1007/s40430-020-02699-3
39. Rahmati S (2014) Direct rapid tooling A2. Comprehensive materials processing. Elsevier, Amsterdam, pp 303–344
40. Levy GN, Schindel R, Kruth JP (2003) Rapid manufacturing and rapid tooling with layer manufacturing (LM) technologies, state of the art and future perspectives. CIRP Ann 52:589–609. https://doi.org/10.1016/S0007-8506(07)60206-6
41. Pilipović A, Raos P, Šercer M (2009) Experimental analysis of properties of materials for rapid prototyping. Int J Adv Manuf Technol 40:105–115. https://doi.org/10.1007/s00170-007-1310-7
42. Rigon D, Ricotta M, Meneghetti G (2020) A literature survey on structural integrity of 3D printed virgin and recycled ABS and PP compounds. Procedia Struct Integr 28:1655–1663. https://doi.org/10.1016/J.PROSTR.2020.10.139
43. Yang Y, Li X, Zheng X, Chen Z, Zhou Q, Chen Y (2018) 3D-printed biomimetic super-hydrophobic structure for microdroplet manipulation and oil/water separation. Adv Mater 30:1704912. https://doi.org/10.1002/ADMA.201704912
44. Li X, Chen Y (2017) Micro-scale feature fabrication using immersed surface accumulation. J Manuf Process 28:531–540. https://doi.org/10.1016/J.JMAPRO.2017.04.022
45. Xu X, Awad A, Robles-Martinez P, Gaisford S, Goyanes A, Basit AW (2021) Vat photopolymerization 3D printing for advanced drug delivery and medical device applications. J Control Release 329:743–757. https://doi.org/10.1016/J.JCONREL.2020.10.008
46. Mao H, Leung Y-S, Li Y, Hu P, Wu W, Chen Y (2017) Multiscale stereolithography using shaped beams. J Micro Nano-Manuf. https://doi.org/10.1115/1.4037832
47. Pan Y, Zhou C, Chen Y (2012) A fast mask projection stereolithography process for fabricating digital models in minutes. J Manuf Sci Eng. https://doi.org/10.1115/1.4007465
48. Zhou C, Chen Y (2012) Additive manufacturing based on optimized mask video projection for improved accuracy and resolution. J Manuf Process 14:107–118. https://doi.org/10.1016/J.JMAPRO.2011.10.002
49. Li X, Mao H, Pan Y, Chen Y (2019) Mask video projection-based stereolithography with continuous resin flow. J Manuf Sci Eng. https://doi.org/10.1115/1.4043765
50. Tumbleston JR, Shirvanyants D, Ermoshkin N, Janusziewicz R, Johnson AR, Kelly D, Chen K, Pinschmidt R, Rolland JP, Ermoshkin A, Samulski ET, DeSimone JM (2015) Continuous liquid interface production of 3D objects. Science 347:1349–1352. https://doi.org/10.1126/SCIENCE.AAA2397
51. He H, Yang Y, Pan Y (2019) Machine learning for continuous liquid interface production: printing speed modelling. J Manuf Syst 50:236–246. https://doi.org/10.1016/J.JMSY.2019.01.004
52. Johnson AR, Caudill CL, Tumbleston JR, Bloomquist CJ, Moga KA, Ermoshkin A, Shirvanyants D, Mecham SJ, Luft JC, De Simone JM (2016) Single-step fabrication of computationally designed microneedles by continuous liquid interface production. PLoS ONE. https://doi.org/10.1371/JOURNAL.PONE.0162518
53. ASTM International—Standards Worldwide (n.d.) https://www.astm.org/. Accessed 29 Aug 2021

54. The 7 categories of Additive Manufacturing, Additive Manufacturing Research Group | Loughborough University (n.d.) https://www.lboro.ac.uk/research/amrg/about/the7categoriesofadditivemanufacturing/. Accessed 29 Aug 2021
55. Designation: F2792—12a (n.d.) https://doi.org/10.1520/F2792-12A.
56. Udroiu R, Braga IC (2017) Polyjet technology applications for rapid tooling. MATEC Web Conf 112:1–6. https://doi.org/10.1051/matecconf/201711203011
57. Hassan Saba M, Mukherjee S, Dutta S, Kumar Mallisetty P, Chandra Murmu N (2021) Electrohydrodynamic jet printing for desired print diameter. Mater Today Proc 46:1749–1754. https://doi.org/10.1016/J.MATPR.2020.07.570
58. Pilipović A, Baršić G, Katić M, Havstad MR (2020) Repeatability and reproducibility assessment of a polyjet technology using X-ray computed tomography. Appl Sci 10:1–14. https://doi.org/10.3390/app10207040
59. Bagheri A, Jin J (2019) Photopolymerization in 3D printing. ACS Appl Polym Mater 1:593–611. https://doi.org/10.1021/acsapm.8b00165
60. O'Neill P, Jolivet L, Kent NJ, Brabazon D (2017) Physical integrity of 3D printed parts for use as embossing tools. Adv Mater Process Technol 3:308–317. https://doi.org/10.1080/2374068X.2017.1330842
61. Gülcan O, Günaydın K, Tamer A (2021) The state of the art of material jetting—a critical review. Polymers (Basel). https://doi.org/10.3390/polym13162829
62. Revilla-León M, Özcan M (2019) Additive manufacturing technologies used for processing polymers: current status and potential application in prosthetic dentistry. J Prosthodont 28:146–158. https://doi.org/10.1111/jopr.12801
63. Lee J, An J, Chua CK (2017) Fundamentals and applications of 3D printing for novel materials. Appl Mater Today 7:120–133. https://doi.org/10.1016/j.apmt.2017.02.004
64. Obikawa T, Yoshino M, Shinozuka J (1999) Sheet steel lamination for rapid manufacturing. J Mater Process Technol 90:171–176
65. Li Y, Wang S, Tian Q, Ding X (2015) Feature representation for statistical-learning-based object detection: a review. Pattern Recognit 48:3542–3559. https://doi.org/10.1016/j.patcog.2015.04.018
66. Gu C, Liu C, Zhang J, Huang H, Jia X (2015) Green scheduling for cloud data centers using renewable resources. In: Proceedings of IEEE INFOCOM, Institute of Electrical and Electronics Engineers Inc. pp 354–359. https://doi.org/10.1109/INFCOMW.2015.7179410.
67. Wang P, Liu H, Wang L, Gao RX (2018) Deep learning-based human motion recognition for predictive context-aware human-robot collaboration. CIRP Ann 67:17–20. https://doi.org/10.1016/j.cirp.2018.04.066
68. Weimer D, Scholz-Reiter B, Shpitalni M (2016) Design of deep convolutional neural network architectures for automated feature extraction in industrial inspection. CIRP Ann 65:417–420. https://doi.org/10.1016/j.cirp.2016.04.072
69. Johnson NS, Vulimiri PS, To AC, Zhang X, Brice CA, Kappes BB, Stebner AP (2020) Invited review: machine learning for materials developments in metals additive manufacturing. Addit Manuf 36:101641. https://doi.org/10.1016/j.addma.2020.101641
70. Rostyslav D, Reinforcement Learning Applications (2020) https://perfectial.com/blog/reinforcement-learning-applications/. Accessed 22 Jan 2021
71. Nikolaou N, Reeve H, Brown G (2020) Margin maximization as lossless maximal compression. http://arxiv.org/abs/2001.10318. Accessed 29 Mar 2021
72. Al-Azzam N, Shatnawi I (2021) Comparing supervised and semi-supervised machine learning models on diagnosing breast cancer. Ann Med Surg 62:53–64. https://doi.org/10.1016/j.amsu.2020.12.043
73. Sun C, Shrivastava A, Singh S, Gupta A (2017) Revisiting unreasonable effectiveness of data in deep learning era
74. Singh D, Singh B (2020) Investigating the impact of data normalization on classification performance. Appl Soft Comput 97:105524. https://doi.org/10.1016/j.asoc.2019.105524
75. Späth H (1992) Introduction. Mathematical algorithms for linear regression. Elsevier, Amsterdam, pp 1–15
76. Botchkarev A (2018) Performance metrics (error measures) in machine learning regression forecasting and prognostics: properties and typology. Interdiscip J Inf Knowl Manage 14:45–76. https://doi.org/10.28945/4184
77. Park J, John Park ASD, Mackay S (2003) Practical data acquisition for instrumentation and control systems. Newnes, Boston
78. Li Y, Yu X, Koudas N (2021) Data acquisition for improving machine learning models. Proc VLDB Endow 14:2150–8097. https://doi.org/10.14778/3467861.3467872
79. Google AI Blog: Deep learning for detection of diabetic eye disease (n.d.) https://ai.googleblog.com/2016/11/deep-learning-for-detection-of-diabetic.html. Accessed 8 Jan 2022
80. Roh Y, Heo G, Whang SE (2021) A survey on data collection for machine learning: a big data-ai integration perspective. IEEE Trans Knowl Data Eng 33:1328–1347. https://doi.org/10.1109/TKDE.2019.2946162
81. Nath V, Levinson SE (2014) Machine learning. https://doi.org/10.1007/978-3-319-05606-7_6
82. Mohammed M, Khan MB, Bashie EBM (2016) Machine learning: algorithms and applications. CRC Press, Boca Raton, pp 1–204
83. Aggarwal A, Srivastava A, Agarwal A, Chahal N, Singh D, Alnuaim AA, Alhadlaq A, Lee HN (2022) Two-way feature extraction for speech emotion recognition using deep learning. Sensors 22:2378. https://doi.org/10.3390/S22062378
84. Smith LN, Topin N (2017) Super-convergence: very fast training of neural networks using large learning rates. Artif Intell Mach Learn Multi-domain Oper Appl. https://doi.org/10.48550/arxiv.1708.07120
85. Yang L, Shami A (2020) On hyperparameter optimization of machine learning algorithms: theory and practice. Neurocomputing 415:295–316. https://doi.org/10.1016/j.neucom.2020.07.061
86. IBM Education (2020) What is unsupervised learning?. IBM. pp 1–8. Accessed from https://www.ibm.com/cloud/learn/unsupervised-learning.
87. Michau G, Fink O (2021) Unsupervised transfer learning for anomaly detection: application to complementary operating condition transfer. Knowl Based Syst 216:106816. https://doi.org/10.1016/j.knosys.2021.106816
88. Shi Z, Al Mamun A, Kan C, Tian W, Liu C (2022) An LSTM-autoencoder based online side channel monitoring approach for cyber-physical attack detection in additive manufacturing. J Intell Manuf. https://doi.org/10.1007/S10845-021-01879-9
89. What is reinforcement learning?—MATLAB & Simulink—MathWorks 中国, (n.d.). https://ww2.mathworks.cn/help/reinforcement-learning/ug/what-is-reinforcement-learning.html. Accessed 29 June 2021
90. Nguyen H, La HM (2019) Review of deep reinforcement learning for robot manipulation. pp 590–595. https://doi.org/10.1109/IRC.2019.00120.
91. Heuillet A, Couthouis F, Díaz-Rodríguez N (2021) Explainability in deep reinforcement learning. Knowl Based Syst 214:106685. https://doi.org/10.1016/j.knosys.2020.106685
92. Dharmawan AG, Xiong Y, Foong S, Song Soh G (2020) A model-based reinforcement learning and correction framework for process control of robotic wire arc additive manufacturing.

Proc IEEE Int Conf Robot Autom. https://doi.org/10.1109/ICRA40945.2020.9197222
93. Jiao Y, Du P (2016) Performance measures in evaluating machine learning based bioinformatics predictors for classifications. Quant Biol 4:320–330. https://doi.org/10.1007/s40484-016-0081-2
94. Cihan P, Coskun H (2021) Performance comparison of machine learning models for diabetes prediction. In: SIU 2021—29th IEEE Conference on Signal Processing and Communications Applications Conference. https://doi.org/10.1109/SIU53274.2021.9477824
95. Xu Y, Zhou Y, Sekula P, Ding L (2021) Machine learning in construction: from shallow to deep learning. Dev Built Environ 6:100045. https://doi.org/10.1016/j.dibe.2021.100045
96. Herriott C, Spear AD (2020) Predicting microstructure-dependent mechanical properties in additively manufactured metals with machine- and deep-learning methods. Comput Mater Sci. https://doi.org/10.1016/j.commatsci.2020.109599
97. Dong S, Wang P, Abbas K (2021) A survey on deep learning and its applications. Comput Sci Rev 40:100379. https://doi.org/10.1016/j.cosrev.2021.100379
98. Lecun Y, Bengio Y, Hinton G (2015) Deep learning. Nature 521:436–444. https://doi.org/10.1038/nature14539
99. Li Y, Zhou X, Colnaghi T, Wei Y, Marek A, Li H, Bauer S, Rampp M, Stephenson LT (2021) Convolutional neural network-assisted recognition of nanoscale L12 ordered structures in face-centred cubic alloys. Npj Comput Mater 7:1–9. https://doi.org/10.1038/s41524-020-00472-7
100. Saishu Y, Poorjam AH, Christensen MG (2021) A CNN-based approach to identification of degradations in speech signals. Eurasip J Audio Speech Music Process 2021:9. https://doi.org/10.1186/s13636-021-00198-4
101. Esteva A, Chou K, Yeung S, Naik N, Madani A, Mottaghi A, Liu Y, Topol E, Dean J, Socher R (2021) Deep learning-enabled medical computer vision. Npj Digit Med 4:1–9. https://doi.org/10.1038/s41746-020-00376-2
102. Feng S, Fu H, Zhou H, Wu Y, Lu Z, Dong H (2021) A general and transferable deep learning framework for predicting phase formation in materials. Npj Comput Mater 7:1–10. https://doi.org/10.1038/s41524-020-00488-z
103. Banga S, Gehani H, Bhilare S, Patel S, Kara L (2018) 3D topology optimization using convolutional neural networks, ArXiv. http://arxiv.org/abs/1808.07440. Accessed 4 Apr 2021
104. Cang R, Yao H, Ren Y (2019) One-shot generation of near-optimal topology through theory-driven machine learning. CAD Comput Aided Des 109:12–21. https://doi.org/10.1016/j.cad.2018.12.008
105. How recurrent neural networks work by Simeon Kostadinov towards data science (n.d.) https://towardsdatascience.com/learn-how-recurrent-neural-networks-work-84e975feaaf7. Accessed 7 Jan 2022
106. Agatonovic-Kustrin S, Beresford R (2000) Basic concepts of artificial neural network (ANN) modeling and its application in pharmaceutical research. J Pharm Biomed Anal 22:717–727. https://doi.org/10.1016/S0731-7085(99)00272-1
107. Kiang MY (2003) Neural networks. Encyclopedia of information systems. Elsevier, Amsterdam, pp 303–315
108. Kussul E, Baidyk T, Wunsch DC (2010) Classical neural networks. Neural networks and micromechanics. Springer, Berlin, pp 7–25
109. A comprehensive guide to convolutional neural networks—the ELI5 way by Sumit Saha towards data science (n.d.) https://towardsdatascience.com/a-comprehensive-guide-to-convolutional-neural-networks-the-eli5-way-3bd2b1164a53. Accessed 7 Jan 2022
110. Kevin Zhou S, Fichtinger G, Rueckert D (2019) Handbook of medical image computing and computer assisted intervention. Elsevier, Amsterdam, pp 1–1043
111. Computer Vision (2018) https://doi.org/10.1016/C2015-0-05563-0
112. Reimers C, Requena-Mesa C (2020) Deep learning—an opportunity and a challenge for geo- and astrophysics. Knowledge discovery in big data from astronomy and earth observation. Elsevier, Amsterdam, pp 251–265
113. Nie F, Hu Z, Li X (2018) An investigation for loss functions widely used in machine learning. Commun Inf Syst 18:37–52. https://doi.org/10.4310/cis.2018.v18.n1.a2
114. Bridgelall R (n.d.) Introduction to support vector machines
115. Tripathi S, Hemachandra N (2018) Scalable linear classiiers based on exponential loss function. ACM Ref Format. https://doi.org/10.1145/3152494.3152521
116. Duchi J (n.d.) CS229 supplemental lecture notes
117. De Boer PT, Kroese DP, Rubinstein RY (n.d.) A tutorial on the cross-entropy method
118. Zhang W, Wang H, Hartmann C, Weber M, Schutte C, Schutte S (2014) Applications of the cross-entropy method to importance sampling and optimal control of diffusions. Soc Ind Appl Math. https://doi.org/10.1137/14096493X
119. Botev ZI, Kroese DP (2009) The generalized cross entropy method, with applications to probability density estimation. Methodol Comput Appl Probab 13:1
120. Mozaffar M, Ebrahimi A, Cao J (2020) Toolpath design for additive manufacturing using deep reinforcement learning a preprint
121. Audibert J, Michiardi P, Guyard F, Marti S, Zuluaga MA (2020) USAD : unsupervised anomaly detection on multivari-ate time series. p 20. https://doi.org/10.1145/3394486.3403392.
122. Goh GD, Sing SL, Yeong WY (2021) A review on machine learning in 3D printing: applications, potential, and challenges. Springer, Dordrecht
123. Li Y, Wan J, Liu A, Jiao Y, Rainer R (2022) Data-driven chaos indicator for nonlinear dynamics and applications on storage ring lattice design. Nucl Instrum Methods Phys Res Sect A. https://doi.org/10.1016/j.nima.2021.166060
124. Hwang SY, Kim Y, Lee JH (2016) Finite element analysis of residual stress distribution in a thick plate joined using two-pole tandem electro-gas welding. J Mater Process Technol 229:349–360. https://doi.org/10.1016/j.jmatprotec.2015.09.037
125. Khairallah SA, Anderson AT, Rubenchik A, King WE (2016) Laser powder-bed fusion additive manufacturing: physics of complex melt flow and formation mechanisms of pores, spatter, and denudation zones. Acta Mater 108:36–45. https://doi.org/10.1016/j.actamat.2016.02.014
126. Toyserkani E, Khajepour A, Corbin S (2004) 3-D finite element modeling of laser cladding by powder injection: effects of laser pulse shaping on the process. Opt Lasers Eng 41:849–867. https://doi.org/10.1016/S0143-8166(03)00063-0
127. Dai D, Gu D (2014) Thermal behavior and densification mechanism during selective laser melting of copper matrix composites: Simulation and experiments. Mater Des 55:482–491. https://doi.org/10.1016/j.matdes.2013.10.006
128. Gouge M, Michaleris P, Denlinger E, Irwin J (2018) The finite element method for the thermo-mechanical modeling of additive manufacturing processes. Thermo-mechanical modeling of additive manufacturing. Elsevier Inc, Amsterdam, pp 19–38
129. Nie P, Ojo OA, Li Z (2014) Numerical modeling of microstructure evolution during laser additive manufacturing of a nickel-based superalloy. Acta Mater 77:85–95. https://doi.org/10.1016/j.actamat.2014.05.039

130. Michaleris P (2014) Modeling metal deposition in heat transfer analyses of additive manufacturing processes. Finite Elem Anal Des 86:51–60. https://doi.org/10.1016/j.finel.2014.04.003
131. Jalalahmadi B, Liu J, Liu Z, Vechart A, Weinzapfel N (2021) An integrated computational materials engineering predictive platform for fatigue prediction and qualification of metallic parts built with additive manufacturing. J Tribol. https://doi.org/10.1115/1.4050941
132. Rajan K (2005) Materials informatics. Mater Today 8:38–45. https://doi.org/10.1016/S1369-7021(05)71123-8
133. Razvi SS, Feng S, Narayanan A, Lee YTT, Witherell P (2019) IDETC2019-98415 A review of machine learning applications in additive manufacturing.
134. Jin Z, Zhang Z, Demir K, Gu GX (2020) Machine learning for advanced additive manufacturing. Matter 3:1541–1556. https://doi.org/10.1016/j.matt.2020.08.023
135. Zhu JH, Zhang WH, Xia L (2016) Topology optimization in aircraft and aerospace structures design. Arch Comput Methods Eng 23:595–622. https://doi.org/10.1007/s11831-015-9151-2
136. Liu Z, Li M, Tay YWD, Weng Y, Wong TN, Tan MJ (2020) Rotation nozzle and numerical simulation of mass distribution at corners in 3D cementitious material printing. Addit Manuf 34:101190. https://doi.org/10.1016/j.addma.2020.101190
137. Laufer F, Roth D, Binz H (2019) An investigation into the influence of mass distribution on conceptual lightweight design. Procedia CIRP. https://doi.org/10.1016/j.procir.2019.04.304
138. Cheng B, Chou K (2020) A numerical investigation of support structure designs for overhangs in powder bed electron beam additive manufacturing. J Manuf Process 49:187–195. https://doi.org/10.1016/j.jmapro.2019.11.018
139. Han Q, Gu H, Soe S, Setchi R, Lacan F, Hill J (2018) Manufacturability of AlSi10Mg overhang structures fabricated by laser powder bed fusion. Mater Des 160:1080–1095. https://doi.org/10.1016/j.matdes.2018.10.043
140. Vantyghem G, De Corte W, Shakour E, Amir O (2020) 3D printing of a post-tensioned concrete girder designed by topology optimization. Autom Constr 112:103084. https://doi.org/10.1016/j.autcon.2020.103084
141. Mirzendehdel AM, Suresh K (2016) Support structure constrained topology optimization for additive manufacturing. CAD Comput Aided Des 81:1–13. https://doi.org/10.1016/j.cad.2016.08.006
142. Mantovani S, Campo GA, Ferrari A (2020) Additive manufacturing and topology optimization: A design strategy for a steering column mounting bracket considering overhang constraints. Proc Inst Mech Eng Part C. https://doi.org/10.1177/0954406220917717
143. Gaynor AT, Guest JK (2014) Topology optimization for additive manufacturing: Considering maximum overhang constraint. In: AIAA Aviation 2014—15th AIAA/ISSMO Multidisciplinary Analysis and Optimization Conference, American Institute of Aeronautics and Astronautics Inc., 2014. https://doi.org/10.2514/6.2014-2036
144. Brackett D, Ashcroft I, Hague R (n.d.) Topology optimization for additive manufacturing
145. Gu GX, Chen CT, Buehler MJ (2018) De novo composite design based on machine learning algorithm. Extrem Mech Lett 18:19–28. https://doi.org/10.1016/j.eml.2017.10.001
146. Wilt JK, Yang C, Gu GX (2020) Accelerating auxetic metamaterial design with deep learning. Adv Eng Mater 22:1901266. https://doi.org/10.1002/adem.201901266
147. Ozguc S, Pan L, Weibel JA (2021) Topology optimization of microchannel heat sinks using a homogenization approach. Int J Heat Mass Transf 169:120896. https://doi.org/10.1016/j.ijheatmasstransfer.2020.120896
148. Cheng L, Liu J, Liang X, To AC (2018) Coupling lattice structure topology optimization with design-dependent feature evolution for additive manufactured heat conduction design. Comput Methods Appl Mech Eng 332:408–439. https://doi.org/10.1016/j.cma.2017.12.024
149. Vogiatzis P, Chen S, Wang X, Li T, Wang L (2017) Topology optimization of multi-material negative Poisson's ratio metamaterials using a reconciled level set method. CAD Comput Aided Des 83:15–32. https://doi.org/10.1016/j.cad.2016.09.009
150. Tejani GG, Savsani VJ, Patel VK (2016) Adaptive symbiotic organisms search (SOS) algorithm for structural design optimization. J Comput Des Eng 3:226–249. https://doi.org/10.1016/j.jcde.2016.02.003
151. Tejani GG, Kumar S, Gandomi AH (2021) Multi-objective heat transfer search algorithm for truss optimization. Eng Comput 37:641–662. https://doi.org/10.1007/s00366-019-00846-6
152. Tejani GG, Savsani VJ, Bureerat S, Patel VK, Savsani P (2019) Topology optimization of truss subjected to static and dynamic constraints by integrating simulated annealing into passing vehicle search algorithms. Eng Comput 35:499–517. https://doi.org/10.1007/s00366-018-0612-8
153. Kumar S, Kumar R, Agarwal RP, Samet B (2020) A study of fractional Lotka-Volterra population model using Haar wavelet and Adams-Bashforth-Moulton methods. Math Methods Appl Sci 43:5564–5578. https://doi.org/10.1002/mma.6297
154. Tejani GG, Pholdee N, Bureerat S, Prayogo D, Gandomi AH (2019) Structural optimization using multi-objective modified adaptive symbiotic organisms search. Expert Syst Appl 125:425–441. https://doi.org/10.1016/j.eswa.2019.01.068
155. Gu GX, Chen CT, Richmond DJ, Buehler MJ (2018) Bioinspired hierarchical composite design using machine learning: simulation, additive manufacturing, and experiment. Mater Horizons 5:939–945. https://doi.org/10.1039/c8mh00653a
156. Singh K, Kapania RK (2021) Accelerated optimization of curvilinearly stiffened panels using deep learning. Thin-Walled Struct 161:107418. https://doi.org/10.1016/j.tws.2020.107418
157. Singh K, Zhao W, Jrad M, Kapania RK (2019) Hybrid optimization of curvilinearly stiffened shells using parallel processing. J Aircr 56:1068–11079. https://doi.org/10.2514/1.C035069
158. MSC Nastran (n.d.) https://www.mscsoftware.com/de/product/msc-nastran. Accessed 17 Apr 2021
159. Sosnovik I, Oseledets I (2019) Neural networks for topology optimization. Russ J Numer Anal Math Model 34:215–223. https://doi.org/10.1515/RNAM-2019-0018
160. Harish B, Eswara Sai Kumar K, Srinivasan B (2020) Topology optimization using convolutional neural network. Advances in multidisciplinary analysis and optimization. Springer, Singapore, pp 301–307
161. Grierson D, Rennie AEW, Quayle SD, Agarwal R, Ruta G (2021) Machine learning for additive manufacturing. Encyclopedia. https://doi.org/10.3390/encyclopedia1030048
162. Shi Y, Zhang Y, Baek S, De Backer W, Harik R (2018) Manufacturability analysis for additive manufacturing using a novel feature recognition technique. CAD Solut LLC 15:941–952. https://doi.org/10.1080/16864360.2018.1462574
163. Williams G, Meisel NA, Simpson TW, McComb C (2019) Design repository effectiveness for 3D convolutional neural networks: application to additive manufacturing. J Mech Des Trans ASME 141:1–12. https://doi.org/10.1115/1.4044199
164. Yao X, Moon SK, Bi G (2017) A hybrid machine learning approach for additive manufacturing design feature recommendation. Rapid Prototyp J 23:983–997. https://doi.org/10.1108/RPJ-03-2016-0041
165. Huang Q, Nouri H, Xu K, Chen Y, Sosina S, Dasgupta T (2014) Statistical predictive modeling and compensation of geometric

deviations of three-dimensional printed products. J Manuf Sci Eng Trans ASME 136:1–10. https://doi.org/10.1115/1.4028510
166. Zhu Z, Anwer N, Huang Q, Mathieu L (2018) Machine learning in tolerancing for additive manufacturing. CIRP Ann 67:157–160. https://doi.org/10.1016/j.cirp.2018.04.119
167. Ghadai S, Balu A, Krishnamurthy A, Sarkar S (2017) Learning and visualizing localized geometric features using 3D-CNN: an application to manufacturability analysis of drilled holes. Accessed from http://arxiv.org/abs/1711.04851.
168. Lederer A, Conejo AJ, Maier KA, Xiao W, Umlauft J, Hirche S (2021) Gaussian process-based real-time learning for safety critical applications
169. Guo Liu JL, Zhang X (2021) Additive manufacturing of structural materials. Mater Sci Eng R Rep. https://doi.org/10.1016/j.mser.2020.100596
170. Additive Manufacturing Materials, Additive Manufacturing (n.d.) https://www.additivemanufacturing.media/kc/what-is-additive-manufacturing/am-materials. Accessed 28 May 2022
171. Hannifin P (2022) Solve the mysteries of the universe. 29: 1–60
172. Hoon Kang S, Lemes Jorge V, Ribeiro Teixeira F, Scotti A (2022) Pyrometrical interlayer temperature measurement in WAAM of thin wall: strategies, limitations and functionality. Metals 12:765. https://doi.org/10.3390/MET12050765
173. Tagawa Y, Maskeliūnas R, Damaševičius R (2021) Acoustic anomaly detection of mechanical failures in noisy real-life factory environments. Electronics 10:2329. https://doi.org/10.3390/ELECTRONICS10192329
174. Guo AXY, Cheng L, Zhan S, Zhang S, Xiong W, Wang Z, Wang G, Cao SC (2022) Biomedical applications of the powder-based 3D printed titanium alloys: a review. J Mater Sci Technol 125:252–264. https://doi.org/10.1016/J.JMST.2021.11.084
175. Liu J, Ye J, Momin F, Zhang X, Li A (2022) Nonparametric Bayesian framework for material and process optimization with nanocomposite fused filament fabrication. Addit Manuf 54:102765. https://doi.org/10.1016/J.ADDMA.2022.102765
176. Zhang X, Saniie J, Bakhtiari S, Heifetz A (2022) Compression of pulsed infrared thermography data with unsupervised learning for nondestructive evaluation of additively manufactured metals. IEEE Access 10:9094–9107. https://doi.org/10.1109/ACCESS.2022.3141654
177. Busachi A, Erkoyuncu J, Colegrove P, Martina F, Watts C, Drake R (2017) A review of additive manufacturing technology and cost estimation techniques for the defence sector. CIRP J Manuf Sci Technol 19:117–128. https://doi.org/10.1016/j.cirpj.2017.07.001
178. Verlinden B, Duflou JR, Collin P, Cattrysse D (2008) Cost estimation for sheet metal parts using multiple regression and artificial neural networks: a case study. Int J Prod Econ 111:484–492. https://doi.org/10.1016/j.ijpe.2007.02.004
179. Niazi A, Dai JS, Balabani S, Seneviratne L (2006) Product cost estimation: technique classification and methodology review. J Manuf Sci Eng Trans ASME 128:563–575. https://doi.org/10.1115/1.2137750
180. Bikmukhametov T, Jäschke J (2020) Combining machine learning and process engineering physics towards enhanced accuracy and explainability of data-driven models R. Comput Chem Eng. https://doi.org/10.1016/j.compchemeng.2020.106834
181. Deng S, Yeh TH (2011) Using least squares support vector machines for the airframe structures manufacturing cost estimation. Int J Prod Econ 131:701–708. https://doi.org/10.1016/j.ijpe.2011.02.019
182. Sajadfar N, Ma Y (2015) A hybrid cost estimation framework based on feature-oriented data mining approach. Adv Eng Inform 29:633–647. https://doi.org/10.1016/j.aei.2015.06.001
183. Chan SL, Lu Y, Wang Y (2018) Data-driven cost estimation for additive manufacturing in cybermanufacturing. J Manuf Syst 46:115–126. https://doi.org/10.1016/j.jmsy.2017.12.001
184. Kai C, Leong S (2020) Microstructure evolution and mechanical property response via 3D printing parameter development of Al–Sc alloy. Virtual Phys Prototyp. https://doi.org/10.1080/17452759.2019.1698967
185. Jiang J, Xiong Y, Zhang Z, Rosen DW (2020) Machine learning integrated design for additive manufacturing. J Intell Manuf. https://doi.org/10.1007/s10845-020-01715-6
186. Rosen DW, Rosen DW (2014) Research supporting principles for design for additive manufacturing and strategies for AM research supporting principles for design for additive manufacturing: this paper provides a comprehensive review on current design principles and strategies for AM. Virtual Phys Prototyp 9:225–232. https://doi.org/10.1080/17452759.2014.951530
187. Gardner JM, Hunt KA, Ebel AB, Rose ES, Zylich SC, Jensen BD, Wise KE, Siochi EJ, Sauti G (2019) Machines as craftsmen: localized parameter setting optimization for fused filament fabrication 3D printing. Adv Mater Technol 4:1800653. https://doi.org/10.1002/admt.201800653
188. Deka A, Behdad S (2019) Part separation technique for assembly-based design in additive manufacturing using genetic algorithm. Proc Manuf 2019:764–771. https://doi.org/10.1016/j.promfg.2019.06.208
189. Abarghooei H, Arabi H, Seyedein SH, Mirzakhani B (2017) Modeling of steady state hot flow behavior of API-X70 microalloyed steel using genetic algorithm and design of experiments. Appl Soft Comput J 52:471–477. https://doi.org/10.1016/j.asoc.2016.10.021
190. Kumar K, Zindani D, Davim P (2019) Sustainable engineering products and manufacturing technologies. Elsevier, Amsterdam
191. Mohamed OA, Masood SH, Bhowmik JL (2017) Influence of processing parameters on creep and recovery behavior of FDM manufactured part using definitive screening design and ANN. Rapid Prototyp J 23:998–1010. https://doi.org/10.1108/RPJ-12-2015-0198
192. Jiang J, Hu G, Li X, Xu X, Zheng P, Stringer J (2019) Analysis and prediction of printable bridge length in fused deposition modelling based on back propagation neural network. Virtual Phys Prototyp 14:253–266. https://doi.org/10.1080/17452759.2019.1576010
193. Omar A, Syed H, Jahar L (2016) Processed by fused deposition modeling additive manufacturing. Adv Prod Eng Manage 11:227–238
194. Bayraktar Ö, Uzun G, Çakiroğlu R, Guldas A (2017) Experimental study on the 3D-printed plastic parts and predicting the mechanical properties using artificial neural networks. Polym Adv Technol 28:1044–1051. https://doi.org/10.1002/pat.3960
195. Sood AK, Equbal A, Toppo V, Ohdar RK, Mahapatra SS (2012) An investigation on sliding wear of FDM built parts. CIRP J Manuf Sci Technol 5:48–54. https://doi.org/10.1016/j.cirpj.2011.08.003
196. Sood AK, Ohdar RK, Mahapatra SS (2012) Experimental investigation and empirical modelling of FDM process for compressive strength improvement. J Adv Res 3:81–90. https://doi.org/10.1016/j.jare.2011.05.001
197. Moradi M, SalehMeiabadi M, Moghadam MK, Ardabili S, Band SS, Mosavi A (2020) Enhancing 3D printing producibility in polylactic acid using fused filament fabrication and machine learning. Mapp Intim. https://doi.org/10.20944/preprints202012.0487.v1
198. Zhang M, Sun CN, Zhang X, Goh PC, Wei J, Hardacre D, Li H (2019) High cycle fatigue life prediction of laser additive manufactured stainless steel: a machine learning approach. Int

J Fatigue 128:105194. https://doi.org/10.1016/j.ijfatigue.2019.105194
199. Tapia G, Khairallah S, Matthews M, King WE, Elwany A (2018) Gaussian process-based surrogate modeling framework for process planning in laser powder-bed fusion additive manufacturing of 316L stainless steel. Int J Adv Manuf Technol 94:3591–3603. https://doi.org/10.1007/s00170-017-1045-z
200. Tapia G, Elwany AH, Sang H (2016) Prediction of porosity in metal-based additive manufacturing using spatial Gaussian process models. Addit Manuf 12:282–290. https://doi.org/10.1016/j.addma.2016.05.009
201. Aoyagi K, Wang H, Sudo H, Chiba A (2019) Simple method to construct process maps for additive manufacturing using a support vector machine. Addit Manuf 27:353–362. https://doi.org/10.1016/j.addma.2019.03.013
202. Wang C, Tan XP, Tor SB, Lim CS (2020) Machine learning in additive manufacturing: state-of-the-art and perspectives. Addit Manuf 36:101538. https://doi.org/10.1016/j.addma.2020.101538
203. Chowdhury S, Anand S (2016) Artificial neural network based geometric compensation for thermal deformation in additive manufacturing processes. ASME Int. https://doi.org/10.1115/msec2016-8784
204. Liu S, Shin YC (2019) Additive manufacturing of Ti6Al4V alloy: a review. Mater Des 164:107552. https://doi.org/10.1016/J.MATDES.2018.107552
205. Khorasani AM, Gibson I, Awan US, Ghaderi A (2019) The effect of SLM process parameters on density, hardness, tensile strength and surface quality of Ti-6Al-4V. Addit Manuf 25:176–186. https://doi.org/10.1016/J.ADDMA.2018.09.002
206. Majumdar T, Bazin T, Ribeiro EMC, Frith JE, Birbilis N (2019) Understanding the effects of PBF process parameter interplay on Ti-6Al-4V surface properties. PLoS ONE 14:e0221198. https://doi.org/10.1371/JOURNAL.PONE.0221198
207. Egan DS, Dowling DP (2019) Influence of process parameters on the correlation between in-situ process monitoring data and the mechanical properties of Ti-6Al-4V non-stochastic cellular structures. Addit Manuf 30:100890. https://doi.org/10.1016/J.ADDMA.2019.100890
208. Levkulich NC, Semiatin SL, Gockel JE, Middendorf JR, DeWald AT, Klingbeil NW (2019) The effect of process parameters on residual stress evolution and distortion in the laser powder bed fusion of Ti-6Al-4V. Addit Manuf 28:475–484. https://doi.org/10.1016/J.ADDMA.2019.05.015
209. Aslani K-E, Kitsakis K, Kechagias JD, Vaxevanidis NM, Manolakos DE (2020) On the application of grey Taguchi method for benchmarking the dimensional accuracy of the PLA fused filament fabrication process. SN Appl Sci 2(6):1–11. https://doi.org/10.1007/S42452-020-2823-Z
210. Aslani KE, Vakouftsi F, Kechagias JD, Mastorakis NE (2019) Surface roughness optimization of poly-jet 3D printing using Grey Taguchi method. In: 2019 3rd International Conference on Control, Artificial Intelligence, Robotics & Optimization (ICCAIRO). pp 213–218. https://doi.org/10.1109/ICCAIRO47923.2019.00041.
211. Narayana PL, Kim JH, Lee J, Choi S-W, Lee S, Park CH, Yeom J-T, Reddy NGS, Hong J-K (2021) Optimization of process parameters for direct energy deposited Ti-6Al-4V alloy using neural networks. Int J Adv Manuf Technol 114:3269–3283. https://doi.org/10.1007/S00170-021-07115-1
212. Reddy NS, Panigrahi BB, Ho CM, Kim JH, Lee CS (2015) Artificial neural network modeling on the relative importance of alloying elements and heat treatment temperature to the stability of α and β phase in titanium alloys. Comput Mater Sci 107:175–183. https://doi.org/10.1016/J.COMMATSCI.2015.05.026
213. Lang V (2021) Data-based process development and control in multi-material jetting technology. Ceram Appl 9:53–57
214. Sander G, Babu AP, Gao X, Jiang D, Birbilis N (2021) On the effect of build orientation and residual stress on the corrosion of 316L stainless steel prepared by selective laser melting. Corros Sci 179:109149. https://doi.org/10.1016/j.corsci.2020.109149
215. Zhang B, Dembinski L, Coddet C (2013) The study of the laser parameters and environment variables effect on mechanical properties of high compact parts elaborated by selective laser melting 316L powder. Mater Sci Eng A 584:21–31. https://doi.org/10.1016/j.msea.2013.06.055
216. Liu Q, Wu H, Paul MJ, He P, Peng Z, Gludovatz B, Kruzic JJ, Wang CH, Li X (2020) Machine-learning assisted laser powder bed fusion process optimization for AlSi10Mg: new microstructure description indices and fracture mechanisms. Acta Mater 201:316–328. https://doi.org/10.1016/j.actamat.2020.10.010
217. Kamath C, Fan YJ (2018) Regression with small data sets: a case study using code surrogates in additive manufacturing. Knowl Inf Syst 57:475–493. https://doi.org/10.1007/s10115-018-1174-1
218. Fang SF, Wang MP, Song M (2009) An approach for the aging process optimization of Al-Zn-Mg-Cu series alloys. Mater Des 30:2460–2467. https://doi.org/10.1016/j.matdes.2008.10.008
219. Read N, Wang W, Essa K, Attallah MM (2015) Selective laser melting of AlSi10Mg alloy: process optimisation and mechanical properties development. Mater Des 65:417–424. https://doi.org/10.1016/j.matdes.2014.09.044
220. Zhang Z, Liu Z, Wu D (2020) Prediction of melt pool temperature in directed energy deposition using machine learning. Addit Manuf 37:101692. https://doi.org/10.1016/j.addma.2020.101692
221. Omar S, Ngadi A, Jebur HH (2013) Machine learning techniques for anomaly detection: an overview. Int J Comput Appl 79:33–41. https://doi.org/10.5120/13715-1478
222. Jin Z, Zhang Z, Ott J, Gu GX (2021) Precise localization and semantic segmentation detection of printing conditions in fused filament fabrication technologies using machine learning. Addit Manuf 37:101696. https://doi.org/10.1016/j.addma.2020.101696
223. Wang P, Yang Y, Moghaddam NS (2022) Process modeling in laser powder bed fusion towards defect detection and quality control via machine learning: the state-of-the-art and research challenges. J Manuf Process 73:961–984. https://doi.org/10.1016/J.JMAPRO.2021.11.037
224. Ye Z, Liu C, Tian W, Kan C (2021) In-situ point cloud fusion for layer-wise monitoring of additive manufacturing. J Manuf Syst 61:210–222. https://doi.org/10.1016/j.jmsy.2021.09.002
225. Egan DS, Ryan CM, Parnell AC, Dowling DP (2021) Using in-situ process monitoring data to identify defective layers in Ti-6Al-4V additively manufactured porous biomaterials. J Manuf Process 64:1248–1254. https://doi.org/10.1016/j.jmapro.2021.03.002
226. Qin J, Hu F, Liu Y, Witherell P, Wang CCL, Rosen DW, Simpson TW, Lu Y, Tang Q (2022) Research and application of machine learning for additive manufacturing. Addit Manuf 52:102691. https://doi.org/10.1016/j.addma.2022.102691
227. Kodaira Y, Miura T, Ito S, Emori K, Yonezu A, Nagatsuka H (2021) Evaluation of crack propagation behavior of porous polymer membranes. Polym Test 96:107124. https://doi.org/10.1016/j.polymertesting.2021.107124
228. Yang K, Yu L, Xia M, Xu T, Li W (2021) Nonlinear RANSAC with crossline correction: an algorithm for vision-based curved cable detection system. Opt Lasers Eng 141:106417. https://doi.org/10.1016/j.optlaseng.2020.106417
229. Muhammad W, Brahme AP, Ibragimova O, Kang J, Inal K (2021) A machine learning framework to predict local strain distribution and the evolution of plastic anisotropy & fracture in additively manufactured alloys. Int J Plast 136:102867. https://doi.org/10.1016/j.ijplas.2020.102867

230. Muñoz JA, Pavlov M, Cheverikin V, Komissarov A, Gromov A (2021) Heterogeneity consequences on the mechanical and microstructural evolution of an AlSi11Cu alloy obtained by selective laser melting. Mater Charact 174:110989. https://doi.org/10.1016/j.matchar.2021.110989
231. Ghoncheh MH, Sanjari M, Zoeram AS, Cyr E, Amirkhiz BS, Lloyd A, Haghshenas M, Mohammadi M (2021) On the microstructure and solidification behavior of new generation additively manufactured Al-Cu-Mg-Ag-Ti-B alloys. Addit Manuf 37:101724. https://doi.org/10.1016/j.addma.2020.101724
232. Gur S, Wolf L, Golgher L, Blinder P (2019) Unsupervised microvascular image segmentation using an active contours mimicking neural network. In: Proceedings of the IEEE/CVF international conference on computer vision. pp 10721–10730. https://doi.org/10.1109/ICCV.2019.01082.
233. Koch G (2015) Siamese neural networks for one-shot image recognition,
234. Pan Y, He H, Xu J, Feinerman A (2017) Study of separation force in constrained surface projection stereolithography. Rapid Prototyp J 23:353–361. https://doi.org/10.1108/RPJ-12-2015-0188
235. He H, Xu J, Yu X, Pan Y (2018) Effect of constrained surface texturing on separation force in projection stereolithography. J Manuf Sci Eng. https://doi.org/10.1115/1.4040322
236. Xu W, Jambhulkar S, Zhu Y, Ravichandran D, Kakarla M, Vernon B, Lott DG, Cornella JL, Shefi O, Miquelard-Garnier G, Yang Y, Song K (2021) 3D printing for polymer/particle-based processing: a review. Compos Part B Eng 223:109102. https://doi.org/10.1016/J.COMPOSITESB.2021.109102
237. Mostafaei A, Stevens EL, Hughes ET, Biery SD, Hilla C, Chmielus M (2016) Powder bed binder jet printed alloy 625: densification, microstructure and mechanical properties. Mater Des 108:126–135. https://doi.org/10.1016/J.MATDES.2016.06.067
238. Yegyan Kumar A, Wang J, Bai Y, Huxtable ST, Williams CB (2019) Impacts of process-induced porosity on material properties of copper made by binder jetting additive manufacturing. Mater Des 182:108001. https://doi.org/10.1016/J.MATDES.2019.108001
239. Zhu Y, Wu Z, Hartley WD, Sietins JM, Williams CB, Yu HZ (2020) Unraveling pore evolution in post-processing of binder jetting materials: X-ray computed tomography, computer vision, and machine learning. Addit Manuf 34:101183. https://doi.org/10.1016/J.ADDMA.2020.101183
240. Mostafaei A, Toman J, Stevens EL, Hughes ET, Krimer YL, Chmielus M (2017) Microstructural evolution and mechanical properties of differently heat-treated binder jet printed samples from gas- and water-atomized alloy 625 powders. Acta Mater 124:280–289. https://doi.org/10.1016/J.ACTAMAT.2016.11.021
241. Mohammad S, Hojjatzadeh H, Parab ND, Yan W, Guo Q, Xiong L, Zhao C, Qu M, Escano LI, Xiao X, Fezzaa K, Everhart W, Sun T, Chen L (2019) Pore elimination mechanisms during 3D printing of metals. Nat Commun. https://doi.org/10.1038/s41467-019-10973-9
242. Everton SK, Hirsch M, Stavroulakis PI, Leach RK, Clare AT (2016) Review of in-situ process monitoring and in-situ metrology for metal additive manufacturing. Mater Des 95:431–445. https://doi.org/10.1016/J.MATDES.2016.01.099
243. Lu QY, Wong CH (2018) Additive manufacturing process monitoring and control by non-destructive testing techniques: challenges and in-process monitoring. Virtual Phys Prototyp 13:39–48. https://doi.org/10.1080/17452759.2017.1351201
244. Landron C, Maire E, Bouaziz O, Adrien J, Lecarme L, Bareggi A (2011) Validation of void growth models using X-ray microtomography characterization of damage in dual phase steels. Acta Mater 59:7564–7573. https://doi.org/10.1016/J.ACTAMAT.2011.08.046
245. Cai X, Malcolm AA, Wong BS, Fan Z (2015) Measurement and characterization of porosity in aluminium selective laser melting parts using X-ray CT. Virtual Phys Prototy 10:195–206. https://doi.org/10.1080/17452759.2015.1112412
246. Flodberg G, Pettersson H, Yang L (2018) Pore analysis and mechanical performance of selective laser sintered objects. Addit Manuf 24:307–315. https://doi.org/10.1016/J.ADDMA.2018.10.001
247. Dimiduk DM, Holm EA, Niezgoda SR (2018) Perspectives on the impact of machine learning, deep learning, and artificial intelligence on materials, processes, and structures engineering. Integr Mater Manuf Innov 7(3):157–172. https://doi.org/10.1007/S40192-018-0117-8
248. Cha Y-J, Choi W, Büyüköztürk O (2017) Deep learning-based crack damage detection using convolutional neural networks. Comput Civ Infrastruct Eng 32:361–378. https://doi.org/10.1111/MICE.12263
249. Cunningham R, Narra SP, Montgomery C, Beuth J, Rollett AD (2017) Synchrotron-based X-ray microtomography characterization of the effect of processing variables on porosity formation in laser power-bed additive manufacturing of Ti-6Al-4V. JOM. https://doi.org/10.1007/s11837-016-2234-1
250. Romano S, Brandão A, Gumpinger J, Gschweitl M, Beretta S (2017) Qualification of AM parts: extreme value statistics applied to tomographic measurements. Mater Des 131:32–48. https://doi.org/10.1016/J.MATDES.2017.05.091
251. Wu Z, Alorf A, Yang T, Li L, Zhu Y (2019) Robust X-ray sparse-view phase tomography via hierarchical synthesis convolutional neural networks. https://arxiv.org/abs/1901.10644v1. Accessed 31 Aug 2021
252. Jolliffe IT, Cadima J (2016) Principal component analysis: a review and recent developments. Philos Trans R Soc A 374:2065. https://doi.org/10.1098/RSTA.2015.0202
253. Cramer CL, Nandwana P, Lowden RA, Elliott AM (2019) Infiltration studies of additive manufacture of WC with Co using binder jetting and pressureless melt method. Addit Manuf 28:333–343. https://doi.org/10.1016/J.ADDMA.2019.04.009
254. Mostafaei A, Rodriguez De Vecchis P, Nettleship I, Chmielus M (2019) Effect of powder size distribution on densification and microstructural evolution of binder-jet 3D-printed alloy 625. Mater Des 162:375–383. https://doi.org/10.1016/J.MATDES.2018.11.051
255. Khanzadeh M, Chowdhury S, Marufuzzaman M, Tschopp MA, Bian L (2018) Porosity prediction: supervised-learning of thermal history for direct laser deposition. J Manuf Syst 47:69–82. https://doi.org/10.1016/j.jmsy.2018.04.001
256. Li Y, Shi Z, Liu C, Tian W, Kong Z, Williams CB (2021) Augmented time regularized generative adversarial network (ATR-GAN) for data augmentation in online process anomaly detection. IEEE Trans Autom Sci Eng. https://doi.org/10.1109/TASE.2021.3118635
257. Becker P, Roth C, Roennau A, Dillmann R (2020) Acoustic anomaly detection in additive manufacturing with long short-term memory neural networks. IEEE 7th Int Conf Ind Eng Appl ICIEA 2020:921–926. https://doi.org/10.1109/ICIEA49774.2020.9102002
258. Print Quality Guide, (n.d.). https://www.simplify3d.com/support/print-quality-troubleshooting/. Accessed 1 June 2022
259. Datsiou KC, Spirrett F, Ashcroft I, Magallanes M, Christie S, Goodridge R (2021) Laser powder bed fusion of soda lime silica glass: optimisation of processing parameters and evaluation of part properties. Addit Manuf 39:101880. https://doi.org/10.1016/j.addma.2021.101880
260. Vaithilingam J, Goodridge RD, Hague RJM, Christie SDR, Edmondson S (2016) The effect of laser remelting on the surface chemistry of Ti6al4V components fabricated by selective

laser melting. J Mater Process Technol 232:1–8. https://doi.org/10.1016/j.jmatprotec.2016.01.022
261. Snow Z, Diehl B, Reutzel EW, Nassar A (2021) Toward in-situ flaw detection in laser powder bed fusion additive manufacturing through layerwise imagery and machine learning. J Manuf Syst 59:12–26. https://doi.org/10.1016/j.jmsy.2021.01.008
262. Baumgartl H, Tomas J, Buettner R, Merkel M (2020) A deep learning-based model for defect detection in laser-powder bed fusion using in-situ thermographic monitoring. Prog Addit Manuf 5:277–285. https://doi.org/10.1007/s40964-019-00108-3
263. Scime L, Beuth J (2018) Anomaly detection and classification in a laser powder bed additive manufacturing process using a trained computer vision algorithm. Addit Manuf 19:114–126. https://doi.org/10.1016/j.addma.2017.11.009
264. Mojahed Yazdi R, Imani F, Yang H (2020) A hybrid deep learning model of process-build interactions in additive manufacturing. J Manuf Syst 57:460–468. https://doi.org/10.1016/j.jmsy.2020.11.001
265. Tammas-Williams S, Withers PJ, Todd I, Prangnell PB (2017) The influence of porosity on fatigue crack initiation in additively manufactured titanium components. Sci Rep 7:1–13. https://doi.org/10.1038/s41598-017-06504-5
266. Beretta S, Romano S (2017) A comparison of fatigue strength sensitivity to defects for materials manufactured by AM or traditional processes. Int J Fatigue 94:178–191. https://doi.org/10.1016/j.ijfatigue.2016.06.020
267. Masuo H, Tanaka Y, Morokoshi S, Yagura H, Uchida T, Yamamoto Y, Murakami Y (2018) Influence of defects, surface roughness and HIP on the fatigue strength of Ti-6Al-4V manufactured by additive manufacturing. Int J Fatigue 117:163–179. https://doi.org/10.1016/j.ijfatigue.2018.07.020
268. Nassar AR, Gundermann MA, Reutzel EW, Guerrier P, Krane MH, Weldon MJ (2019) Formation processes for large ejecta and interactions with melt pool formation in powder bed fusion additive manufacturing. Sci Rep 9:1–11. https://doi.org/10.1038/s41598-019-41415-7
269. Gobert C, Reutzel EW, Petrich J, Nassar AR, Phoha S (2018) Application of supervised machine learning for defect detection during metallic powder bed fusion additive manufacturing using high resolution imaging. Addit Manuf 21:517–528. https://doi.org/10.1016/J.ADDMA.2018.04.005
270. Morgan JP (2019) Data fusion for additive manufacturing inspection
271. Liu R, Liu S, Zhang X (2021) A physics-informed machine learning model for porosity analysis in laser powder bed fusion additive manufacturing. Int J Adv Manuf Technol 113:1943–1958. https://doi.org/10.1007/s00170-021-06640-3
272. Ward L, Agrawal A, Choudhary A, Wolverton C (2016) A general-purpose machine learning framework for predicting properties of inorganic materials. Npj Comput Mater 2:1–7. https://doi.org/10.1038/npjcompumats.2016.28
273. Dong G, Leong S, Fang Y, Li J, Thong J, Kai Z, Reddy S, Yee W (2021) Machine learning for 3D printed multi-materials tissue-mimicking anatomical models. Mater Des 211:110125
274. Karmuhilan M, Sood AK (2018) Intelligent process model for bead geometry prediction in WAAM. Mater Today Proc 5:24005–24013. https://doi.org/10.1016/j.matpr.2018.10.193
275. Chaparro BM, Thuillier S, Menezes LF, Manach PY, Fernandes JV (2008) Material parameters identification: gradient-based, genetic and hybrid optimization algorithms. Comput Mater Sci 44:339–346. https://doi.org/10.1016/j.commatsci.2008.03.028
276. Liu S, Stebner AP, Kappes BB, Zhang X (2021) Machine learning for knowledge transfer across multiple metals additive manufacturing printers. Addit Manuf 39:101877. https://doi.org/10.1016/j.addma.2021.101877
277. Singh A, Nath A, Shekhar Roy S, Kumar Lohar A (2022) Modeling of laser aided direct metal deposition of stainless steel using supervised deep learning algorithms. Mater Today Proc. https://doi.org/10.1016/J.MATPR.2022.03.468
278. Ni J, Ling H, Zhang S, Wang Z, Peng Z, Benyshek C, Zan R, Miri AK, Li Z, Zhang X, Lee J, Lee KJ, Kim HJ, Tebon P, Hoffman T, Dokmeci MR, Ashammakhi N, Li X, Khademhosseini A (2019) Three-dimensional printing of metals for biomedical applications. Mater Today Bio 3:100024. https://doi.org/10.1016/J.MTBIO.2019.100024
279. Ni L, Wang D, Wu J, Wang Y, Tao Y, Zhang J, Liu J (2020) Streamflow forecasting using extreme gradient boosting model coupled with Gaussian mixture model. J Hydrol 586:124901. https://doi.org/10.1016/j.jhydrol.2020.124901
280. Chen T, Guestrin C (2016) XGBoost: a scalable tree boosting system. In: Proceedings of ACM SIGKDD International Conference on Knowledge Discovery and Data Mining, Association for Computing Machinery. pp 785–794. https://doi.org/10.1145/2939672.2939785.
281. Fan J, Wu L, Zhang F, Cai H, Zeng W, Wang X, Zou H (2019) Empirical and machine learning models for predicting daily global solar radiation from sunshine duration: a review and case study in China. Renew Sustain Energy Rev 100:186–212. https://doi.org/10.1016/j.rser.2018.10.018
282. Nguyen-Le DH, Tao QB, Nguyen VH, Abdel-Wahab M, Nguyen-Xuan H (2020) A data-driven approach based on long short-term memory and hidden Markov model for crack propagation prediction. Eng Fract Mech 235:107085. https://doi.org/10.1016/j.engfracmech.2020.107085
283. Hochreiter S, Schmidhuber J (1997) Long short-term memory. Neural Comput 9:1735–1780. https://doi.org/10.1162/neco.1997.9.8.1735
284. Khanzadeh M, Chowdhury S, Tschopp MA, Doude HR, Marufuzzaman M, Bian L (2019) In-situ monitoring of melt pool images for porosity prediction in directed energy deposition processes. IISE Trans 51:437–455. https://doi.org/10.1080/24725854.2017.1417656
285. Galeazzi D, Silva RHGe, Viviani AB, Jaeger PR, Schwedersky MB (2022) Evaluation of thermal and geometric properties of martensitic stainless steel thin walls built by additive manufacturing cold metal transfer (CMT) processes. Int J Adv Manuf Technol 120:2151–2165. https://doi.org/10.1007/S00170-022-08921-X
286. Choi TM, Kumar S, Yue X, Chan HL (2022) Disruptive technologies and operations management in the industry 4.0 era and beyond. Prod Oper Manage 31:9–31. https://doi.org/10.1111/POMS.13622
287. Sood SK, Rawat KS, Kumar D (2022) A visual review of artificial intelligence and Industry 4.0 in healthcare. Comput Electr Eng 101:107948. https://doi.org/10.1016/J.COMPELECENG.2022.107948
288. Kumar N, Bhavsar H, Mahesh PVS, Srivastava AK, Bora BJ, Saxena A, Dixit AR (2022) Wire arc additive manufacturing—a revolutionary method in additive manufacturing. Mater Chem Phys 285:126144. https://doi.org/10.1016/J.MATCHEMPHYS.2022.126144
289. Barrionuevo GO, Sequeira-Almeida PM, Ríos S, Ramos-Grez JA, Williams SW (2022) A machine learning approach for the prediction of melting efficiency in wire arc additive manufacturing. Int J Adv Manuf Technol 2022(120):3123–3133. https://doi.org/10.1007/S00170-022-08966-Y
290. Li Y, Mu H, Polden J, Li H, Wang L, Xia C, Pan Z (2022) Towards intelligent monitoring system in wire arc additive manufacturing: a surface anomaly detector on a small dataset. Int J Adv Manuf Technol 2022(120):5225–5242. https://doi.org/10.1007/S00170-022-09076-5

291. Zhou J, Wu X, Chen Y, Yang C, Yang R, Tan J, Liu Y, Qiu L, Cheng HM (2022) 3D printed template-directed assembly of multiscale graphene structures. Adv Funct Mater 32:2105879. https://doi.org/10.1002/ADFM.202105879
292. Think big. Print nano. Your partner for high-precision additive manufacturing. Nanoscribe, (n.d.). https://www.nanoscribe.com/en/. Accessed 18 May 2022
293. Korkmaz ME, Waqar S, Garcia-Collado A, Gupta MK, Krolczyk GM (2022) A technical overview of metallic parts in hybrid additive manufacturing industry. J Mater Res Technol 18:384–395. https://doi.org/10.1016/J.JMRT.2022.02.085
294. Haleem A, Javaid M, Vaishya R (2019) 5D printing and its expected applications in orthopaedics. J Clin Orthop Trauma 10:809. https://doi.org/10.1016/J.JCOT.2018.11.014
295. Gillaspie EA, Matsumoto JS, Morris NE, Downey RJ, Shen KR, Allen MS, Blackmon SH (2016) From 3-dimensional printing to 5-dimensional printing: enhancing thoracic surgical planning and resection of complex tumors. Ann Thorac Surg 101:1958–1962. https://doi.org/10.1016/J.ATHORACSUR.2015.12.075
296. Yang Y, Li X, Chu M, Sun H, Jin J, Yu K, Wang Q, Zhou Q, Chen Y (2019) Electrically assisted 3D printing of nacre-inspired structures with self-sensing capability. Sci Adv. https://doi.org/10.1126/SCIADV.AAU9490
297. Arif ZU, Khalid MY, Ahmed W, Arshad H (2022) A review on four-dimensional (4D) bioprinting in pursuit of advanced tissue engineering applications. Bioprinting 27:e00203. https://doi.org/10.1016/J.BPRINT.2022.E00203
298. Three Areas Holding Back The $10.6B 3D Printing Industry, (n.d.). https://www.forbes.com/sites/michaelmolitch-hou/2022/04/25/three-areas-holding-back-the-106b-3d-printing-industry/?sh=7740ac474935. Accessed 18 May 2022
299. Harris P, Laskowski B, Reutzel E, Earthman JC, Hess AJ (2018) Reliability centered additive manufacturing computational design framework. IEEE Aerosp Conf Proc. https://doi.org/10.1109/AERO.2018.8396824
300. Liu Y, Guo L, Gao H, You Z, Ye Y, Zhang B (2022) Machine vision based condition monitoring and fault diagnosis of machine tools using information from machined surface texture: a review. Mech Syst Signal Process 164:108068. https://doi.org/10.1016/J.YMSSP.2021.108068
301. Ahmad MA, Teredesai A, Eckert C (2018) Interpretable machine learning in healthcare. Proc 2018 Int Conf Healthc Inform ICHI. https://doi.org/10.1109/ICHI.2018.00095
302. Sagi O, Rokach L (2020) Explainable decision forest: transforming a decision forest into an interpretable tree. Inf Fusion 61:124–138. https://doi.org/10.1016/J.INFFUS.2020.03.013
303. Ekanayake IU, Meddage DPP, Rathnayake U (2022) A novel approach to explain the black-box nature of machine learning in compressive strength predictions of concrete using Shapley additive explanations (SHAP). Case Stud Constr Mater 16:e01059
304. Vora HB, Mirani HA, Bhatt V (2021) Traditional machine learning and no code machine learning with its features and application. Int J Trend Sci Res Dev 5:29–32
305. Prathumrat P, Nikzad M, Hajizadeh E, Arablouei R, Sbarski I (2022) Shape memory elastomers: a review of synthesis, design, advanced manufacturing, and emerging applications. Polym Adv Technol 33:1782–1808. https://doi.org/10.1002/PAT.5652
306. Alejandrino JD, Concepcion RS, Lauguico SC, Tobias RR, Venancio L, Macasaet D, Bandala AA, Dadios EP (2020) A machine learning approach of lattice infill pattern for increasing material efficiency in additive manufacturing processes. Int J Mech Eng Robot Res 9:1253–1263. https://doi.org/10.18178/ijmerr.9.9.1253-1263
307. Wei HL, Mukherjee T, Zhang W, Zuback JS, Knapp GL, De A, DebRoy T (2020) Mechanistic models for additive manufacturing of metallic components. Prog Mater Sci. https://doi.org/10.1016/j.pmatsci.2020.100703
308. Wang Y, Müller W-D, Rumjahn A, Schwitalla A (2020) Parameters influencing the outcome of additive manufacturing of tiny medical devices based on PEEK. Materials (Basel) 13:466. https://doi.org/10.3390/ma13020466
309. Dinc NU, Lim J, Kakkava E, Psaltis D, Moser C (2020) Computer generated optical volume elements by additive manufacturing. Nanophotonics 9:4173–4181. https://doi.org/10.1515/nanoph-2020-0196
310. Majeed A, Zhang Y, Ren S, Lv J, Peng T, Waqar S, Yin E (2021) A big data-driven framework for sustainable and smart additive manufacturing. Robot Comput Integr Manuf 67:102026. https://doi.org/10.1016/j.rcim.2020.102026
311. Paraskevoudis K, Karayannis P, Koumoulos EP (2020) Real-time 3D printing remote defect detection (stringing) with computer vision and artificial intelligence. Processes. https://doi.org/10.3390/pr8111464
312. Fountas NA, Vaxevanidis NM (2021) Optimization of fused deposition modeling process using a virus-evolutionary genetic algorithm. Comput Ind 125:103371. https://doi.org/10.1016/j.compind.2020.103371
313. Colosimo BM, Huang Q, Dasgupta T, Tsung F (2018) Opportunities and challenges of quality engineering for additive manufacturing. J Qual Technol 50:233–252. https://doi.org/10.1080/00224065.2018.1487726